

# Highlights from HAWC



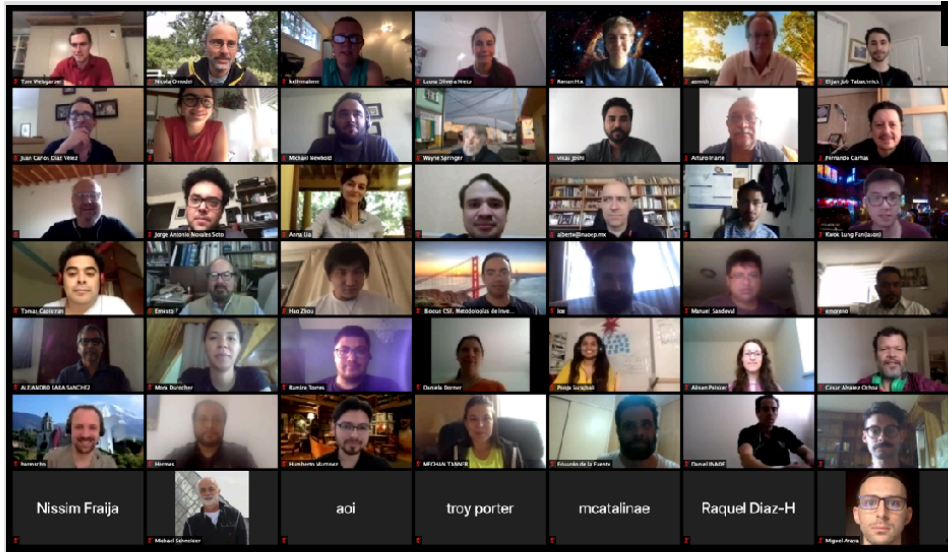
**Multimessenger high energy astrophysics in the era  
of LHAASO : Zoom Meeting, July 27<sup>th</sup> -29<sup>th</sup> 2020**

Sabrina Casanova, IFJ-PAN, Krakow and MPIK, Heidelberg

# Outline

- The HAWC detector
- A selection of HAWC Results
  - TeV Survey Maps
  - Highest Energy Sky
  - Electron and proton accelerators (PWNe, Star Cluster, Microquasars, SNRs)
  - Extended Emission from the GP ( TeV Halos, Fermi Bubbles, GDE, MCs)
  - CR Anisotropy
  - Multimessenger Observations (LIGO and Icecube)
- Outriggers

# Zoom on HAWC



## United States

University of Maryland  
 Los Alamos National Laboratory  
 University of Wisconsin  
 University of Utah  
 University of New Hampshire  
 Pennsylvania State University  
 University of New Mexico  
 Michigan Technological University  
 NASA/Goddard Space Flight Center  
 Georgia Institute of Technology  
 Michigan State University  
 University of Rochester

## Mexico

Instituto Nacional de Astrofísica,  
 Óptica y Electrónica (INAOE)  
 Universidad Nacional Autónoma  
 de México (UNAM)  
 Instituto de Física  
 Instituto de Astronomía  
 Instituto de Geofísica  
 Instituto de Ciencias Nucleares  
 Universidad Politécnica de Pachuca  
 Benemérita Universidad Autónoma de Puebla  
 Universidad Autónoma de Chiapa

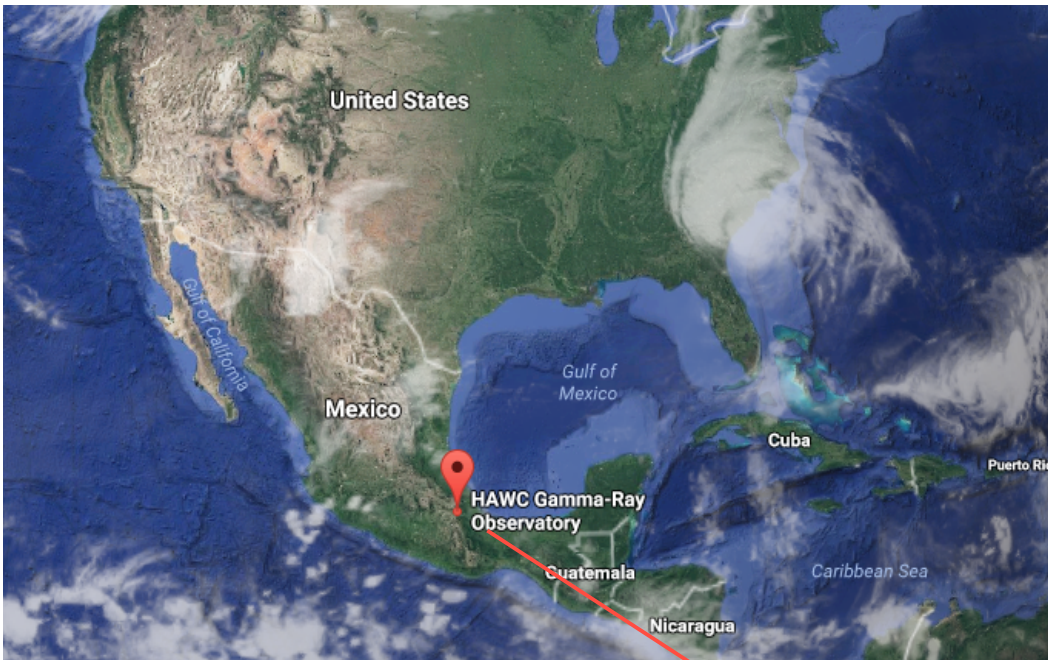
Universidad Autónoma del Estado de  
 Hidalgo  
 Universidad de Guadalajara  
 Universidad Michoacana de San  
 Nicolás de Hidalgo  
 Centro de Investigación y de  
 Estudios Avanzados  
 Instituto Politécnico Nacional  
 Centro de Investigación en  
 Computación – IPN

## Europe

IFJ-PAN, Krakow, Poland  
 Max-Planck Institute for Nuclear  
 Physics

# The HAWC Detector

- Site: Sierra Negra, Mexico, 19°N, 4,100 m altitude.
- Inaugurated **March 2015**.



# High-Altitude Water Cherenkov Gamma-Ray Observatory

Pico de Orizaba  
Puebla, Mexico (19°N)

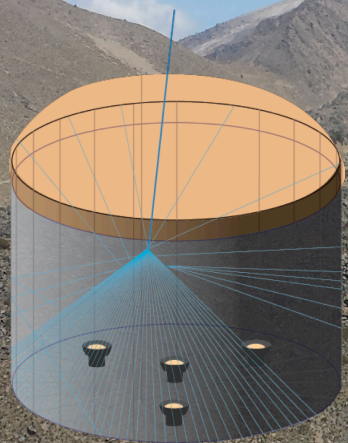
Energy range:  
**~100 GeV - 100TeV**

Field of view:  
**45° from zenith**

Observing time:  
**>95% of the time**

Angular resolution:  
**~0.1° - 1°**

300 ×



5m tall, 7.3 m diameter  
~200,000 L of water

4 PMTs facing upwards collect  
Cherenkov light produced by secondary particles

22,000 m<sup>2</sup>

T-rex for scale



4,100 m.a.s.l.

- Instantaneous FOV 2sr. Daily 8sr (66% of the sky).

# HAWC Water Cherenkov Detectors

- The WCDs are filled with 200,000 l of purified water. The particles from the shower induce **Cherenkov** light in **water**, detected by the 4 PMTs.

Steel frame construction



Large plastic bag container



Water trucks filling the tanks

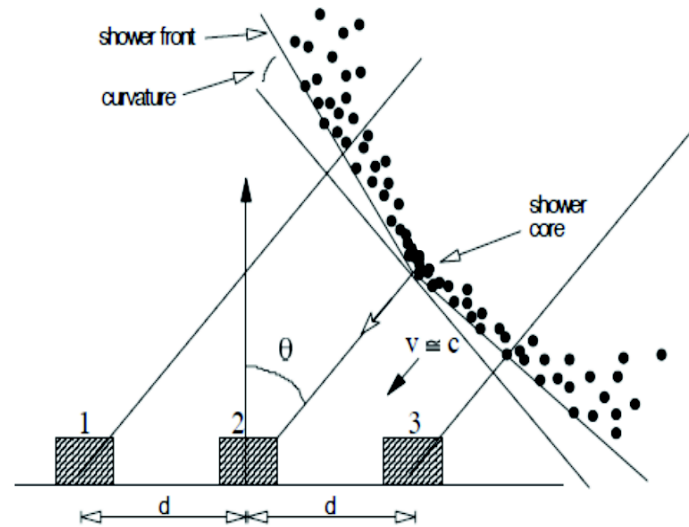
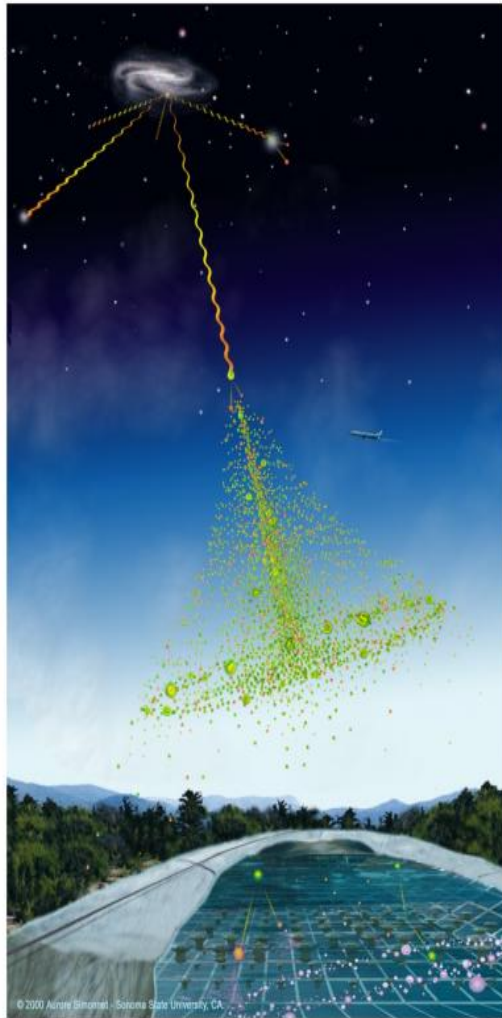


8-inch  
10-inch  
PMTs



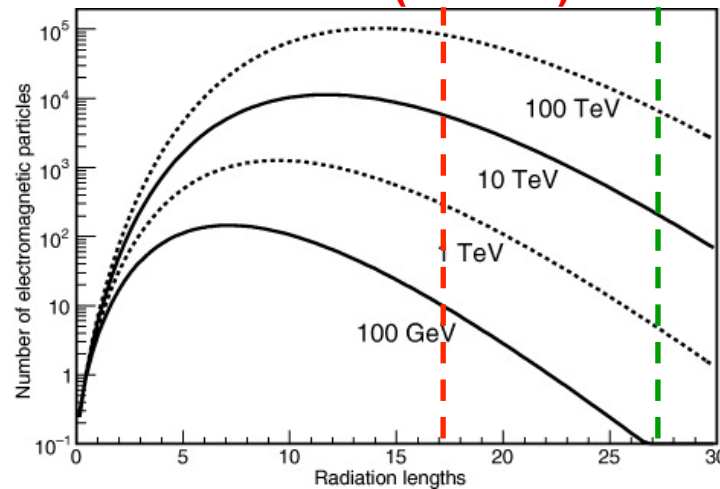
3900 tanker truck trips needed

# Detection Technique



- The particle detectors are tanks full of water. Particles from the shower pass through the water and induce Cherenkov light detected by PMTs.
- High altitude means closer to the shower maximum

**HAWC (4100m)** **Sea level**



**The reconstruction of the events  
Involves determining:**

**Direction of the Event**

**Likelihood of an event to be  $\gamma$**

**Size of the Event**

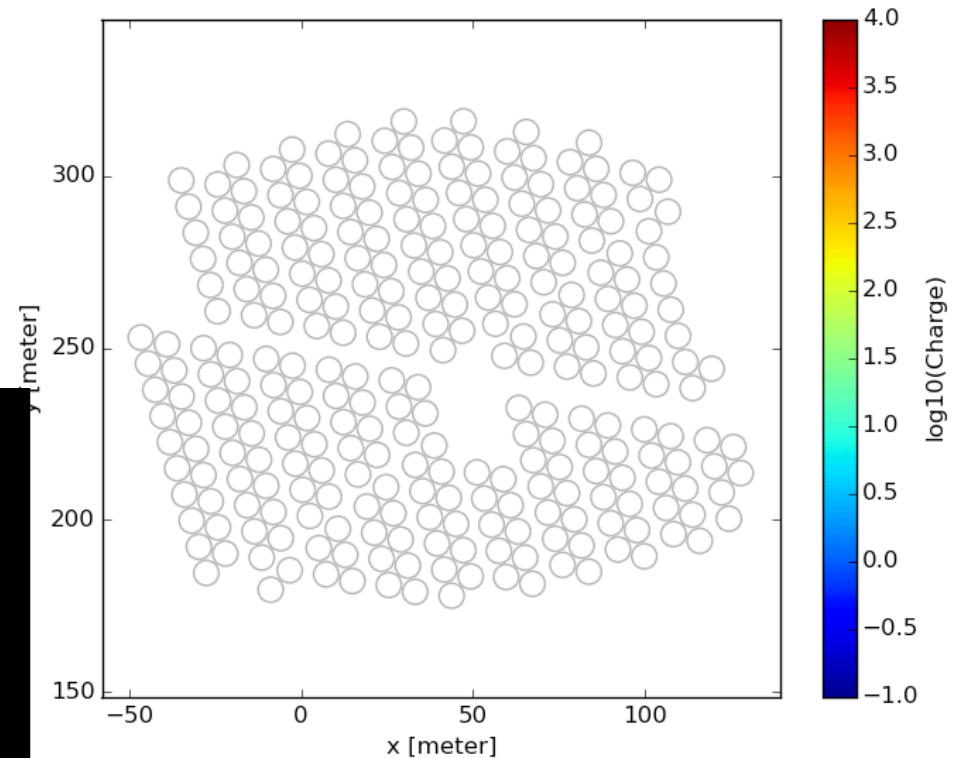
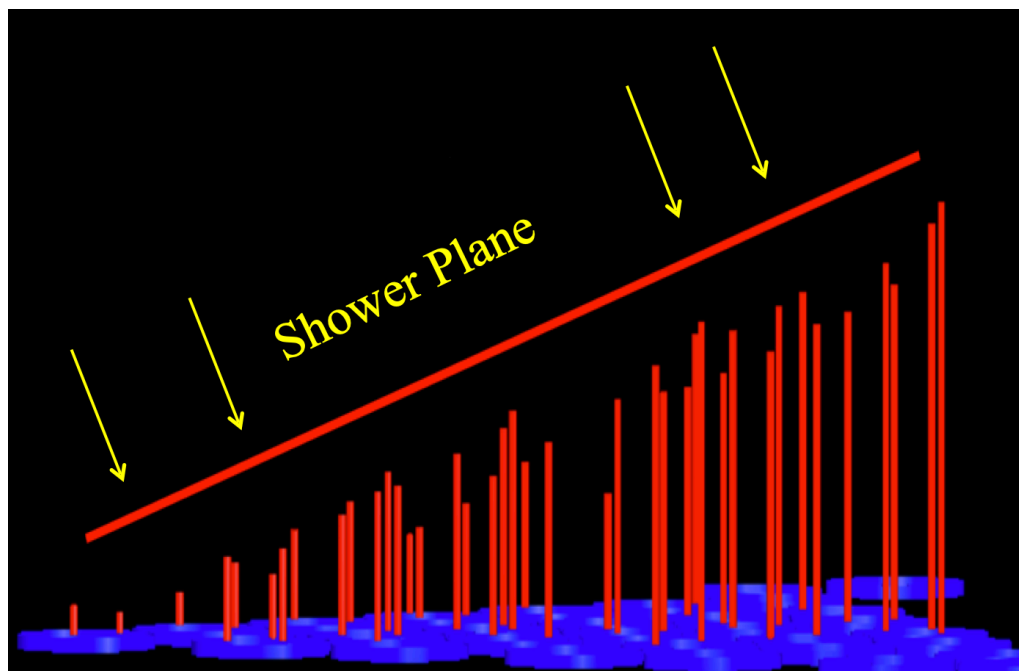
# Direction reconstruction

The concentration of secondary particles is highest along the trajectory of the original primary particle, termed the air shower core.

Determining the position of the core on the ground is key to reconstructing the direction

At first order, we fit a plane to the relative timing of each PMT

Sub-nanosecond precision is needed

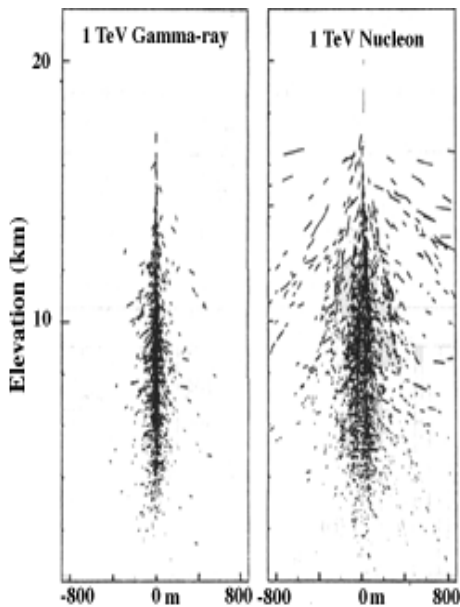




# Gamma-Hadron Separation

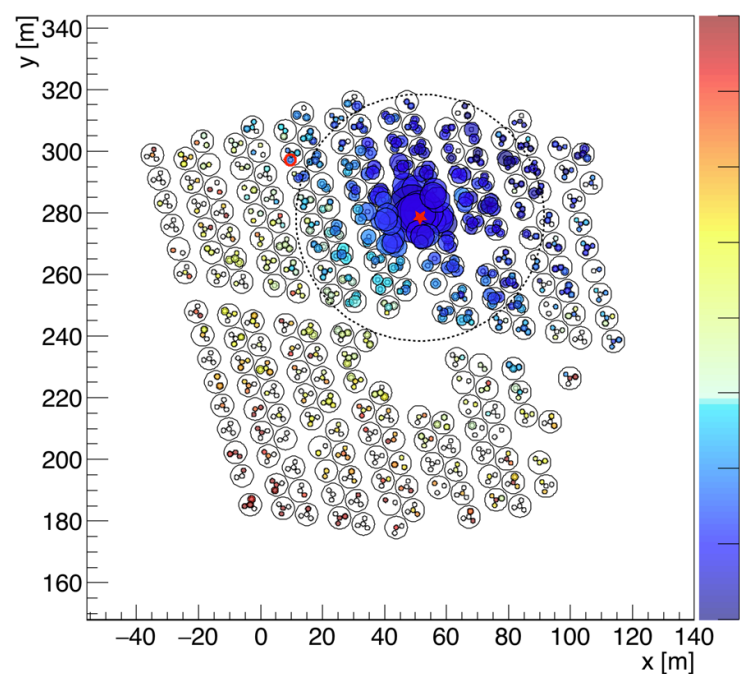
## Simulation

Gamma Hadron



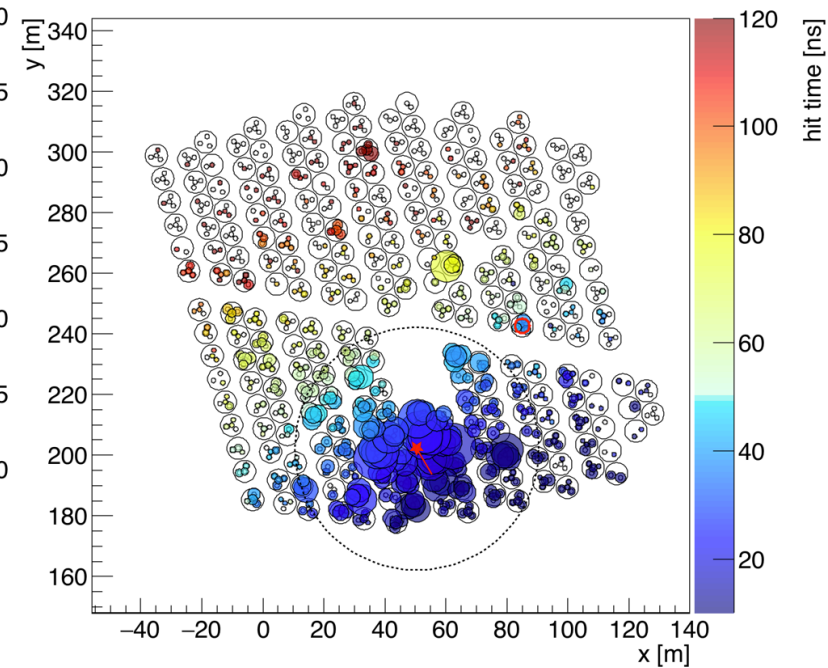
## HAWC Data

Likely Gamma Ray



## HAWC Data

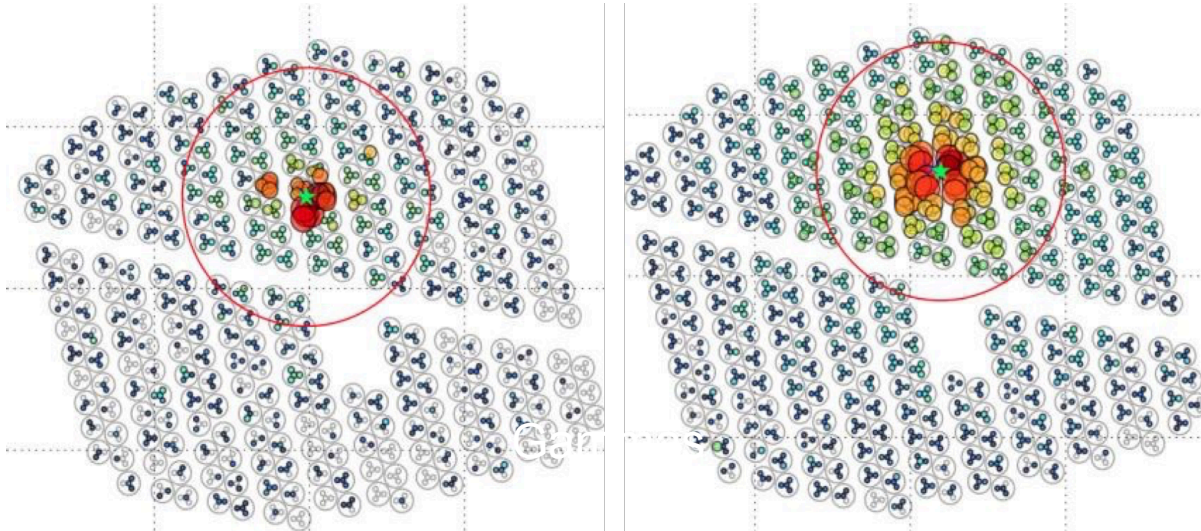
Hadron Shower



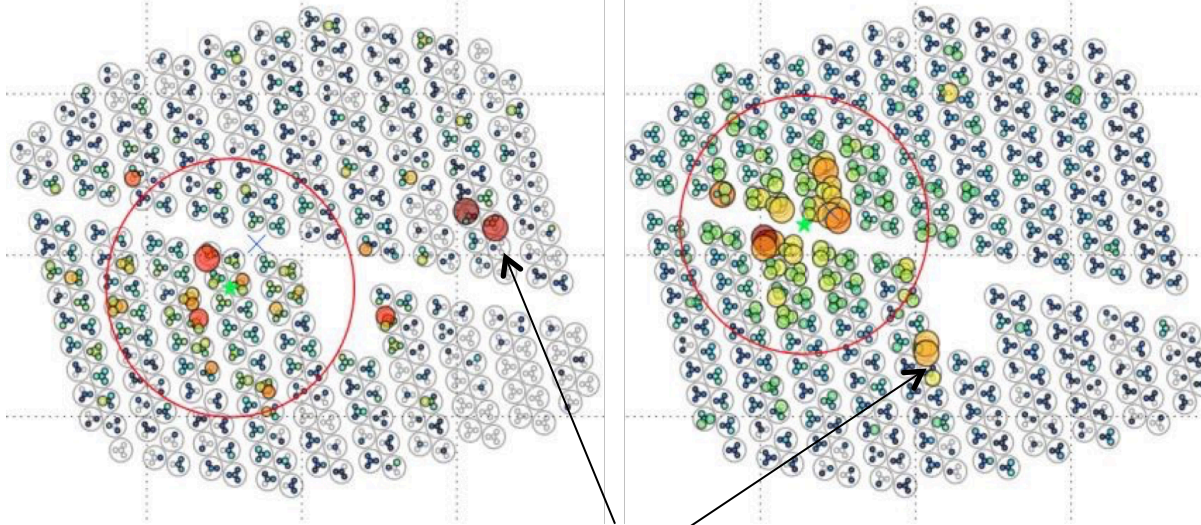
- Main background is hadronic CR, e.g. 400  $\gamma$ /day from the Crab vs 15k CR/s.
- Gamma/hadron can be discriminated based on the event footprint on the detector: gamma-ray showers are more compact, cosmic rays showers tend to "break apart"
- Showers appear quite different particularly above several TeV..

# Montecarlo Shower Simulation

Gammas



Protons



Energy deposited away from the core

# Quantifying the clumpiness: Compactness

$$C = N_{\text{hit}} / C_{\text{xPE40}}$$

$C_{\text{xPE40}}$  is the effective charge measured in the PMT with the largest effective charge outside a radius of 40 meters from the shower core.  $N_{\text{hit}}$  is the number of hit PMTs during the air shower.  $C_{\text{xPE40}}$  is typically large for a hadronic event, so  $C$  is small.

# Quantifying the clumpiness: Pincness

$$P = 1/N \sum_{i=1,N} (\zeta_i - \langle \zeta_i \rangle)^2 / \sigma_{\zeta_i}^2$$

P is defined using the **lateral distribution function of the air shower**.

Each of the PMT hits,  $i$ , has a measured **effective charge  $Q_{\text{eff},i}$** . P is computed using the logarithm of this charge  $\zeta_i = \log_{10}(Q_{\text{eff},i})$ .

For each hit, an expectation is assigned  $\langle \zeta_i \rangle$  by averaging the  $\zeta_i$  in all PMTs contained in an annulus containing the hit, with a width of 5 meters, centered at the air shower core.

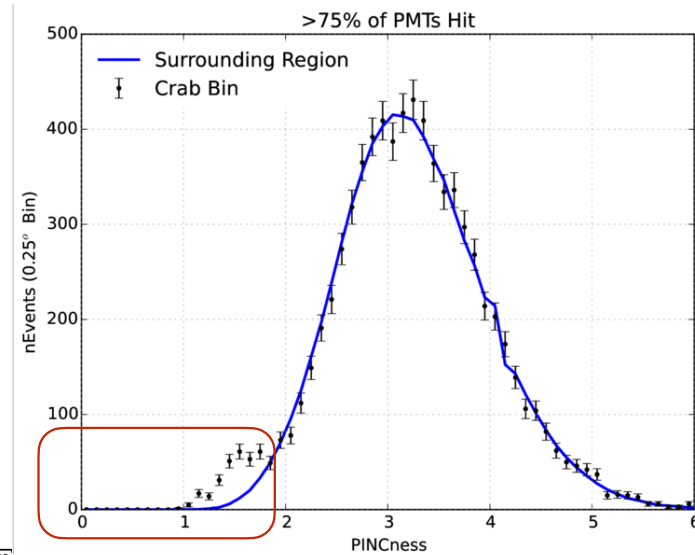
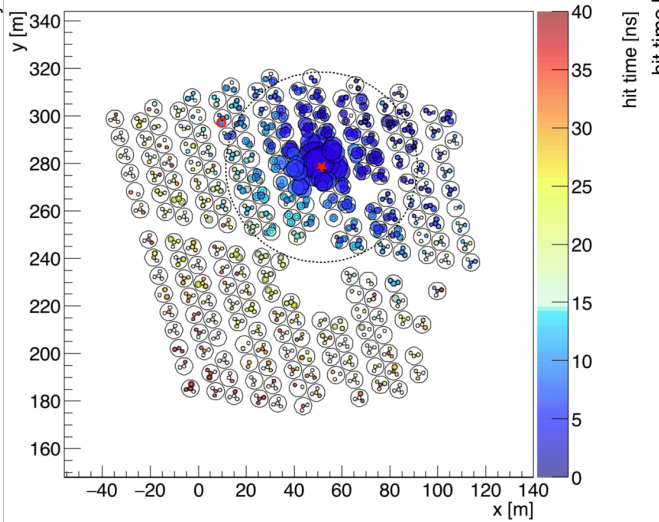
**The higher the accumulated charge within the ring the more likely the event is a hadron.**

# Background Rejection

>99.9% rejection  
for large showers

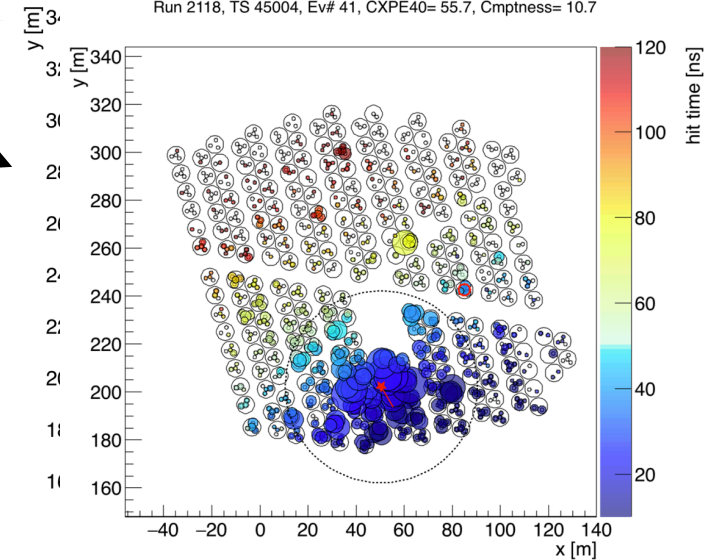
Likely gamma shower

Run 2054, TS 584212, Ev# 226, CXPE40= 21.2, Cmpthness= 28.3

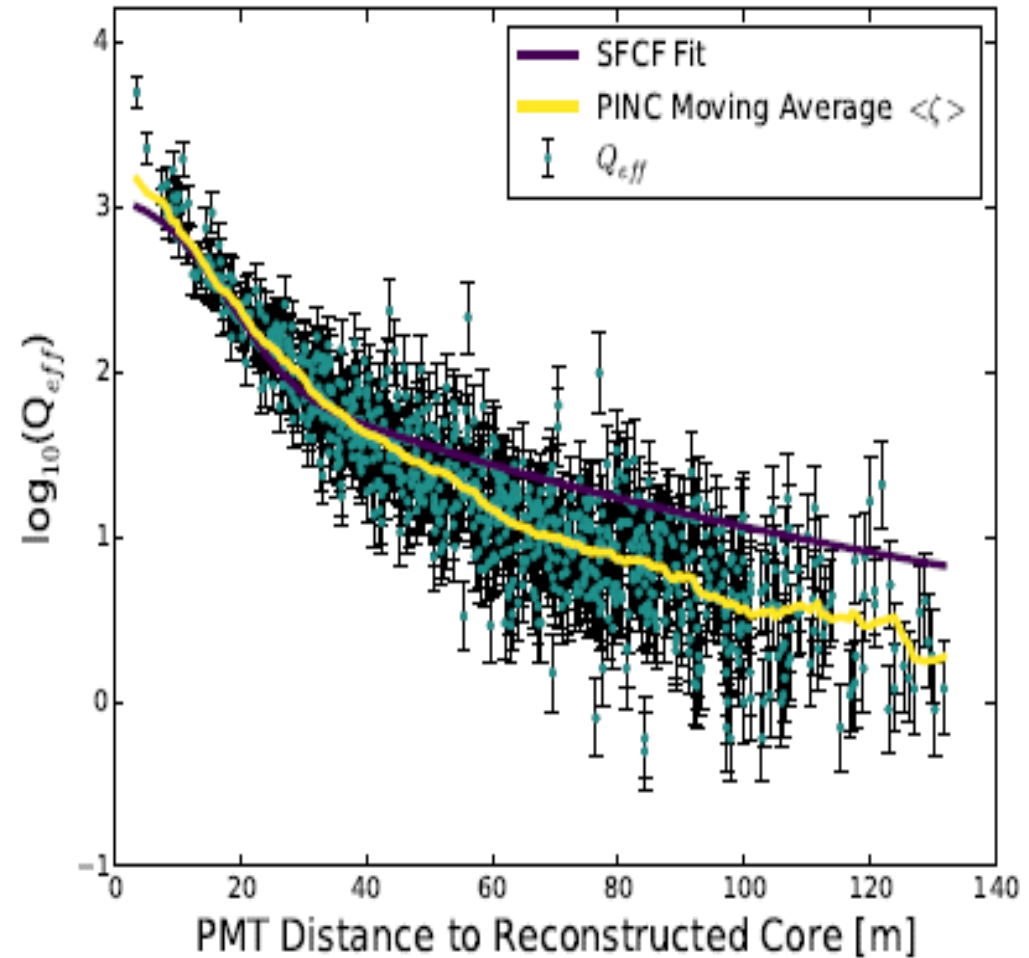
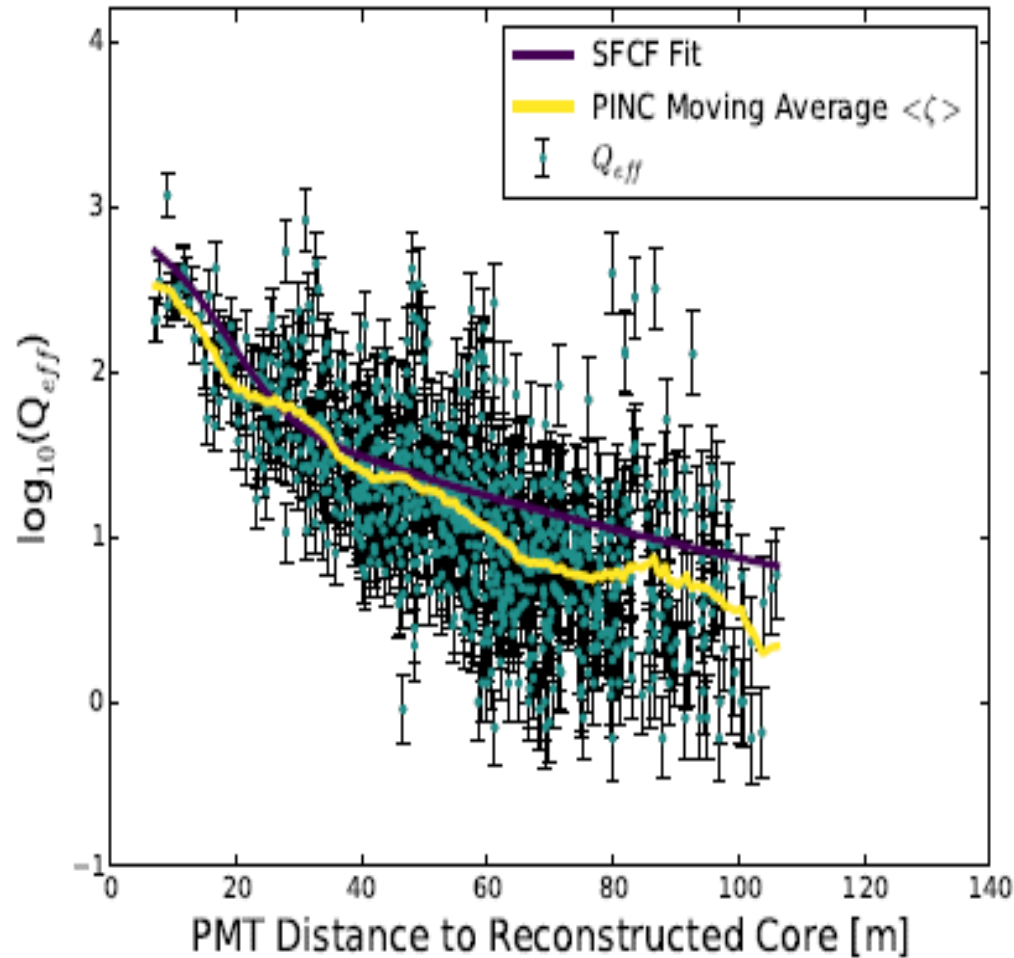


Likely hadron shower

Run 2118, TS 45004, Ev# 41, CXPE40= 55.7, Cmpthness= 10.7

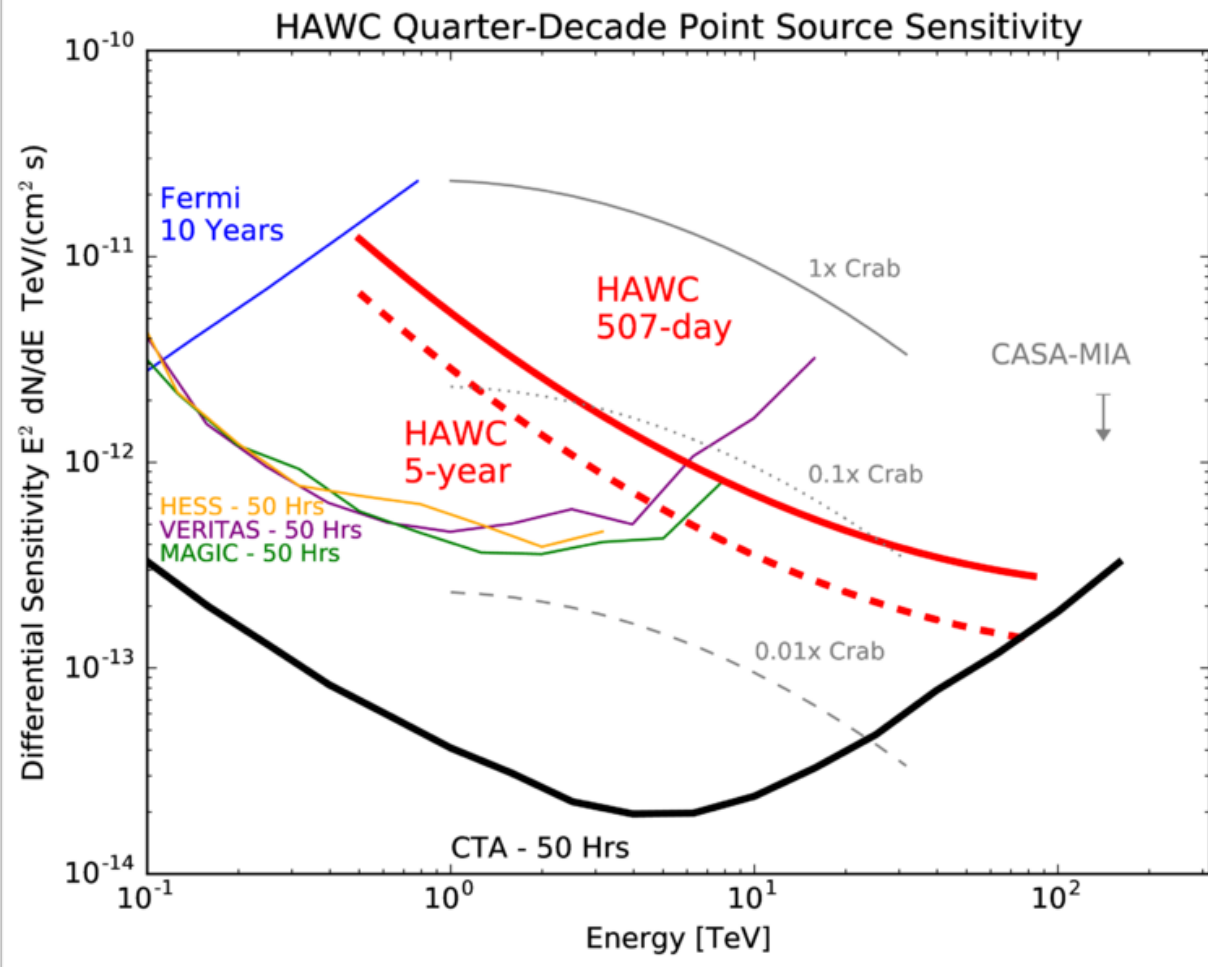


# $\gamma/h$ separation



Lateral distribution functions of an obvious cosmic ray (left) and a photon candidate from the Crab Nebula (right). The cosmic ray has isolated high-charge hits far from the shower core due to penetrating particles in the hadronic air shower. These features are absent in the gamma-ray shower.

# HAWC Sensitivity

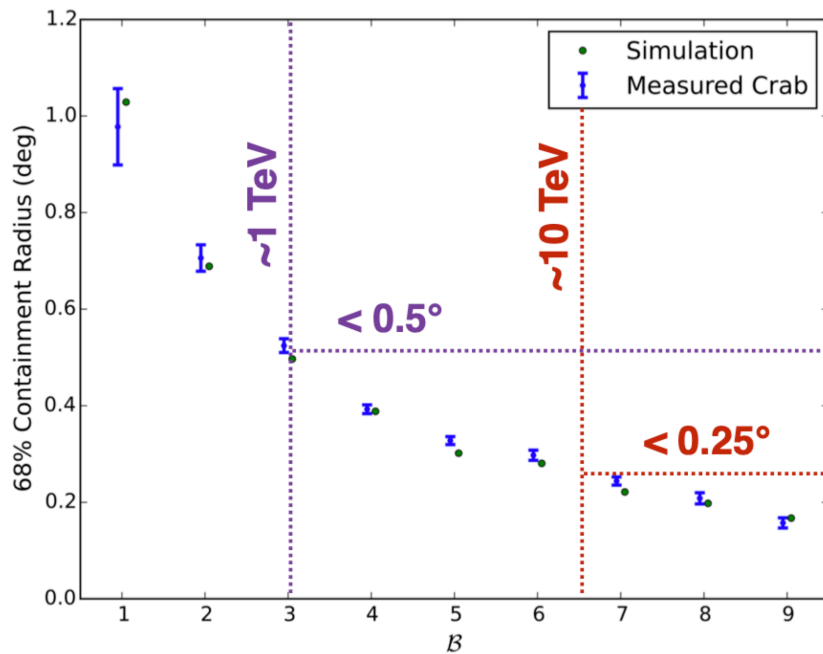


HAWC Collaboration+17

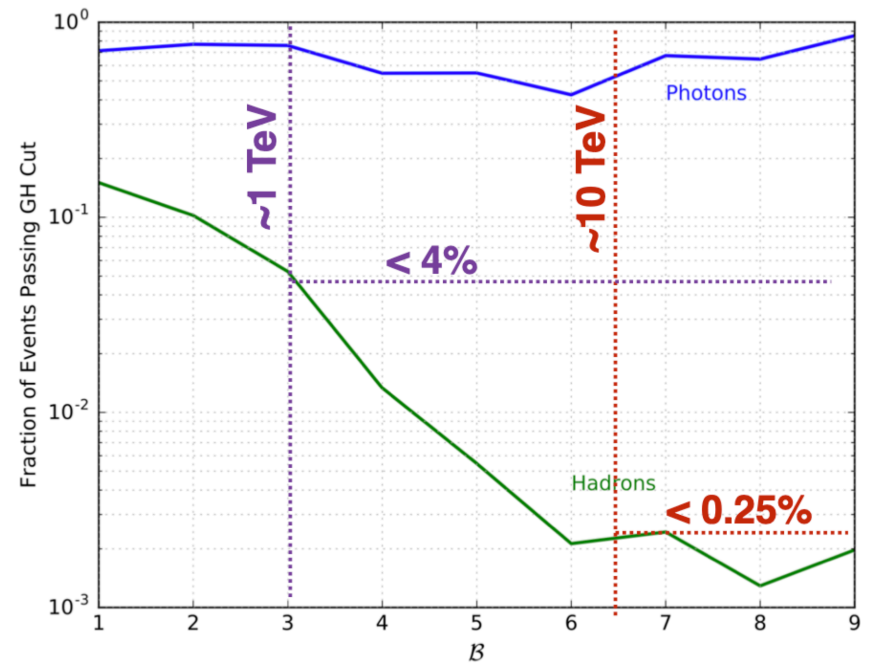
- Instantaneous sensitivity 15-20x less than IACTs.
- Exposure (sr/yr) is 2000-4000x higher than IACTs.
- Above 10 TeV HAWC 1-yr sensitivity is comparable to 50h observation by an IACT.
- Survey  $>$  half the sky to: 40 mCrab [ $5\sigma$ ] (1yr)  $<$  20 mCrab [ $5\sigma$ ] (5yr)

# Summary on reconstruction

Angular resolution



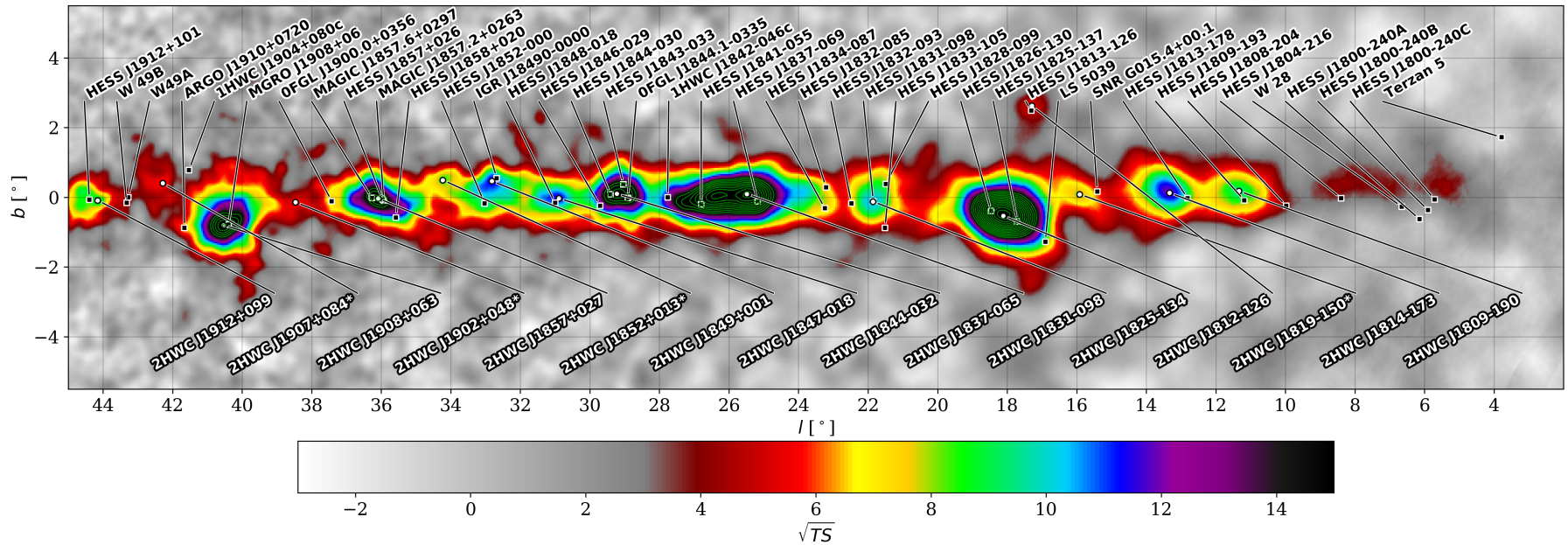
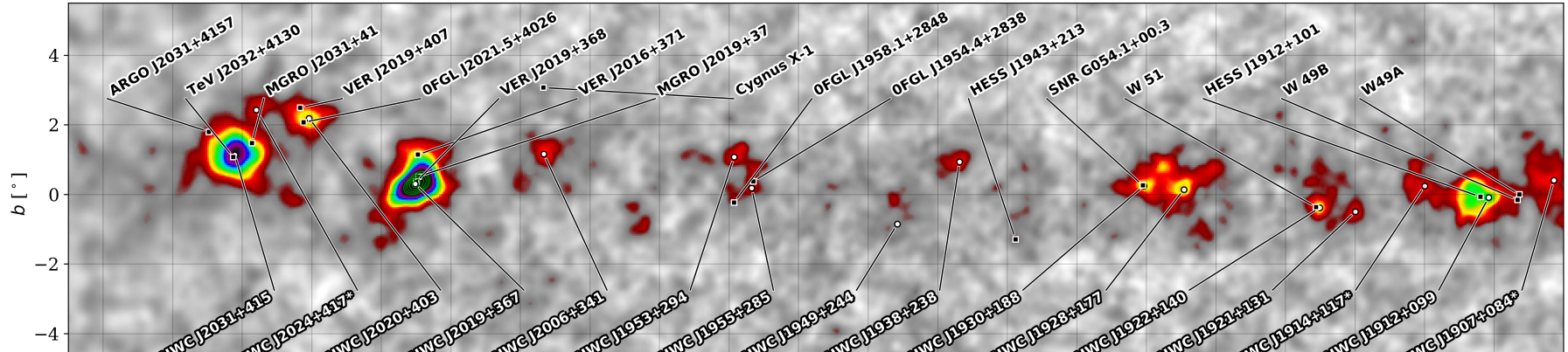
Gamma / Hadron - Cut efficiency



A. U. Abeysekara, *et al*, *ApJ*, **843**, 2017 / arXiv:1701.01778

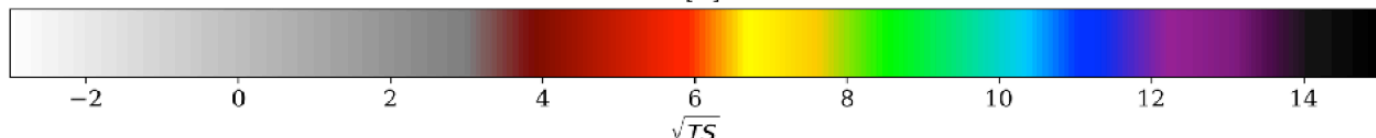
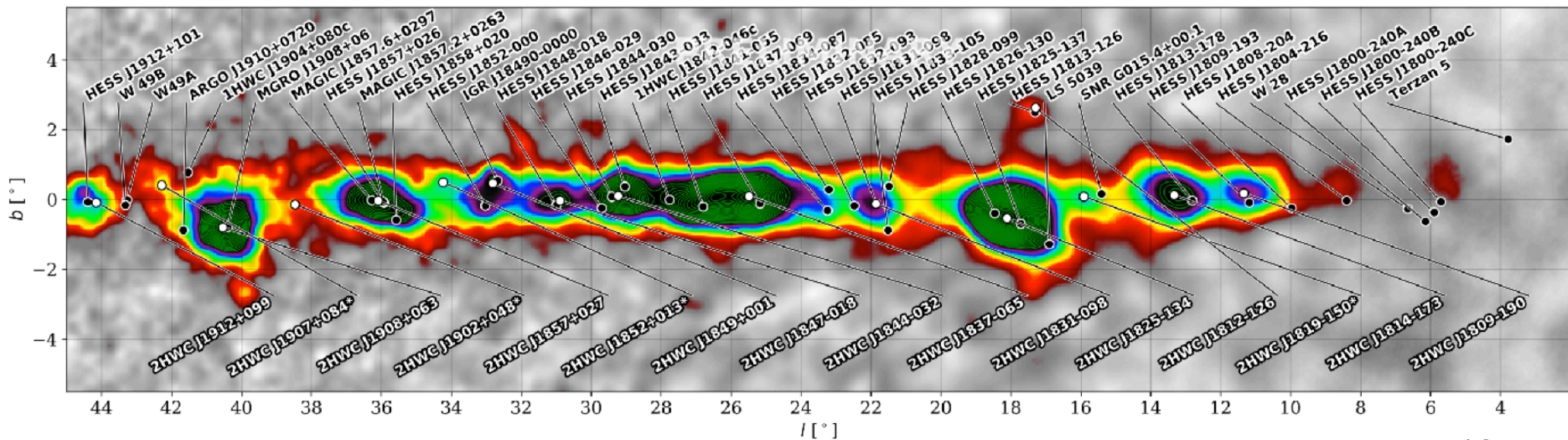
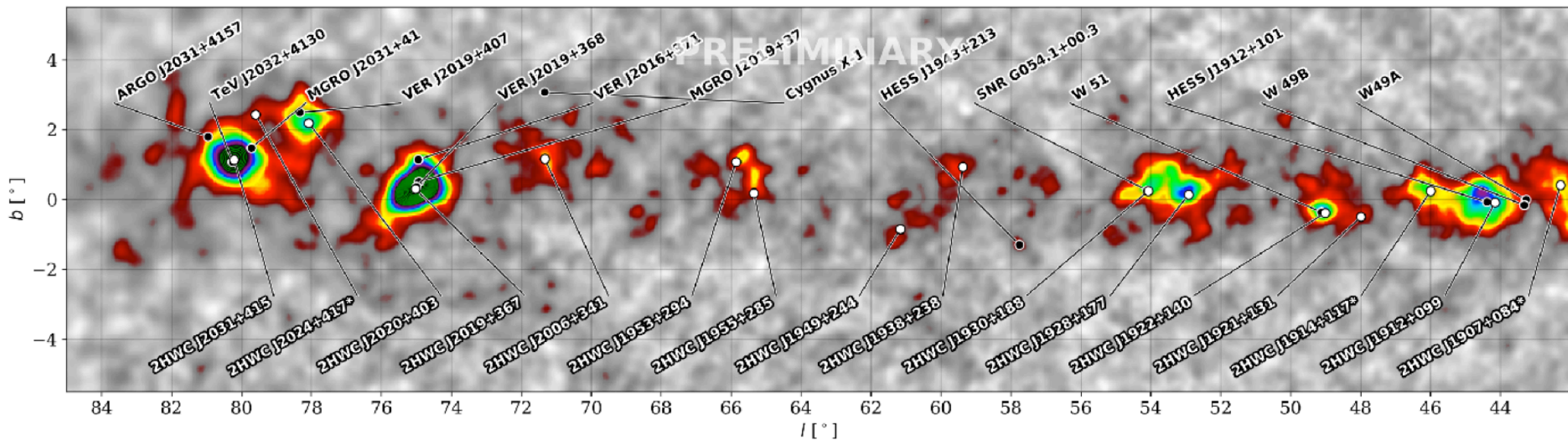


# 2<sup>nd</sup> HAWC Catalog

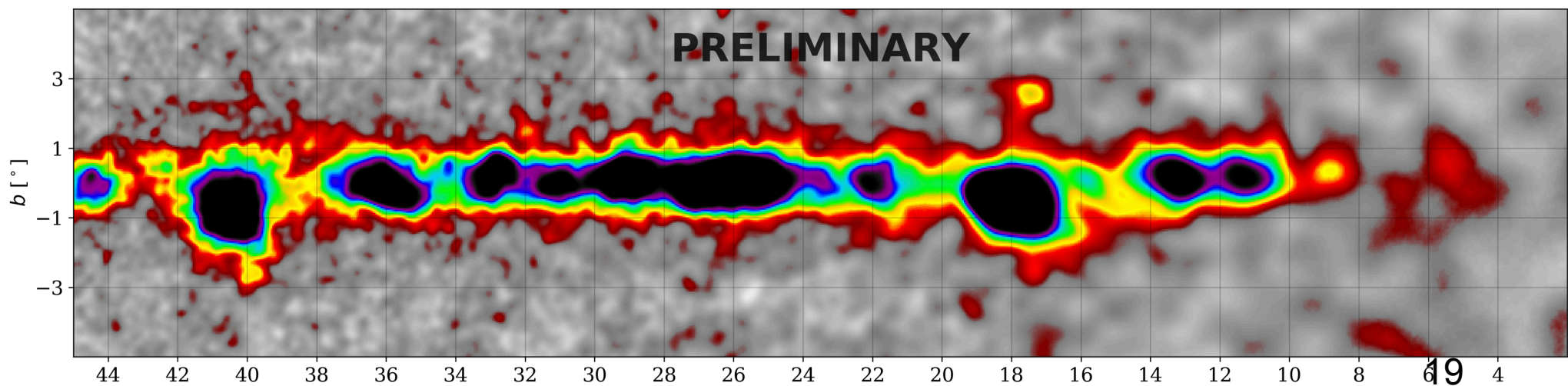
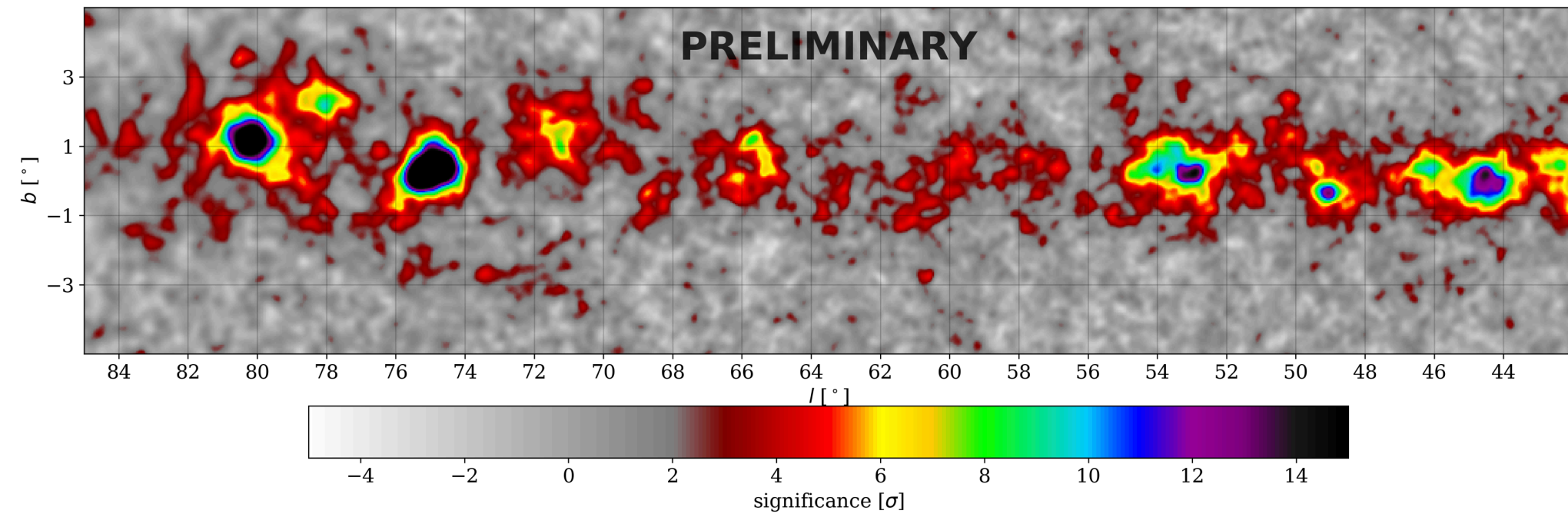


40 sources of which 1/4 are new

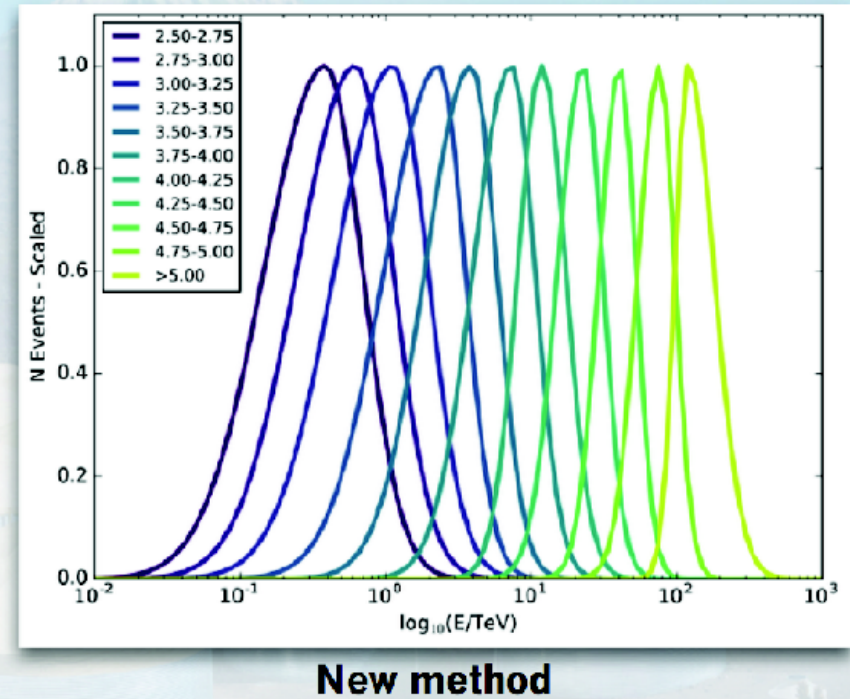
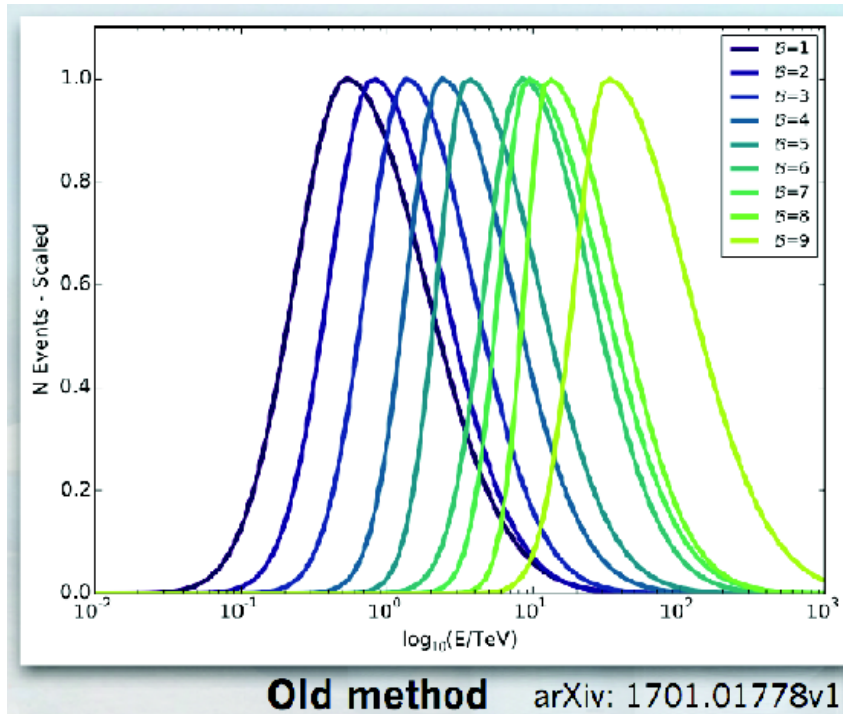
# HAWC 1017d (3 years) map



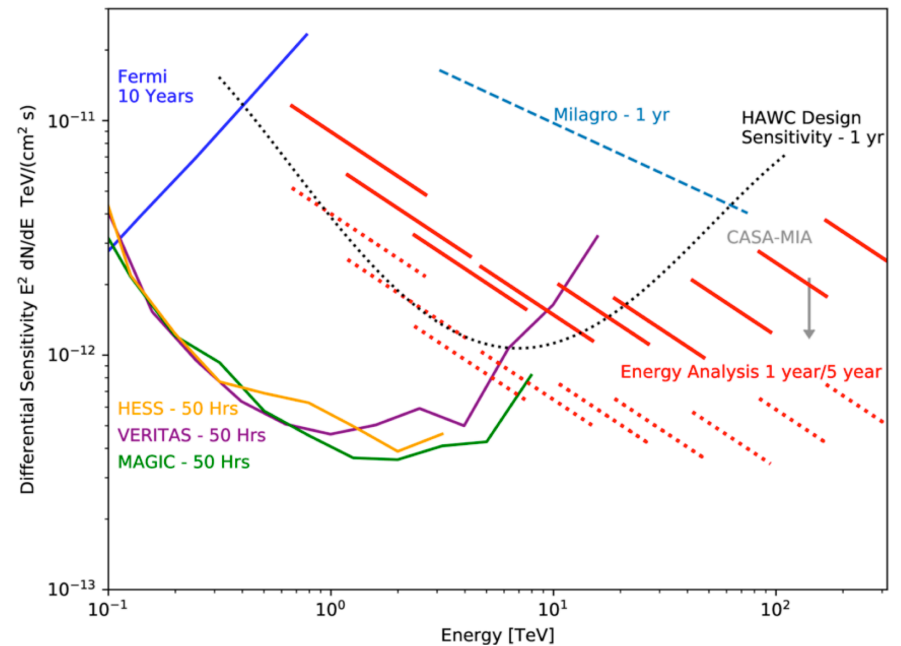
# HAWC maps after 1543 days



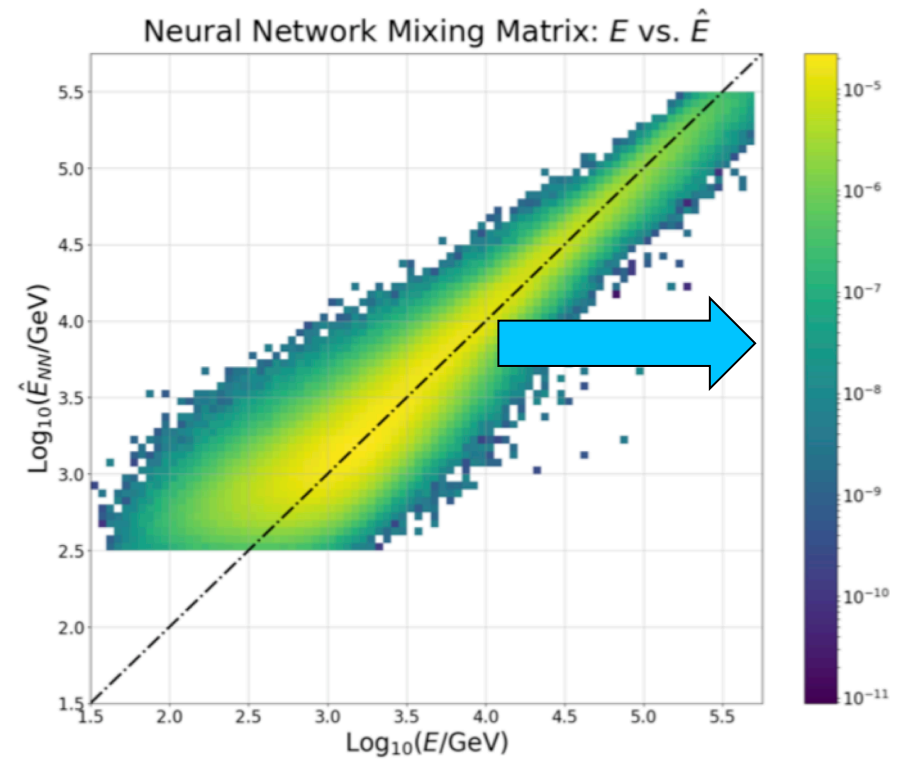
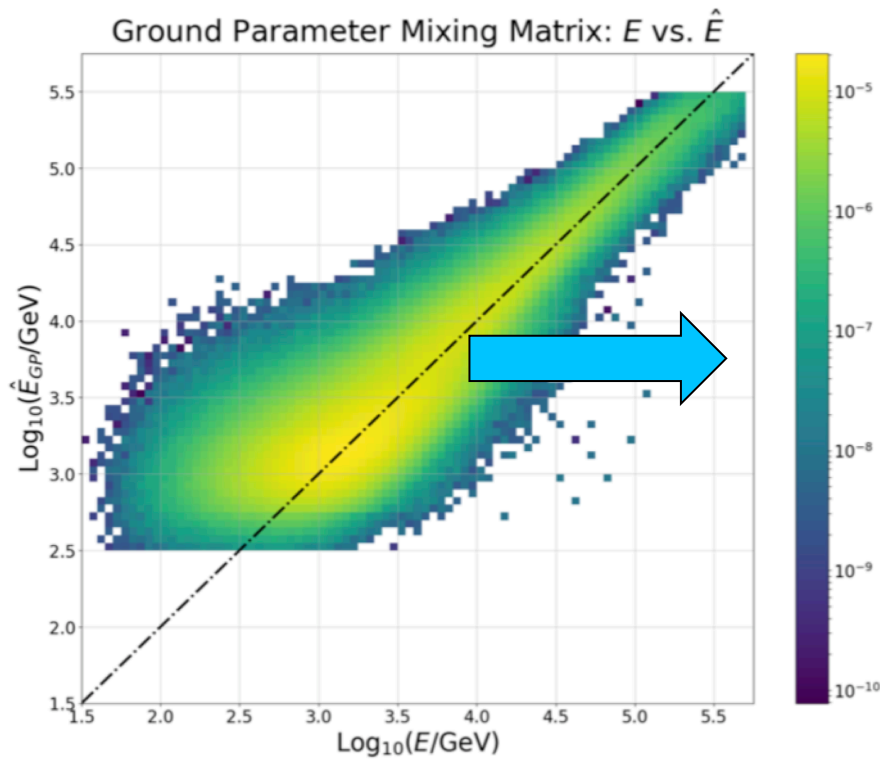
# Event by event Energy Estimator



- Spectral analysis is paramount when understanding the physics of the emission
- Previously the number of PMT seeing lights as energy proxy. No difference between 10 and 50 TeV events
- Event-by-event energy estimation algorithm to distinguish between 10 and 100 TeV photon
- Previously published HAWC papers did not use this algorithm

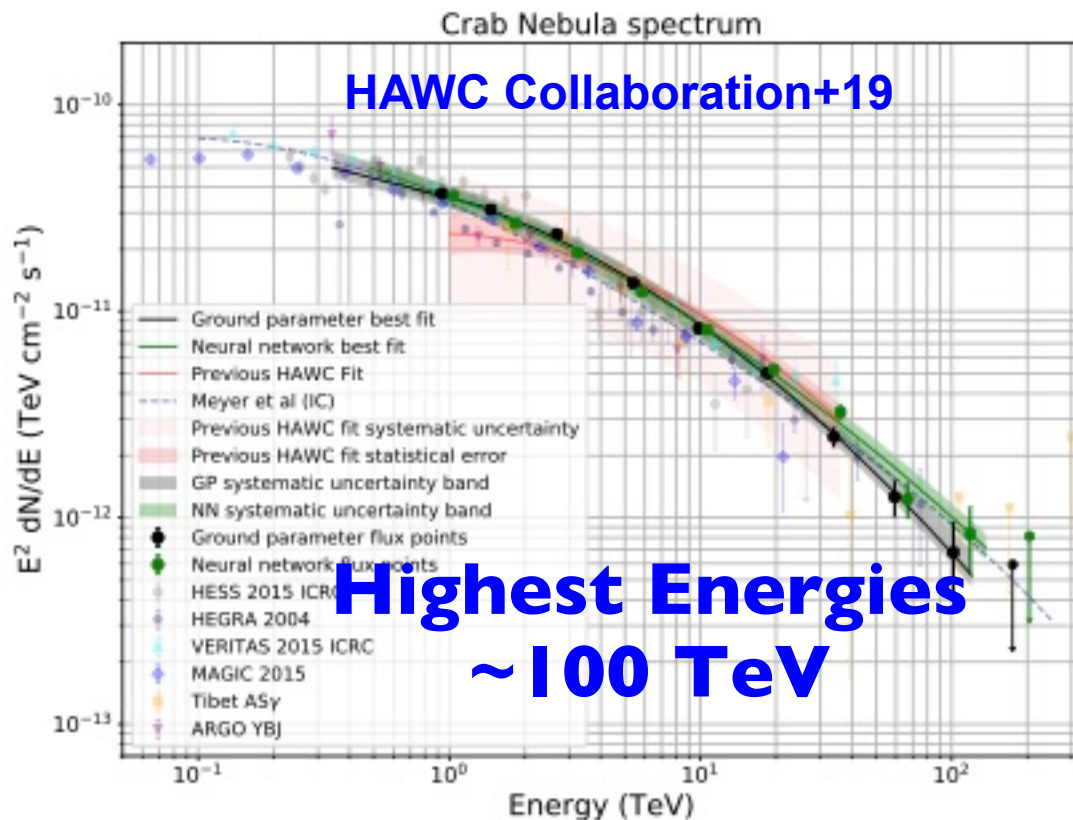


# Breaking degeneracy of highest Energy Events: Energy Estimators



Kelly Malone & Sam Marinelli

# The Crab Spectrum at the highest energies



Two independent energy estimation algorithms (grey and green points/bands above)

837 day dataset

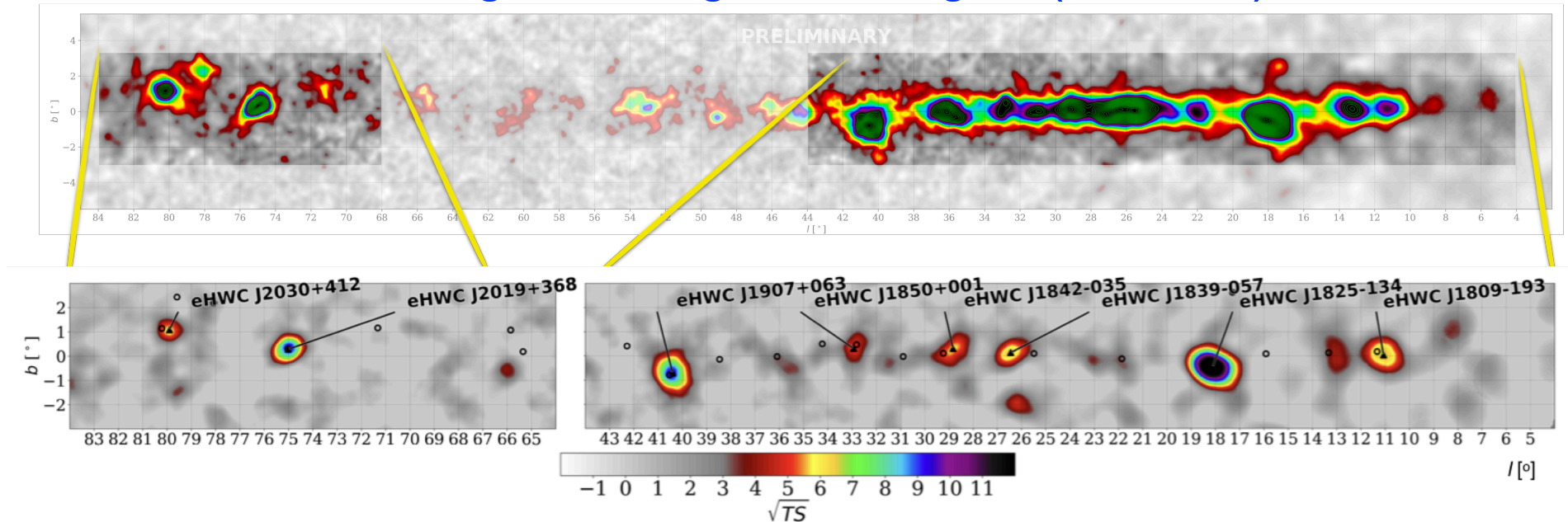
Good agreement at lower energies with previous HAWC paper (ApJ 2007) and IACT measurements

First Crab spectra that goes past 100 TeV in reconstructed energy

The Crab spectrum obtained with the GP method (black) and NN method (green). The error bars on the flux points are statistical only. The shaded grey and green shaded bands denote systematic uncertainties.

# Highest Energy Skymaps (1039 days)

Pushing to the highest energies (>56 TeV)



Acceleration mechanisms: hadronic or leptonic?

Each source has a pulsar within 0.5 deg from the HAWC position

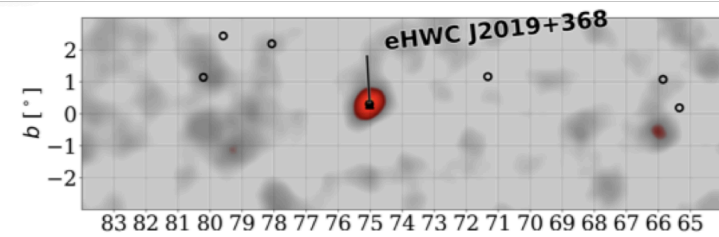
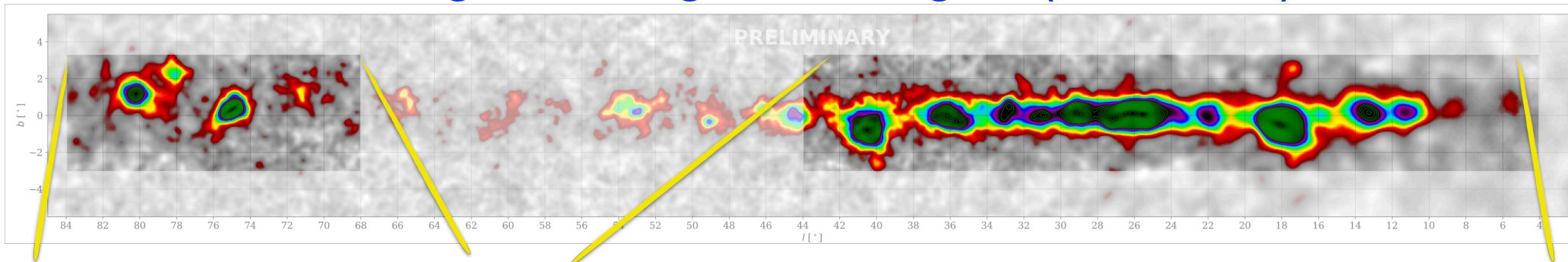
Correlation with neutrinos?

Detailed studies of the sources undergoing

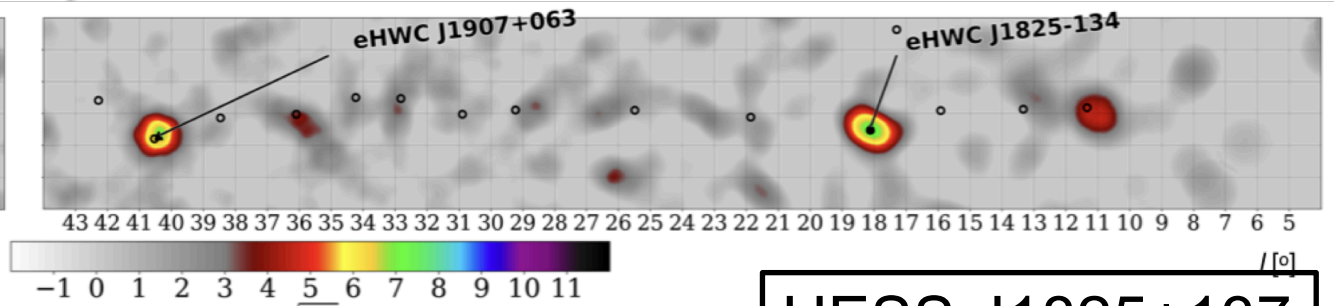
Strongly constraining test of Lorentz invariance (HAWC Coll, 2020)

# Highest Energy Skymaps

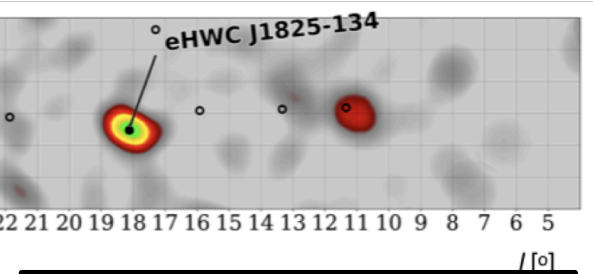
Pushing to the highest energies (>100 TeV)



MGRO 2019+371



MGRO 1908+06



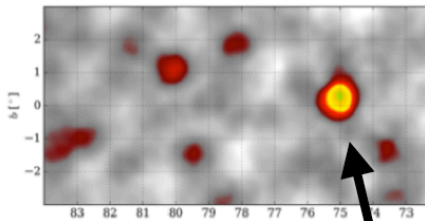
HESS J1825+137  
HESS J1826-130



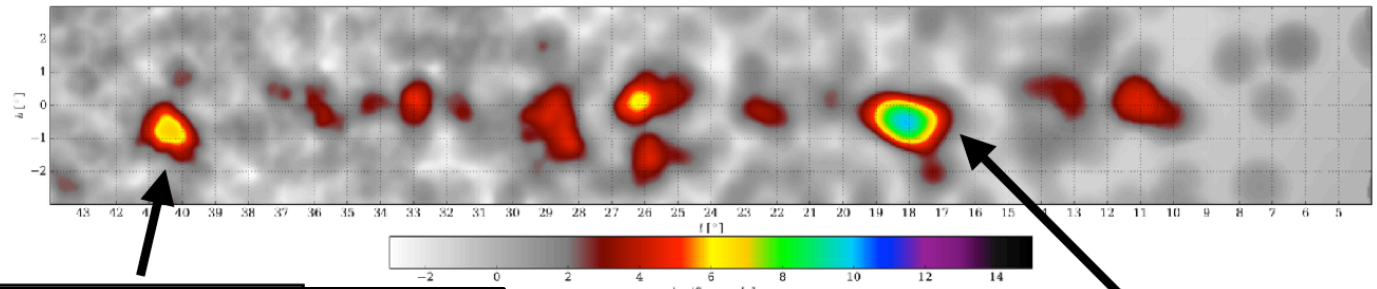
# The Galaxy above 100 TeV

Source name	RA (°)	Dec (°)	Extension > 56 TeV (°)	F ( $10^{-14}$ ph cm $^{-2}$ s $^{-1}$ )	$\sqrt{TS} > 56$ TeV	nearest 2HWC source	Distance to 2HWC source(°)	$\sqrt{TS} > 100$ TeV
eHWC J0534+220	83.61 ± 0.02	22.00 ± 0.03	PS	1.2 ± 0.2	12.0	J0534+220	0.02	4.44
eHWC J1809-193	272.46 ± 0.13	-19.34 ± 0.14	0.34 ± 0.13	2.4 $^{+0.6}_{-0.5}$	6.97	J1809-190	0.30	4.82
eHWC J1825-134	276.40 ± 0.06	-13.37 ± 0.06	0.36 ± 0.05	4.6 ± 0.5	14.5	J1825-134	0.07	7.33
eHWC J1839-057	279.77 ± 0.12	-5.71 ± 0.10	0.34 ± 0.08	1.5 ± 0.3	7.03	J1837-065	0.96	3.06
eHWC J1842-035	280.72 ± 0.15	-3.51 ± 0.11	0.39 ± 0.09	1.5 ± 0.3	6.63	J1844-032	0.44	2.70
eHWC J1850+001	282.59 ± 0.21	0.14 ± 0.12	0.37 ± 0.16	1.1 $^{+0.3}_{-0.2}$	5.31	J1849+001	0.20	3.04
eHWC J1907+063	286.91 ± 0.10	6.32 ± 0.09	0.52 ± 0.09	2.8 ± 0.4	10.4	J1908+063	0.16	7.30
eHWC J2019+368	304.95 ± 0.07	36.78 ± 0.04	0.20 ± 0.05	1.6 $^{+0.3}_{-0.2}$	10.2	J2019+367	0.02	4.85
eHWC J2030+412	307.74 ± 0.09	41.23 ± 0.07	0.18 ± 0.06	0.9 ± 0.2	6.43	J2031+415	0.34	3.07

Galactic Plane, > 56 TeV (0.5 degree extended source assumed)



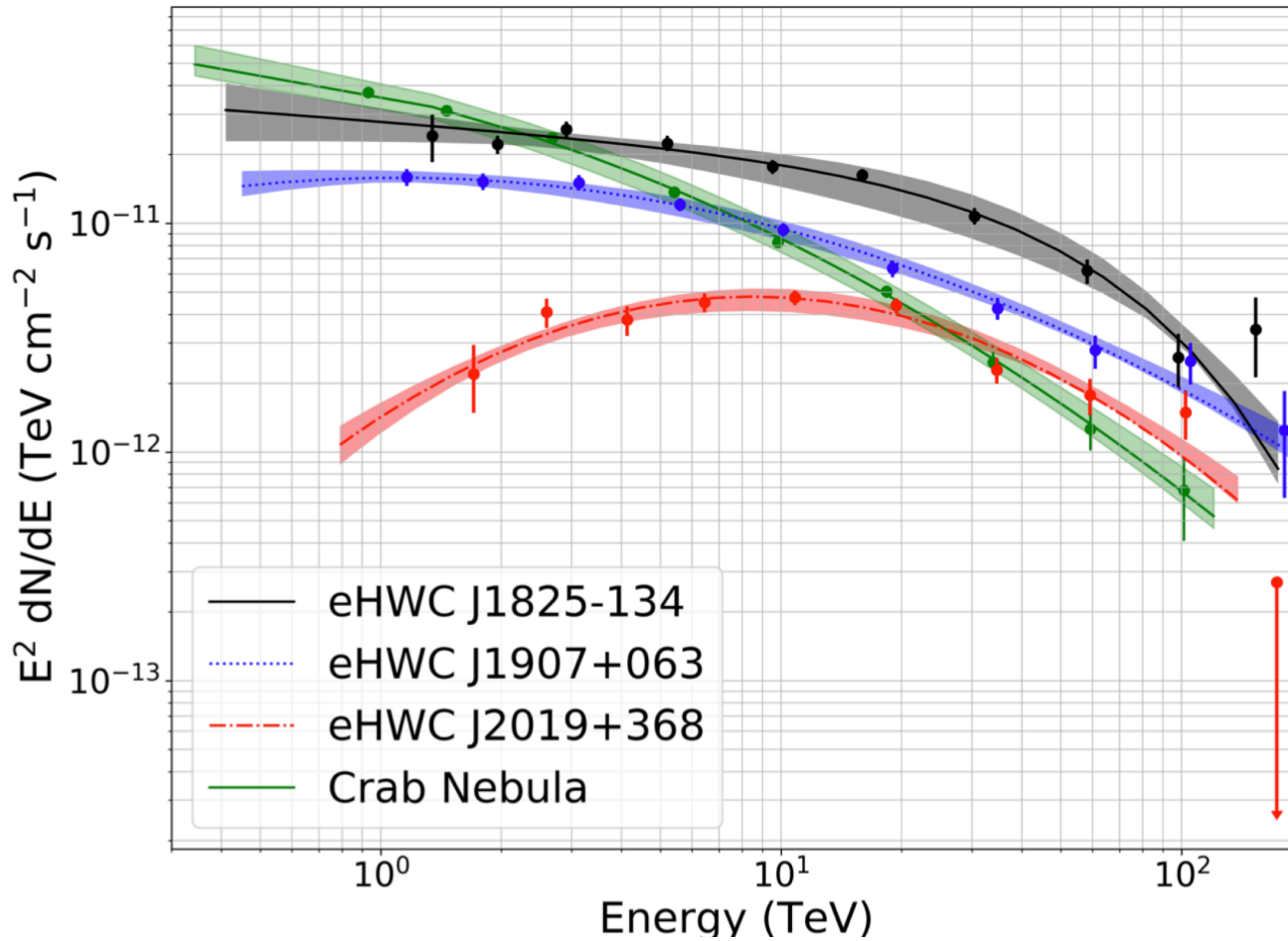
MGRO 2019+371



MGRO 1908+06

HESS J1825+137  
HESS J1826-130

# The Galaxy above 100 TeV: Spectra



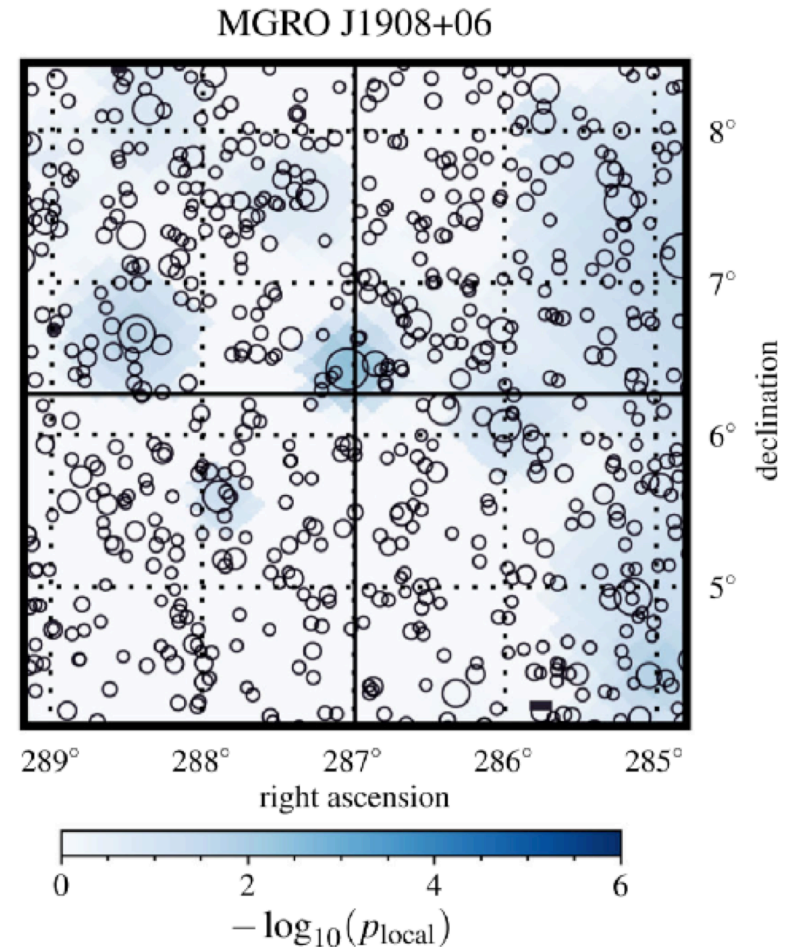
Source	$\sqrt{TS}$	Extension ( $^\circ$ )	$\phi_0$ ( $10^{-13}$ TeV cm $^2$ s $^{-1}$ )	$\alpha$	$E_{cut}$ (TeV)	PL diff
eHWC J1825-134	41.1	$0.53 \pm 0.02$	$2.12 \pm 0.15$	$2.12 \pm 0.06$	$61 \pm 12$	7.4
Source	$\sqrt{TS}$	Extension ( $^\circ$ )	$\phi_0$ ( $10^{-13}$ TeV cm $^2$ s $^{-1}$ )	$\alpha$	$\beta$	PL diff
eHWC J1907+063	37.8	$0.67 \pm 0.03$	$0.95 \pm 0.05$	$2.46 \pm 0.03$	$0.11 \pm 0.02$	6.0
eHWC J2019+368	32.2	$0.30 \pm 0.02$	$0.45 \pm 0.03$	$2.08 \pm 0.06$	$0.26 \pm 0.05$	8.2

# HAWC HE source as neutrino sources

Some HAWC PeV candidates are promising neutrino sources

Neutrinos seen in coincidence with a PeVatron candidate would unambiguously indicate hadronic origin

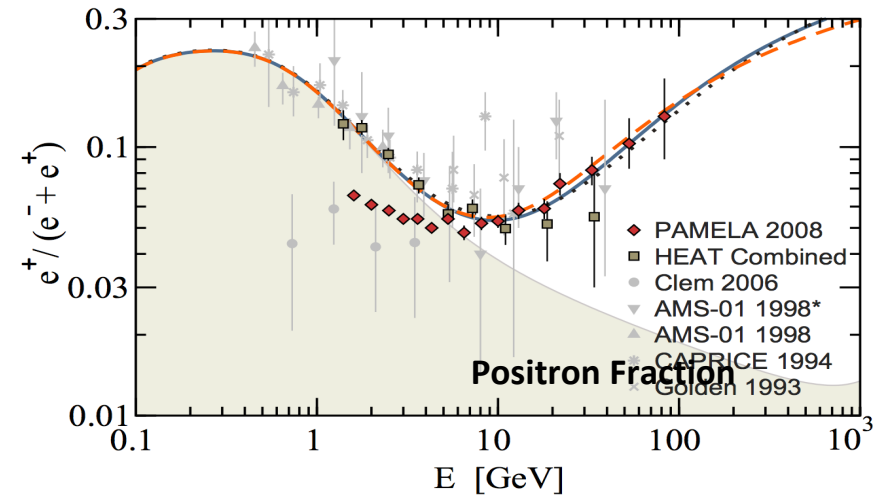
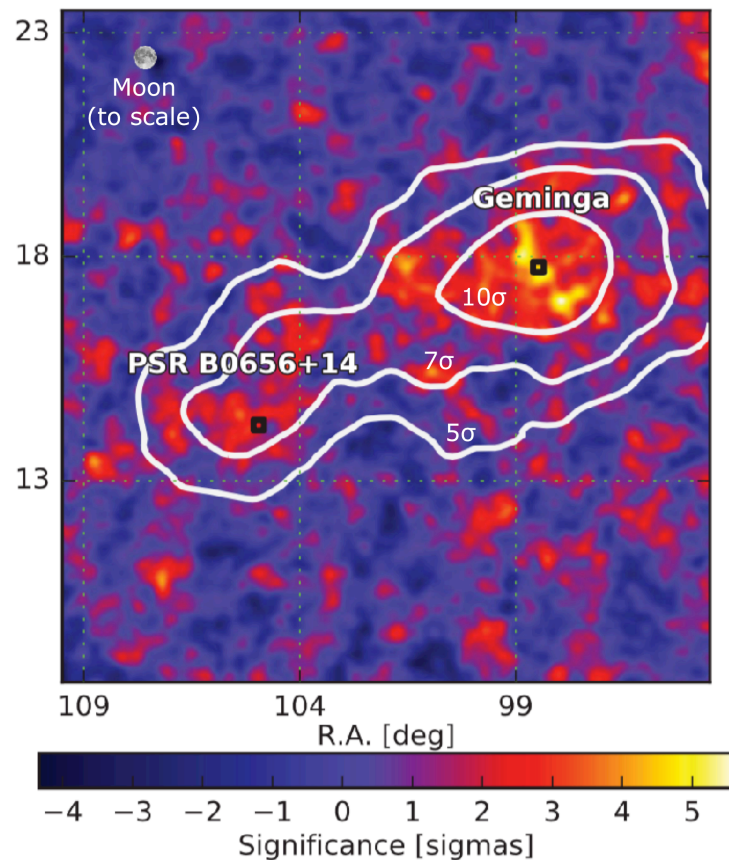
J1908+06 one of best p-values in IceCube point source searches, although still consistent with background-only hypothesis



IceCube,  
European Physics  
Journal (2019)

# Geminga-Monogem

28

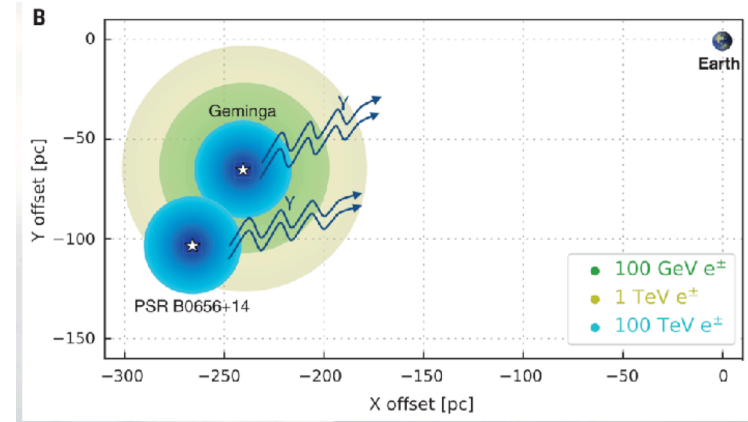
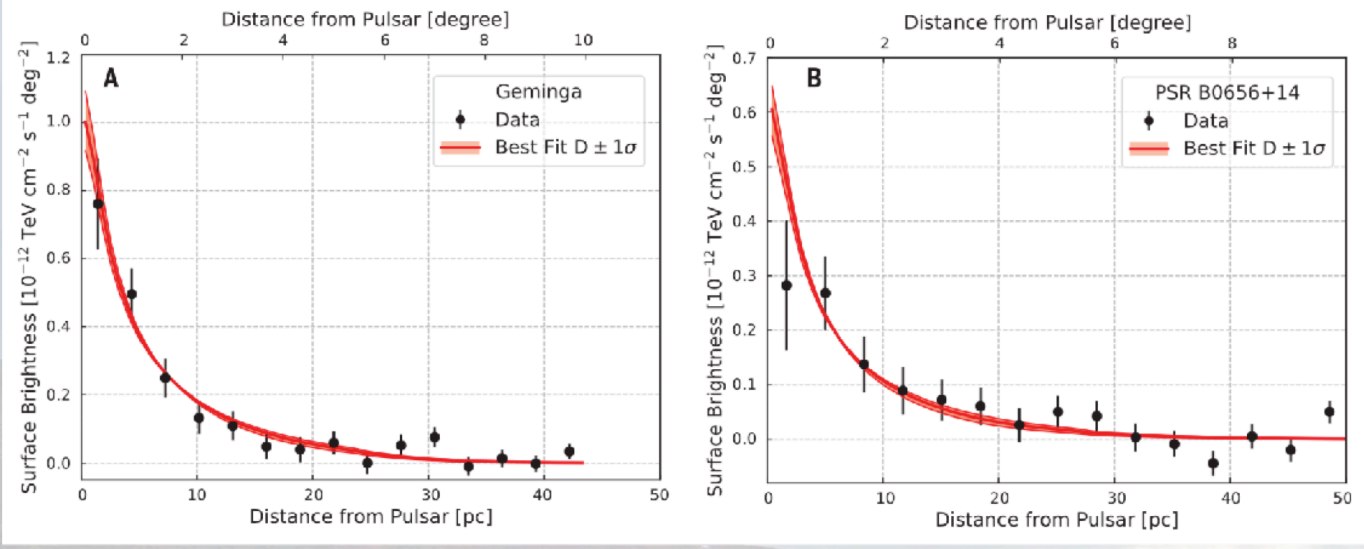


**Aharonian+1995, Yuksel+2009**

- First detection of 2 deg extended emission around Geminga by Milagro in 2009
- Confirmation ( $\sim 13.1\sigma$ ) of Geminga (PSR J0633+1746) by HAWC.
- Discovery ( $\sim 81\sigma$ ) of a new extended source near PSR B0656+14.
- Both pulsars, similar in age and distance, were suggested as contributors of the positron fraction (Aharonian+1995, Yuksel+2009).

# Geminga-Monogem PWNe

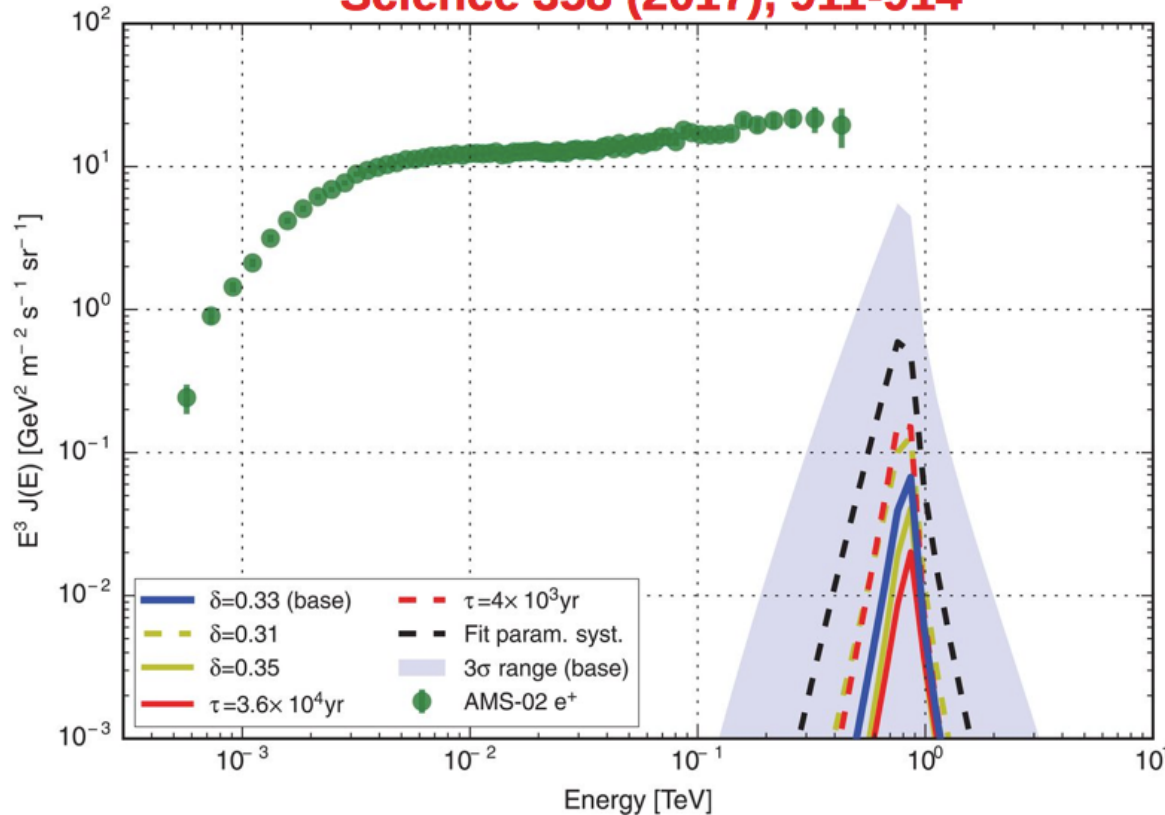
## HAWC, Science 2017



- Geminga and Monogem : about 5 deg ext
- Assuming emission from electrons diffusing in the ISM, then extension is a direct measurement of particle diffusion  $\theta(20\text{TeV}) \propto \sqrt{[D(100\text{TeV})]}$
- $D(100 \text{ TeV}) = (4.5 \pm 1.2) 10^{27} \text{ cm}^2/\text{s}$ , roughly 100 times smaller than diffusion from B/C ratio

# The positron flux at Earth

Science 358 (2017), 911-914



RESEARCH

PARTICLE ASTROPHYSICS

## Extended gamma-ray sources around pulsars constrain the origin of the positron flux at Earth

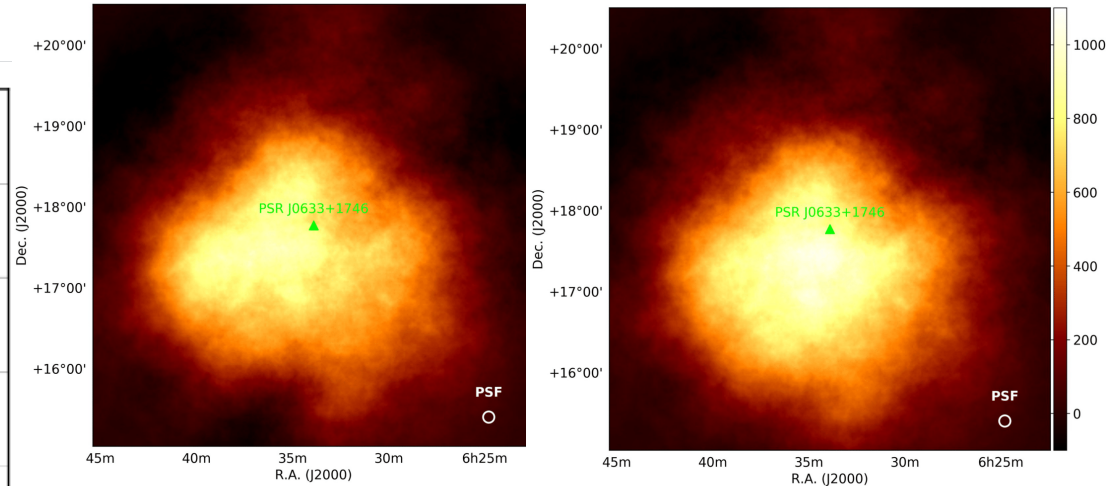
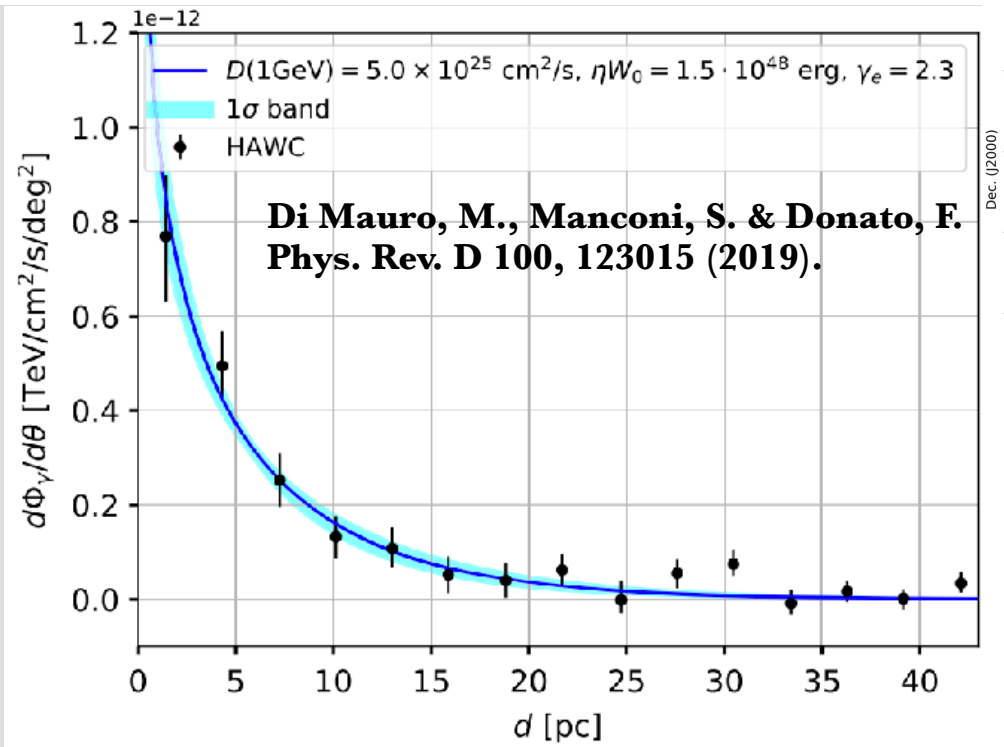
A. U. Abeysekara,<sup>1</sup> A. Albert,<sup>2</sup> R. Alfaro,<sup>3</sup> C. Alvarez,<sup>4</sup> J. D. Álvarez,<sup>5</sup> R. Arceo,<sup>4</sup> J. C. Arteaga-Velázquez,<sup>2</sup> D. Avila Rojas,<sup>2</sup> H. A. Ayala Solares,<sup>6</sup> A. S. Barber,<sup>1</sup> N. Bautista-Elivar,<sup>7</sup> A. Becerril,<sup>8</sup> E. Belmont-Moreno,<sup>9</sup> S. Y. BenZvi,<sup>10</sup> D. Berley,<sup>9</sup> A. Bernal,<sup>10</sup> J. Braun,<sup>11</sup> C. Brisbois,<sup>6</sup> K. S. Caballero-Mora,<sup>4</sup> T. Capistrán,<sup>12</sup> A. Carramiñana,<sup>12</sup> S. Casanova,<sup>13,14</sup> M. Castillo,<sup>5</sup> U. Cotti,<sup>5</sup> J. Cotzomi,<sup>15</sup> S. Coutiño de León,<sup>13</sup> C. De León,<sup>15</sup> E. De la Fuente,<sup>16</sup> B. L. Dingus,<sup>2</sup> M. A. DuVernois,<sup>17</sup> J. C. Díaz-Vélez,<sup>16</sup> R. W. Ellsworth,<sup>17</sup> K. Engel,<sup>9</sup> O. Enríquez-Rivera,<sup>18</sup> D. W. Florino,<sup>9</sup> N. Fraija,<sup>10</sup> J. A. García-González,<sup>3</sup> F. Garfías,<sup>10</sup> M. Gerhardt,<sup>6</sup> A. González Muñoz,<sup>3</sup> M. M. González,<sup>10</sup> J. A. Goodman,<sup>9</sup> Z. Hampel-Arias,<sup>11</sup> J. P. Harding,<sup>2</sup> S. Hernández,<sup>3</sup> A. Hernández-Almada,<sup>3</sup> J. Hinton,<sup>14</sup> B. Hona,<sup>6</sup> C. M. Hui,<sup>10</sup> P. Hüntemeyer,<sup>6</sup> A. Iriarte,<sup>10</sup> A. Jardín-Bliq,<sup>14</sup> V. Joshi,<sup>14</sup> S. Kaufmann,<sup>4</sup> D. Kieda,<sup>1</sup> A. Lara,<sup>18</sup> R. J. Lamer,<sup>20</sup> W. H. Lee,<sup>10</sup> D. Lennarz,<sup>21</sup> H. León Vargas,<sup>3</sup> J. T. Linnemann,<sup>22</sup> A. L. Longinotti,<sup>12</sup> G. Luis Raya,<sup>7</sup> R. Luna-García,<sup>23</sup> R. López-Coto,<sup>14</sup> K. Malone,<sup>24</sup> S. S. Marinelli,<sup>25</sup> O. Martínez,<sup>15</sup> I. Martínez Castellanos,<sup>9</sup> J. Martínez-Castro,<sup>25</sup> H. Martínez-Huerta,<sup>25</sup> J. A. Matthews,<sup>20</sup> P. Miranda-Romagnoli,<sup>26</sup> E. Moreno,<sup>15</sup> M. Mostafá,<sup>24</sup> L. Nellen,<sup>27</sup> M. Newbold,<sup>1</sup> M. U. Nisa,<sup>8</sup> R. Noriega-Papaqui,<sup>26</sup> R. Pelayo,<sup>23</sup> J. Pretz,<sup>24</sup> E. G. Pérez-Pérez,<sup>7</sup> Z. Ren,<sup>20</sup> C. D. Rho,<sup>8</sup> C. Rivière,<sup>9</sup> D. Rosa-González,<sup>12</sup> M. Rosenberg,<sup>24</sup> E. Ruiz-Velasco,<sup>3</sup> H. Salazar,<sup>15</sup> F. Salesa Greus,<sup>15</sup> A. Sandoval,<sup>9</sup> M. Schneider,<sup>28</sup> H. Schorlemmer,<sup>14</sup> G. Sinnis,<sup>2</sup> A. J. Smith,<sup>9</sup> R. W. Springer,<sup>1</sup> P. Surabali,<sup>14</sup> I. Taboada,<sup>22</sup> O. Tibolla,<sup>4</sup> K. Tollefson,<sup>22</sup> I. Torres,<sup>12</sup> T. N. Ukwatta,<sup>2</sup> G. Vianello,<sup>29</sup> T. Weisgarber,<sup>11</sup> S. Westerhoff,<sup>11</sup> I. G. Wisher,<sup>11</sup> J. Wood,<sup>11</sup> T. Yapici,<sup>22</sup> G. Yodh,<sup>30</sup> P. W. Young,<sup>3</sup> A. Zepeda,<sup>25,4</sup> H. Zhou,<sup>24</sup> F. Guo,<sup>2</sup> J. Hahn,<sup>14</sup> H. Li,<sup>2</sup> H. Zhang,<sup>2</sup>

The unexpectedly high flux of cosmic-ray positrons detected at Earth may originate from nearby astrophysical sources, dark matter, or unknown processes of cosmic-ray secondary production. We report the detection, using the High-Altitude Water Cherenkov Observatory (HAWC), of extended tera-electron volt gamma-ray emission coincident with the locations of two nearby middle-aged pulsars (Geminga and PSR B0656+14). The HAWC observations demonstrate that these pulsars are indeed local sources of accelerated leptons, but the measured tera-electron volt emission profile constrains the diffusion of particles away from these sources to be much slower than previously assumed. We demonstrate that the leptons emitted by these objects are therefore unlikely to be the origin of the excess positrons, which may have a more exotic origin.

- From the gamma-ray flux and diffuse information (radial profile) we can estimate the flux of electrons/positrons expected at the Earth.
- Under the assumption of isotropic and homogeneous diffusion, these sources are **unlikely to be the main contributors to the positron excess.**

# Geminga at GeV and TeV

<https://www.mpi-hd.mpg.de/hfm/HESS/pages/home/som/2020/04/>



Diffusion Coefficient from Fermi data is consistent with HAWC Observation

Joint Fermi HAWC Spectrum constrains acceleration efficiency

HESS detected Geminga too

# TeV halos in the outer Galaxy

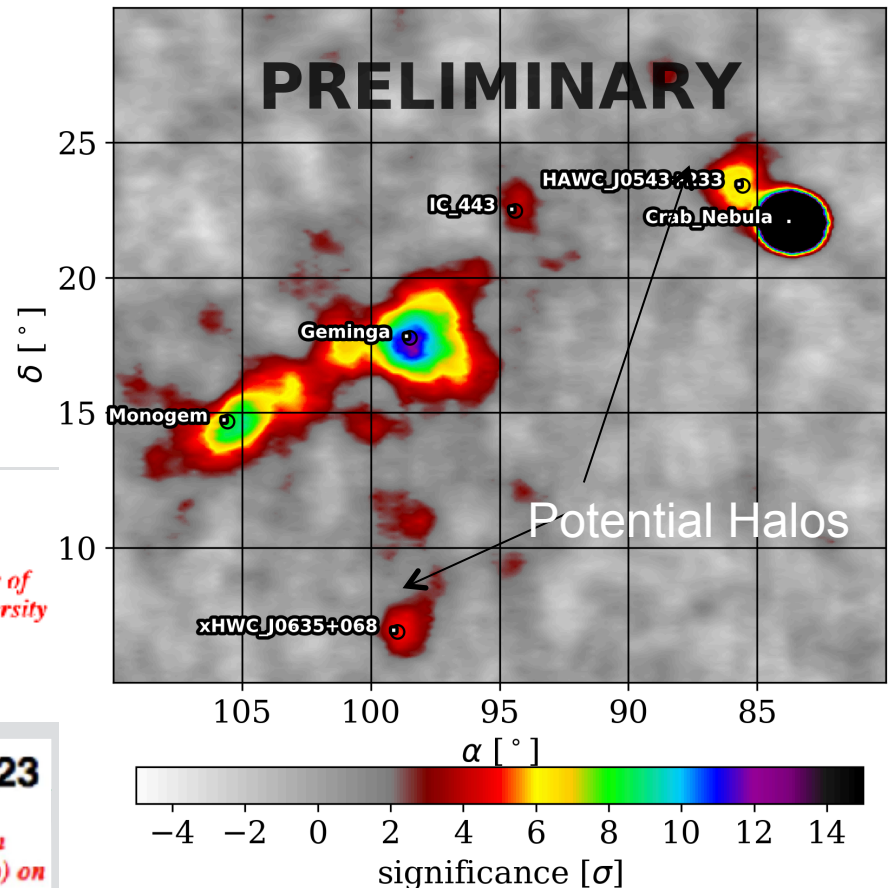
- Highly extended electron clouds, much larger than PWNe
- Hard spectrum sources surrounding PWN
- In the outer galaxy where there is little source confusion :Geminga and PSR B0656+14 and two more potential halos

## HAWC detection of TeV source HAWC J0635+070

ATel #12013; *Chad Brisbois (Michigan Technological University), Colas Riviere (University of Maryland), Henrike Fleischhack (Michigan Technological University), Andrew Smith (University of Maryland) on behalf of the HAWC collaboration*  
 on 6 Sep 2018; 14:47 UT  
 Credential Certification: Colas Riviere (riviere@umd.edu)

## HAWC detection of TeV emission near PSR B0540+23

ATel #10941; *Colas Riviere (University of Maryland), Henrike Fleischhack (Michigan Technological University), Andres Sandoval (Universidad Nacional Autonoma de Mexico) on behalf of the HAWC collaboration*  
 on 9 Nov 2017; 23:11 UT  
 Credential Certification: Colas Riviere (riviere@umd.edu)



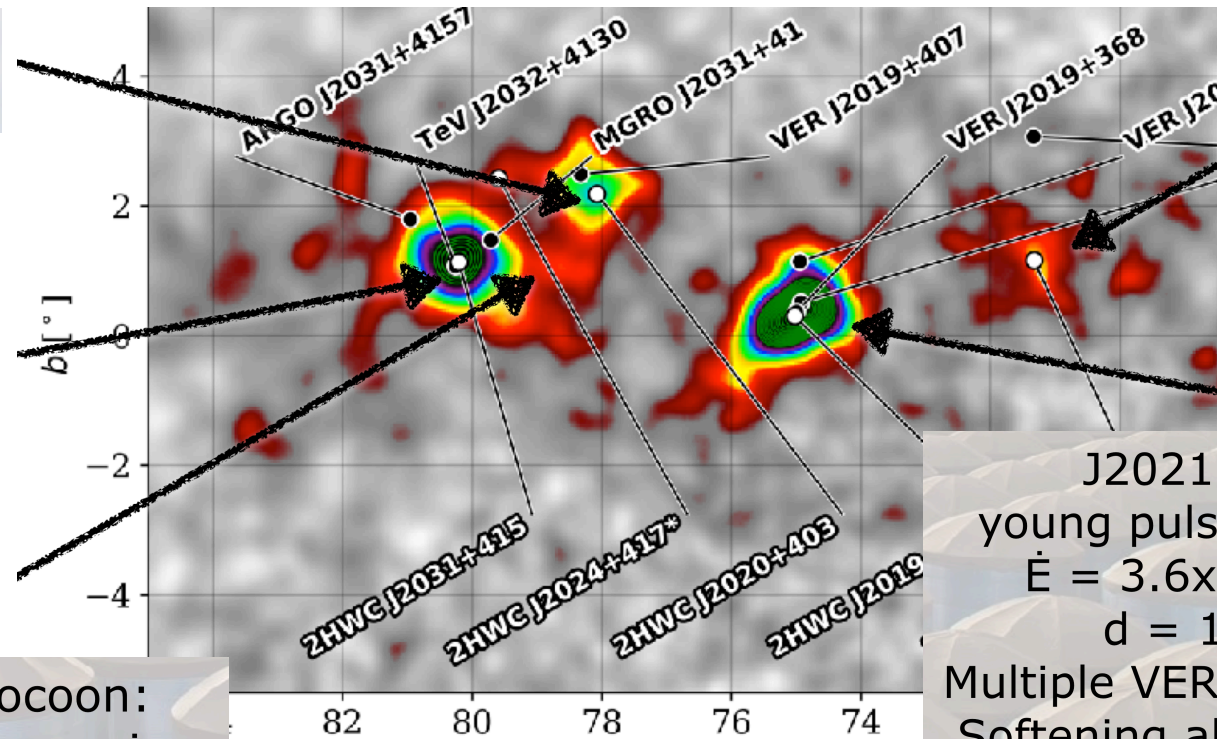


# The Cygnus Region

G78.2+2.1 ( $\gamma$  Cygni SNR)  
Middle aged:  $\sim 6000$  yr

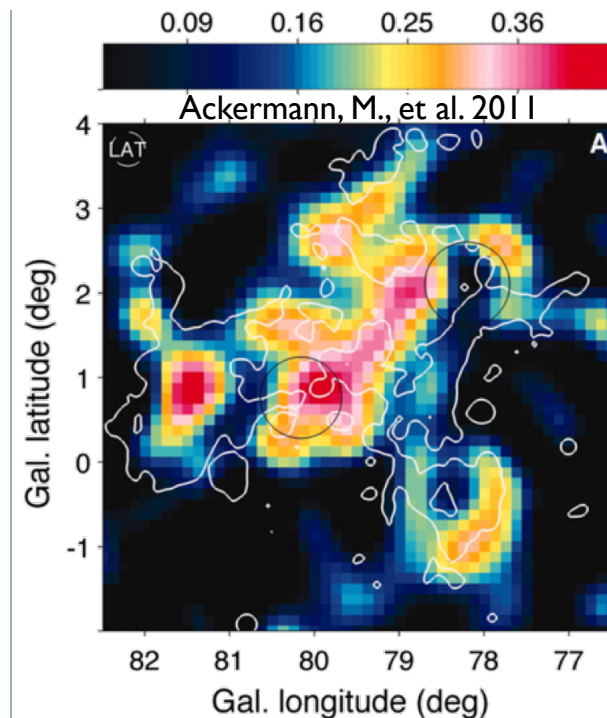
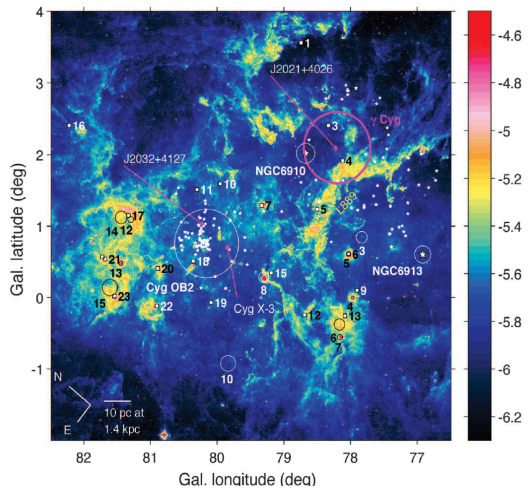
TeV J2031+4130:

Fermi's Cygnus Cocoon:  
Active star formation region

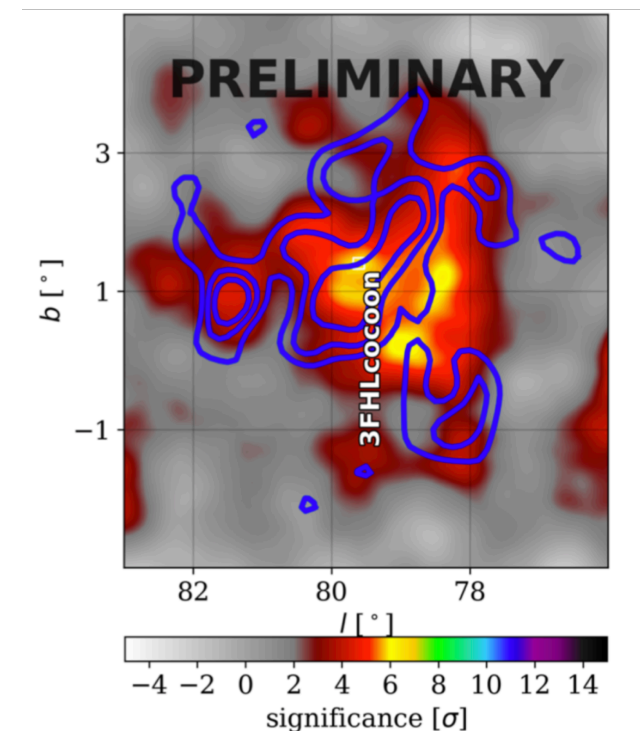


J2021+3651:  
young pulsar: 17.2 kyr  
 $\dot{E} = 3.6 \times 10^{36}$  erg/s  
 $d = 1.8$  kpc  
Multiple VERITAS sources.  
Softening above 30 TeV?

# SFR as CR sources: Fermi-HAWC cocoon



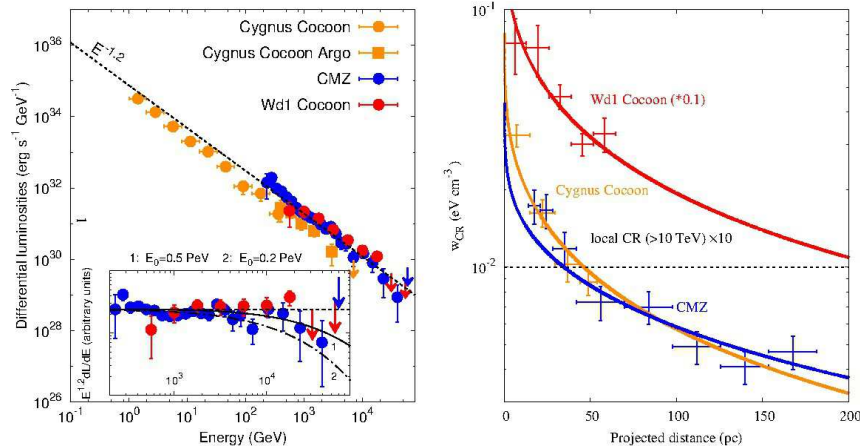
- Star forming region as GCR accelerator ?
- What is the maximum acceleration energy ?
- Cygnus Cocoon detected from GeV energies to TeV energies



- Fermi detected hard and extended emission from Cygnus X, between OB2 and Gamma Cygni SNR
- Cocoon of accelerated CRs

# SFR as CR sources:

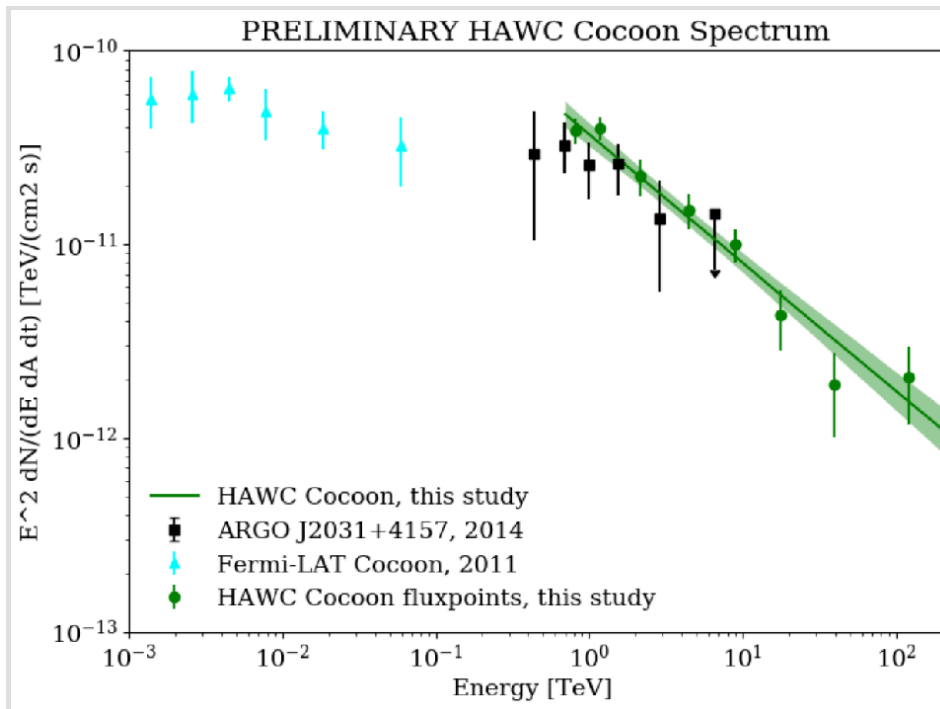
## Fermi-Argo-HAWC cocoon



Can SFR accelerate particles to high energies?

**Candidate: OB2 association in Cygnus Region**

*Fermi detection at GeV (Ackermann et al., **Science** 334, 2011, 'The Cocoon')*



*Argo detection of a counterpart to Fermi cocoon up to several TeV*

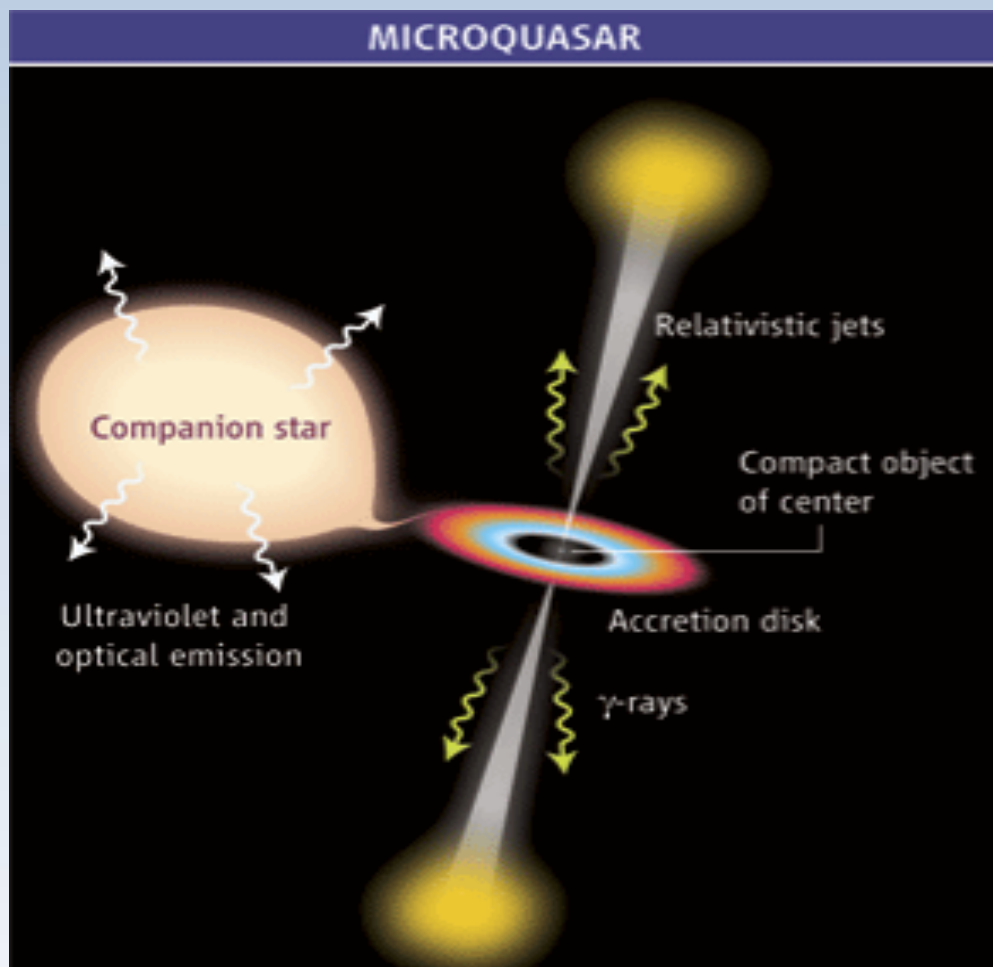
*Aharonian+2019, Nature Astronomy*

*HAWC detection of a TeV counterpart up to 100 TeV*

**Only SFR seen from GeV to 100 TeV!**

Energy budget and diffusion profile consistent with proton acceleration in collective star winds

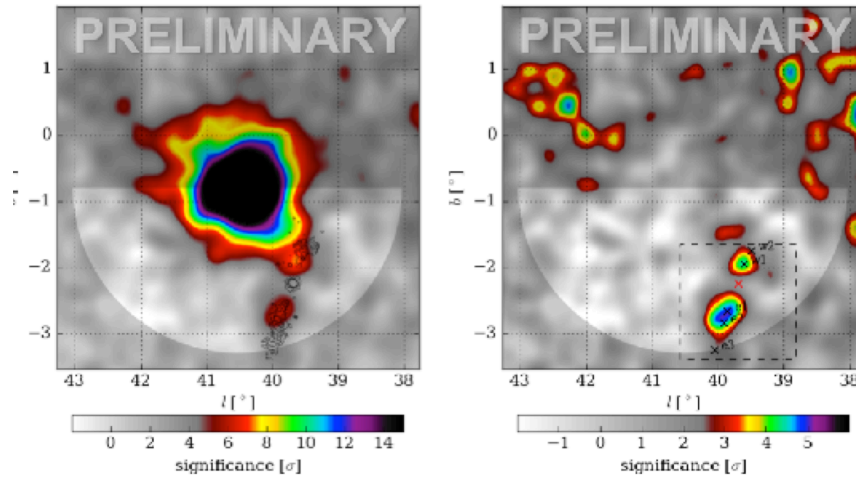
# Microquasars as sources of TeV $\gamma$ s



Compact binaries are extremely interesting astrophysical laboratories, which show periodic or unpredictable flaring activities and mimic the behaviour of AGN on observable timescales.

Microquasars are binaries with accretion disks that can emit X-rays and gamma-rays and have relativistic jets.

Micro-quasars are expected to emit radiation at TeV energies.



- SS 433 is a Galactic micro-quasar observed in radio-X-rays.

- SS433 is a binary system formed by a Supergiant 30 solar masses star and a compact object, either a neutron star or a black hole

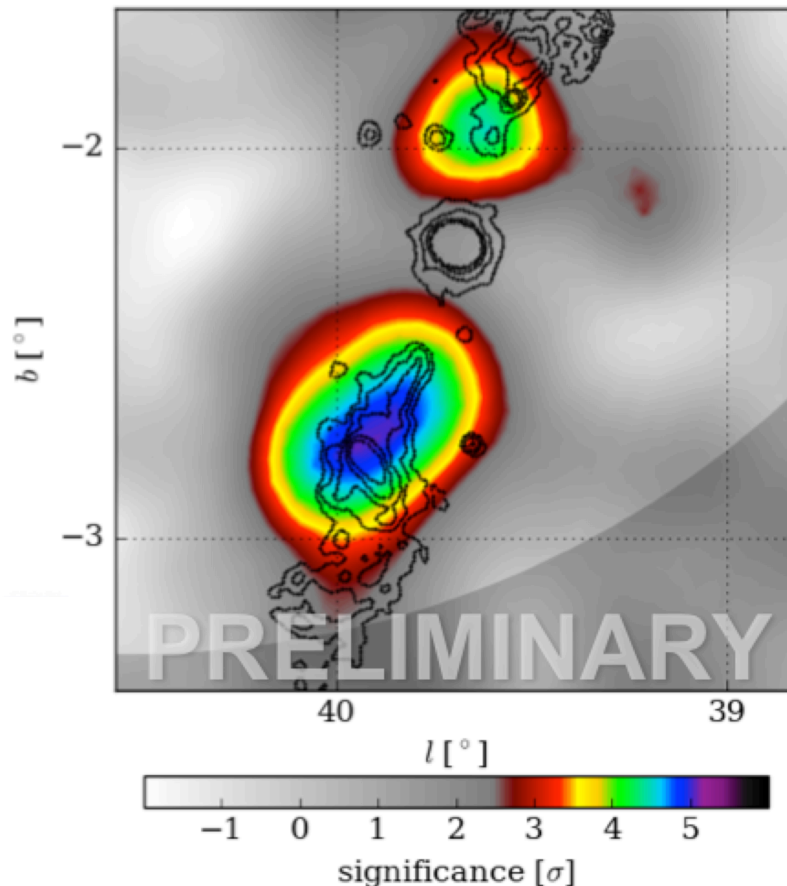
- Two jets, the most powerful known in the Galaxy, extend perpendicular to the line of sight and terminate in W50 nebula and produce western and eastern X-ray lobes

- SS433 jet :  $10^{39-40}$  erg/s

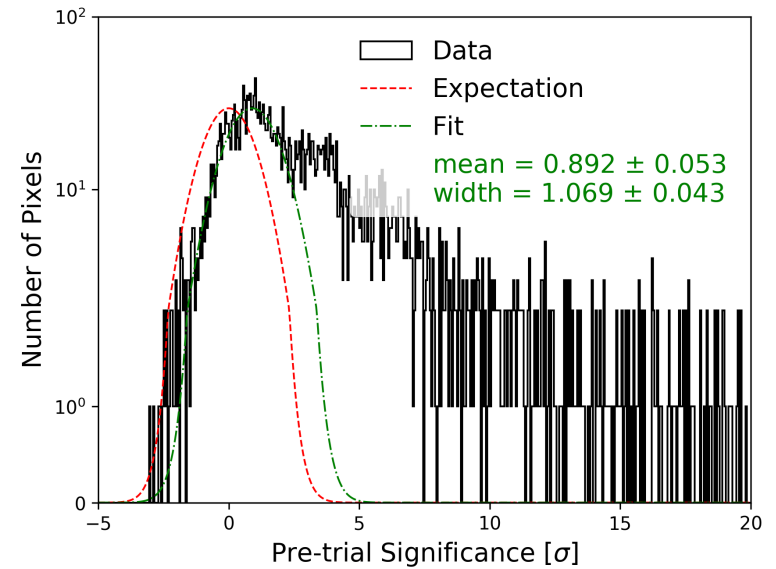
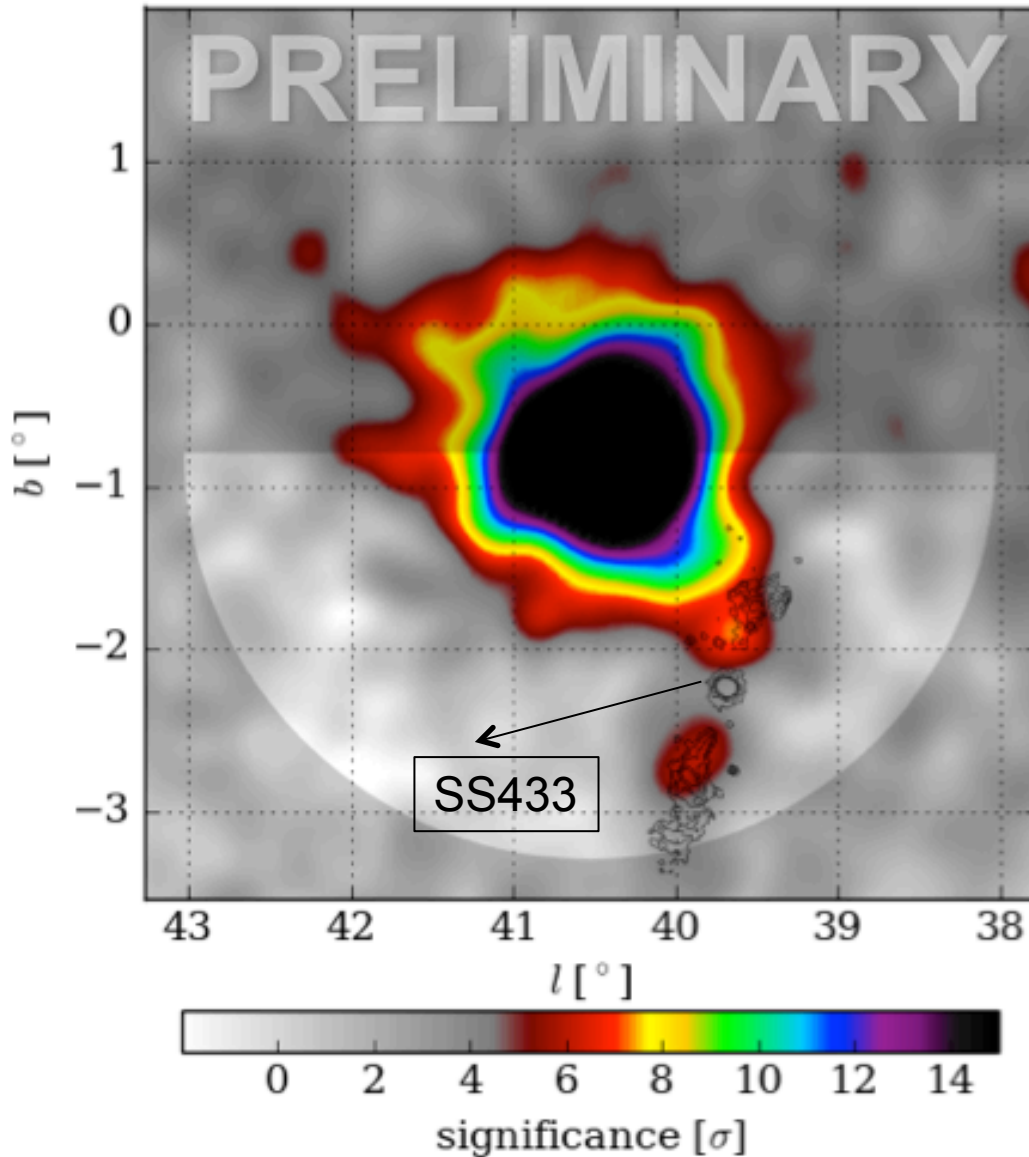
- SS433 jet speed roughly  $c/4$

- Baryon loaded

- Particle acceleration is believed to occur at the lobes where strong radiation is expected to be emitted at GeV and TeV energies



# Region of SS433 dominated by MGRO J1908+06



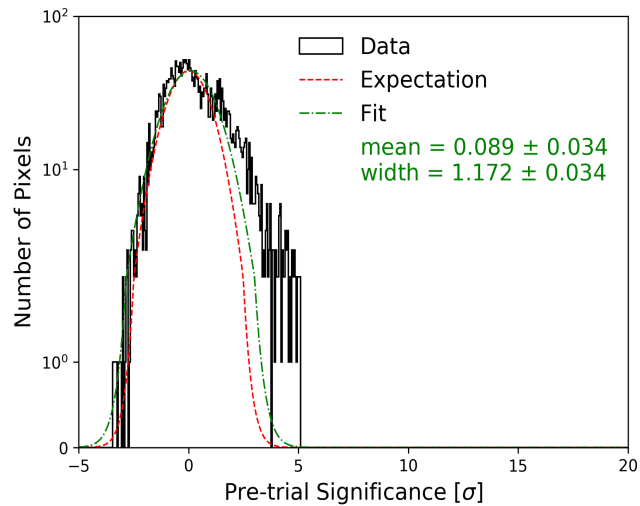
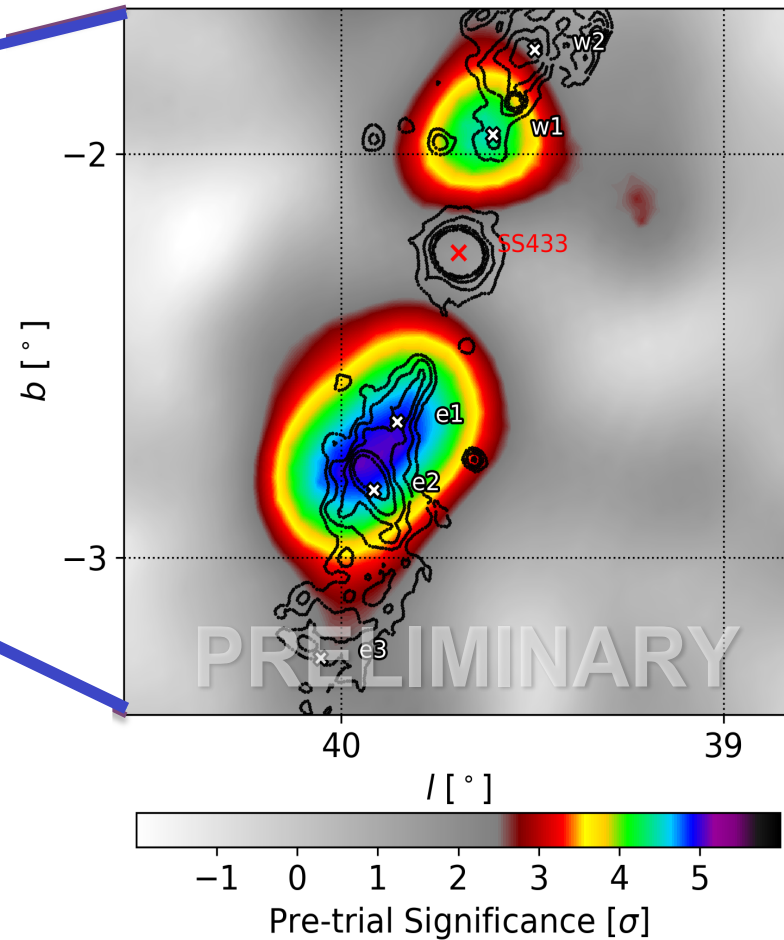
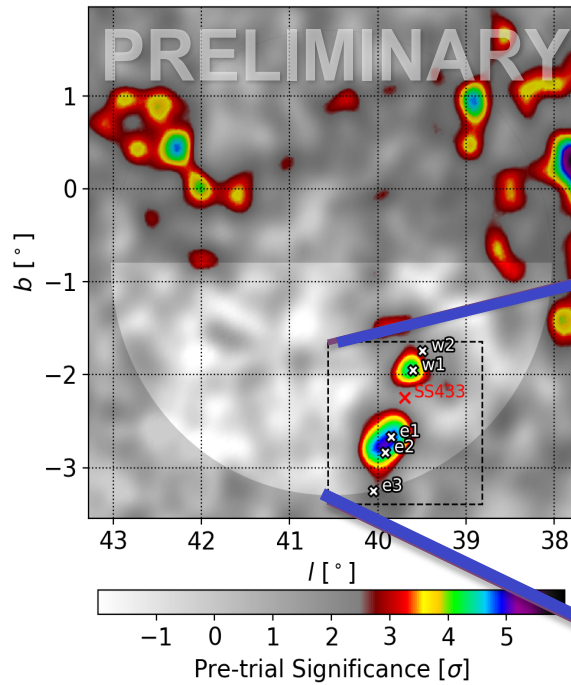
Simultaneous fit of normalisation, spectrum, size for MGRO J1908+06 and normalisation for each SS433 lobes

SS433 lobes spectral index assumed -2

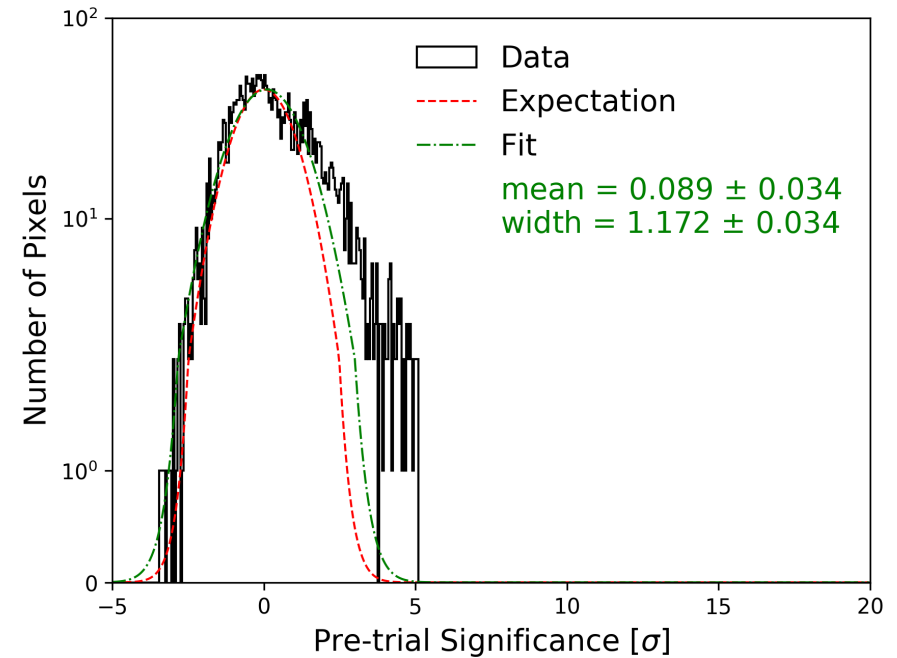
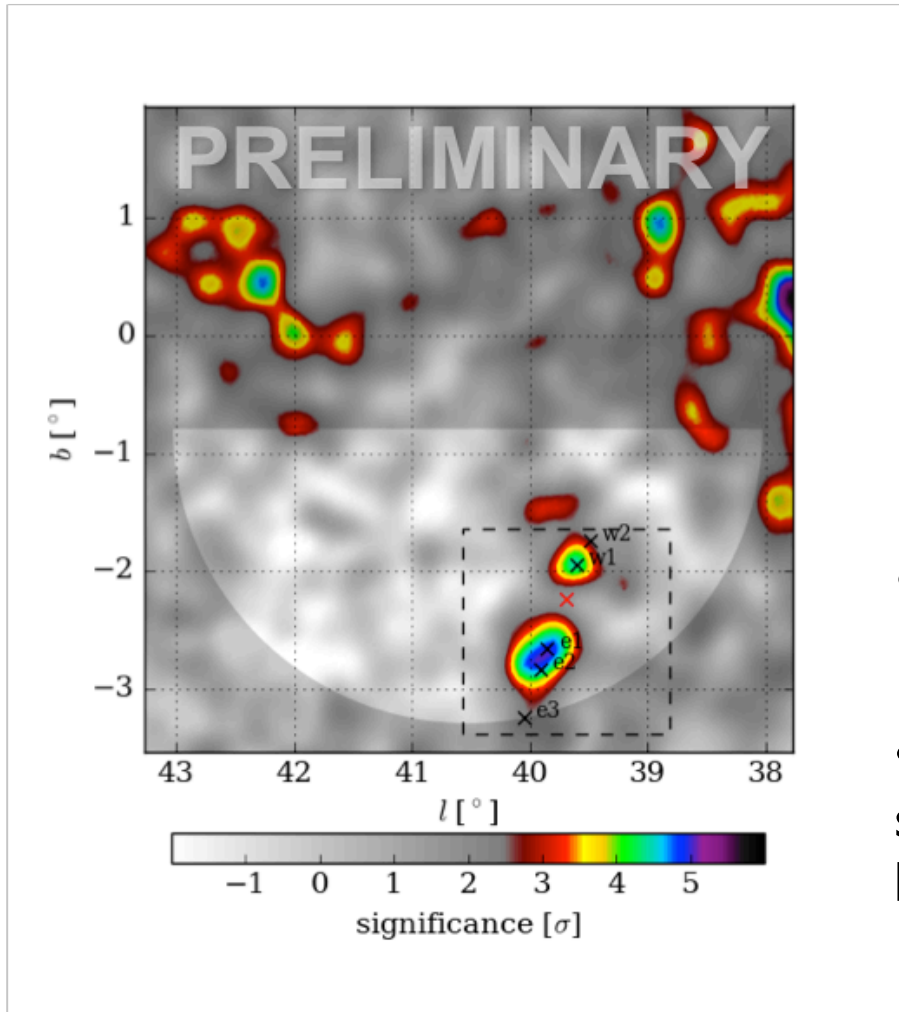
Semi-circular RoI to reduce GDE contamination

# Region of SS433 after subtracting MGRO J1908+06

Nature, Abeysekera et al 2018



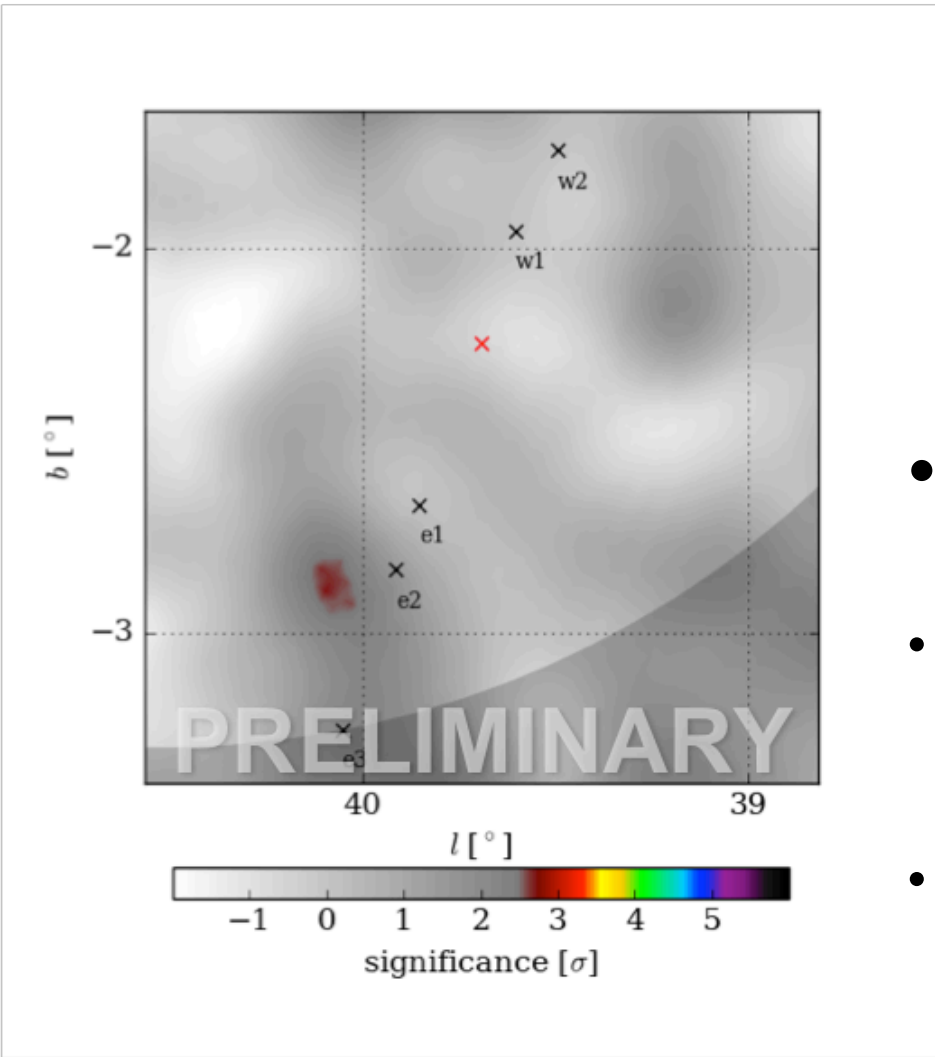
# SS433 lobes



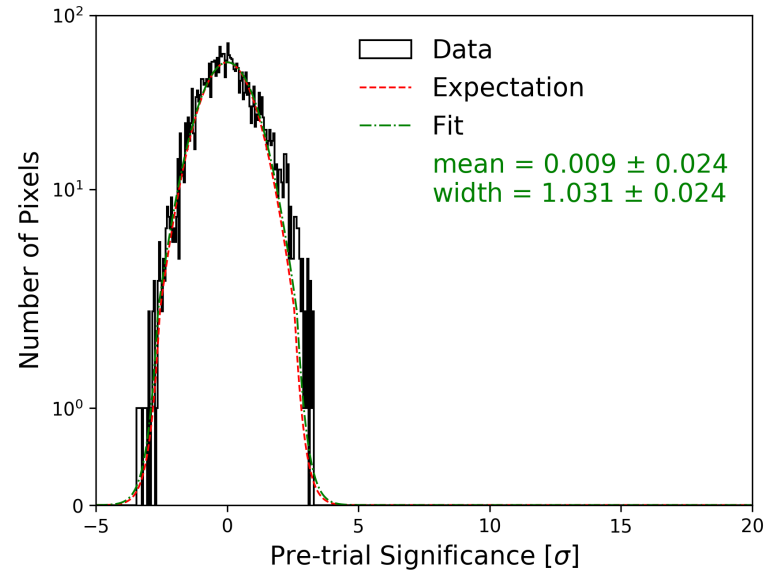
- PL of spectral index -2.0 has been assumed for both lobes.
- The pre-trial significance distribution shows improvement by removing J1908 but high- significance tail still exists



# Residuals



Nature, Abeysekara et al 2018



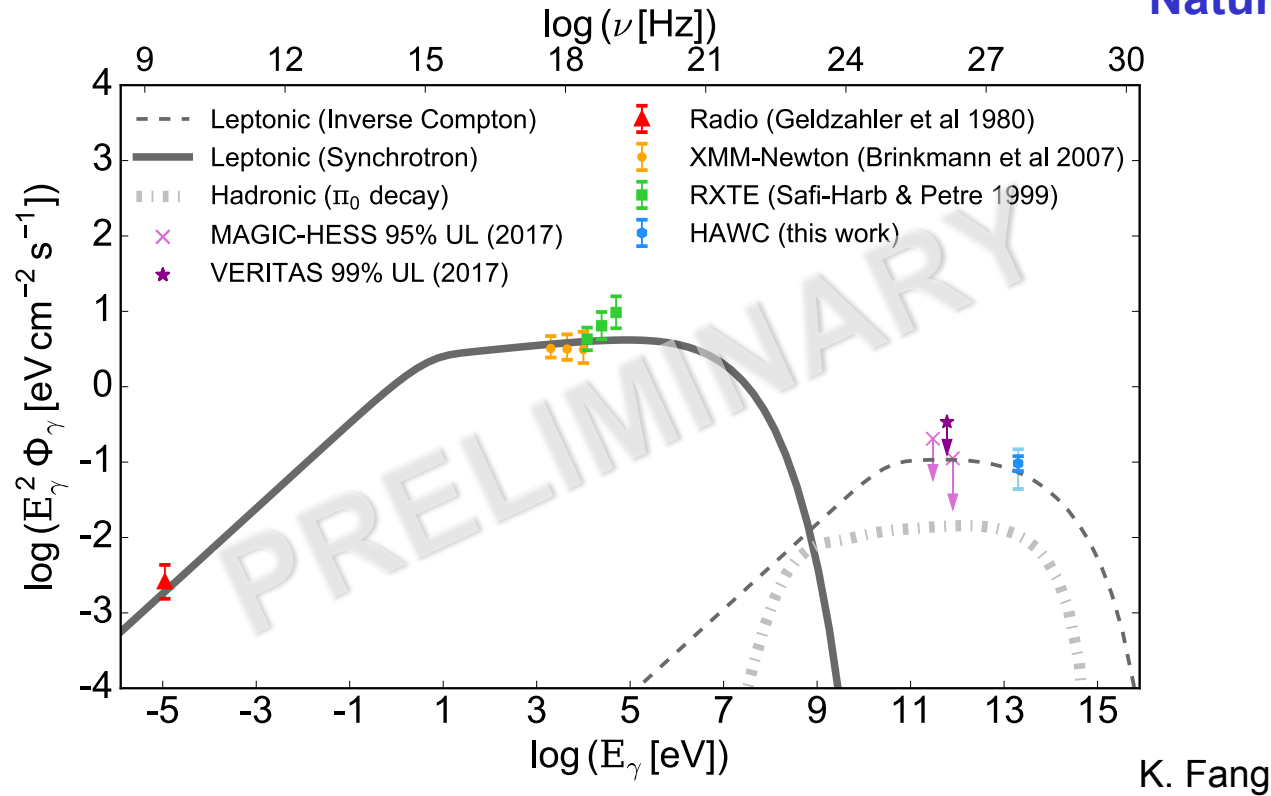
- Residual map after subtracting the lobes as well as J1908.
- The residual significance distribution is zero-mean Gaussian, consistent with background-only distribution.
- The fit of point-like east and west lobes gives  $5.4 \sigma$  post-trial with HAWC's 1017 days of dataset at e1 and w1.
- Upper limits on angular size are 0.25 degree for e1 and 0.35 degree for w1, corresponding to 23 and 34 pc, respectively at 5.5 kpc.

# Origin of the emission

- Composition and spectrum of the particles generating the gamma rays: hadronic ( $\pi^0$  decay) or leptonic (IC) origin?
- Acceleration in magnetic fields or by standing shocks?
- Is there enough energy to accelerate high-energy particles?

# Origin of the emission (e1)

Nature, HAWC Coll 2018



- IC scattering off CMB photons, scattering off optical and infrared suppressed electron acceleration
- Electrons of at least 130 TeV required in a magnetic field of 16 microGauss
- Hadronic emission assumes 10% conversion of jet energy into protons and 0.05 cm<sup>-3</sup> density

# Origin of the emission

Leptonic model does a good job of explaining the gamma ray emission, requires  $\sim 0.5\%$  of jet power going into electron acceleration.

In hadronic-only scenario protons of at least 250 TeV produce gamma in proton-proton interaction and secondary leptons radio and X-rays via synchrotron radiation.

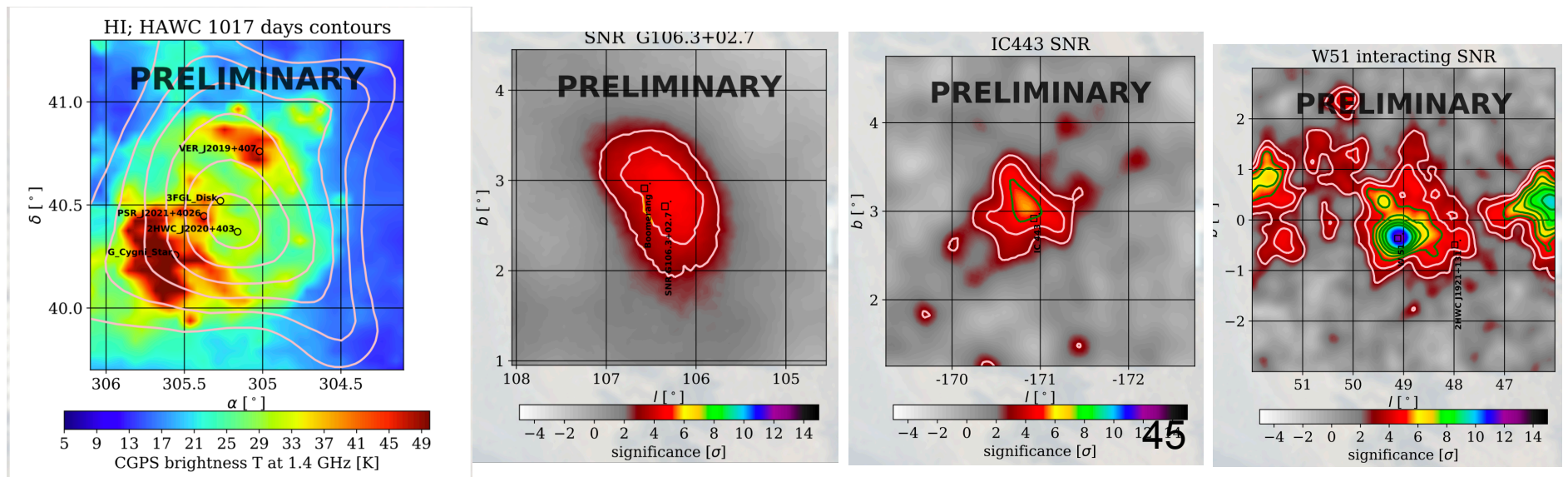
Energy budget of  $3 \times 10^{50}$  erg  $\sim 100\%$  of jet energy over 30000 year lifetime of SS 433 must go into accelerating protons to explain the observed gamma-ray emission.

Acceleration is occurring in the jets, not in the central binary:

1. Emission region is  $\sim 40$  pc from central binary.
2. Diffusion length scale is  $\sim 35$  pc at these energies, assuming ISM diffusion coefficient
3. Advection length scale is  $\sim 4$  pc.

# Testing the SNR paradigm

- SNRs postulated main sources of CRs in our Galaxy
- tens TeV to hundreds TeV emission crucial to test acceleration up to PeV energies
- HAWC detection of significant TeV  $\gamma$ -ray emission from middle-aged three SNRs:  $\gamma$ -Cygni, IC 433, and W51C. Combined fits of Fermi and HAWC data describing the GeV-TeV emission as pion decay spectrum
- HAWC J2227+610 associated to G106.3+2.7 possibly accelerating hadrons up to 800 TeV



Middle-aged SNR, ~6000 yrs [Lozinskaya et al., 2000]).

Distance: ~1.7 kpc.

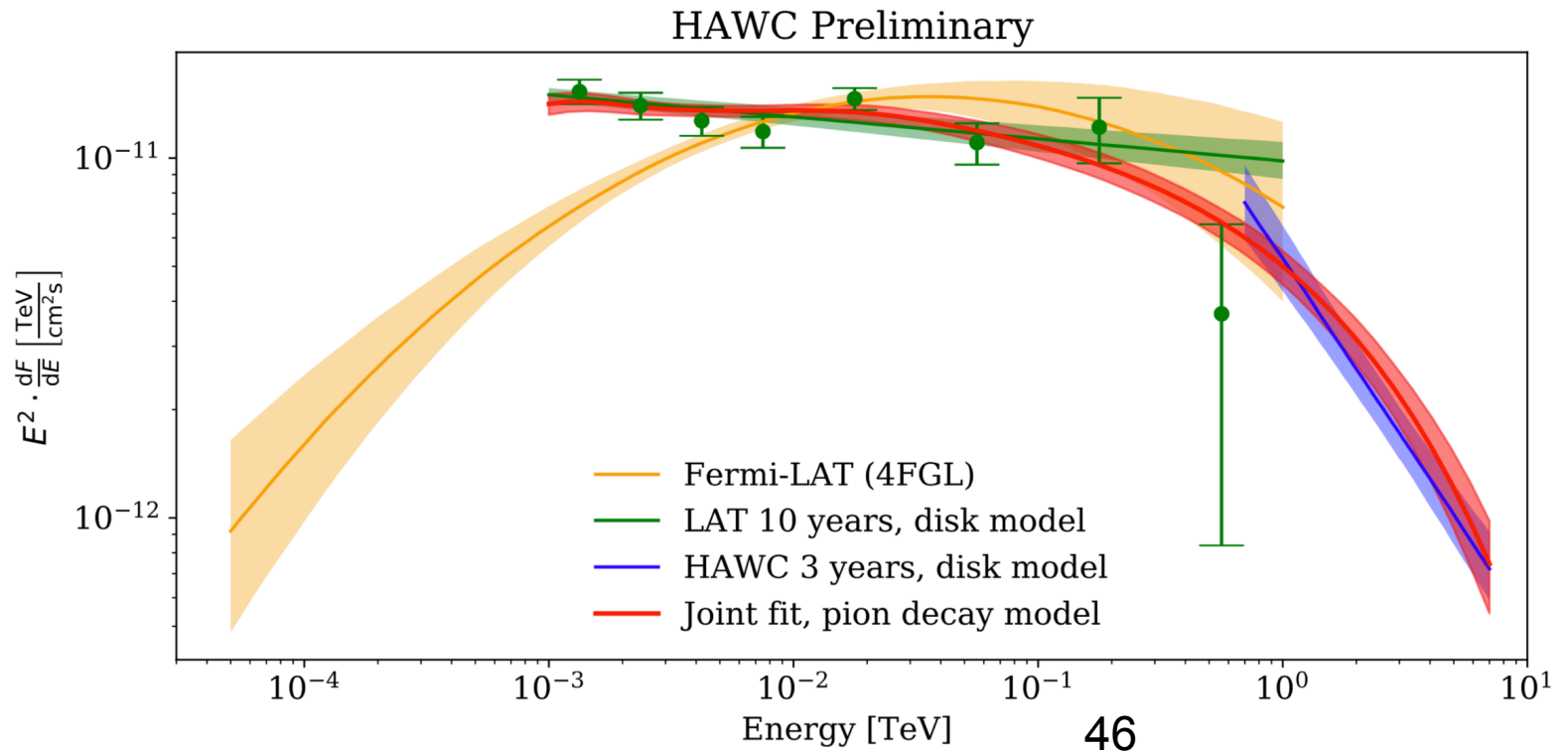
X-ray/radio shell, enhanced emission at northern/southern edge.

Seen up to TeV energies.

Leptonic or hadronic emission?

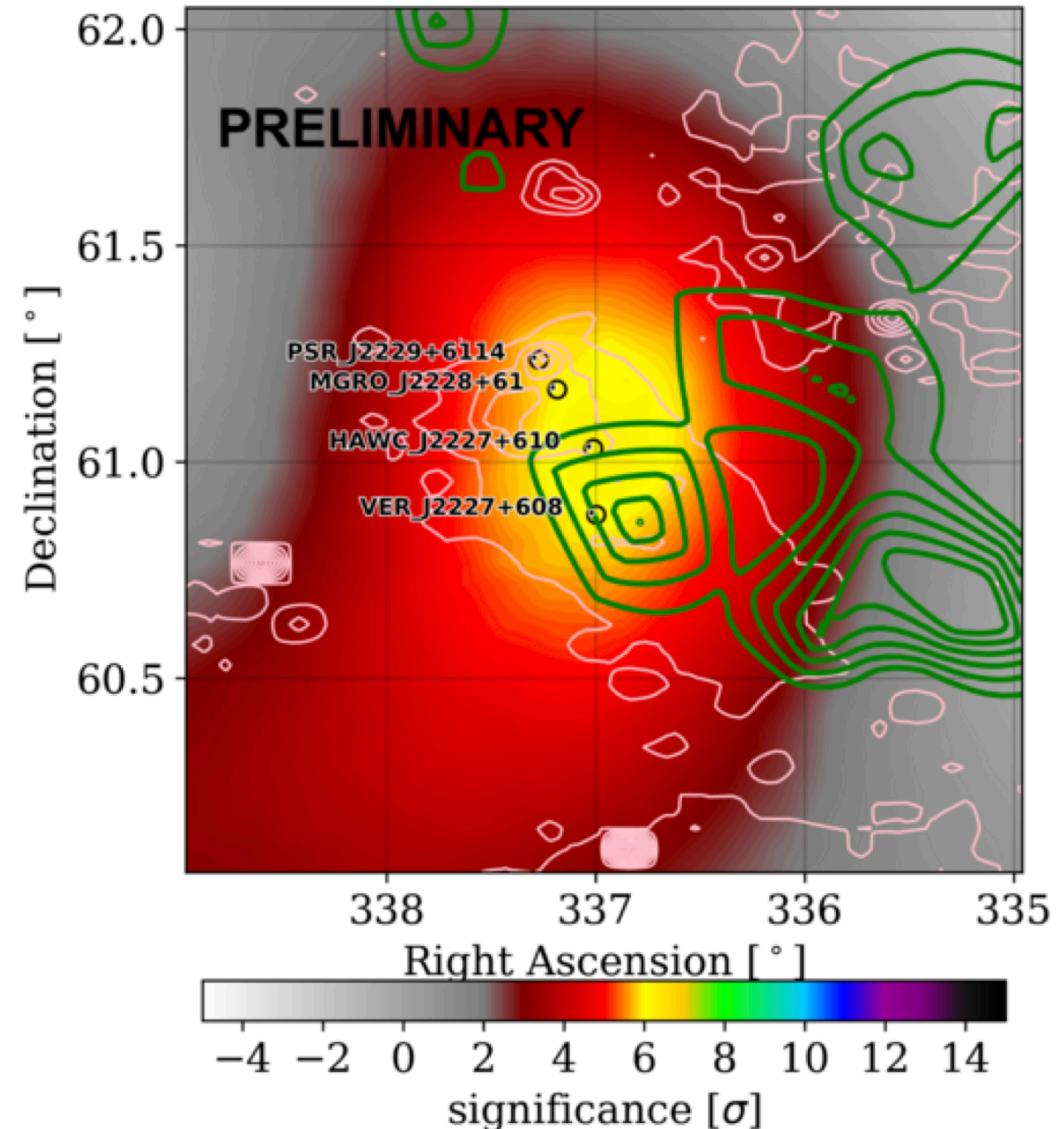
**$\gamma$ -Cygni**

## Combined Fermi - HAWC fit to $\gamma$ Cygni



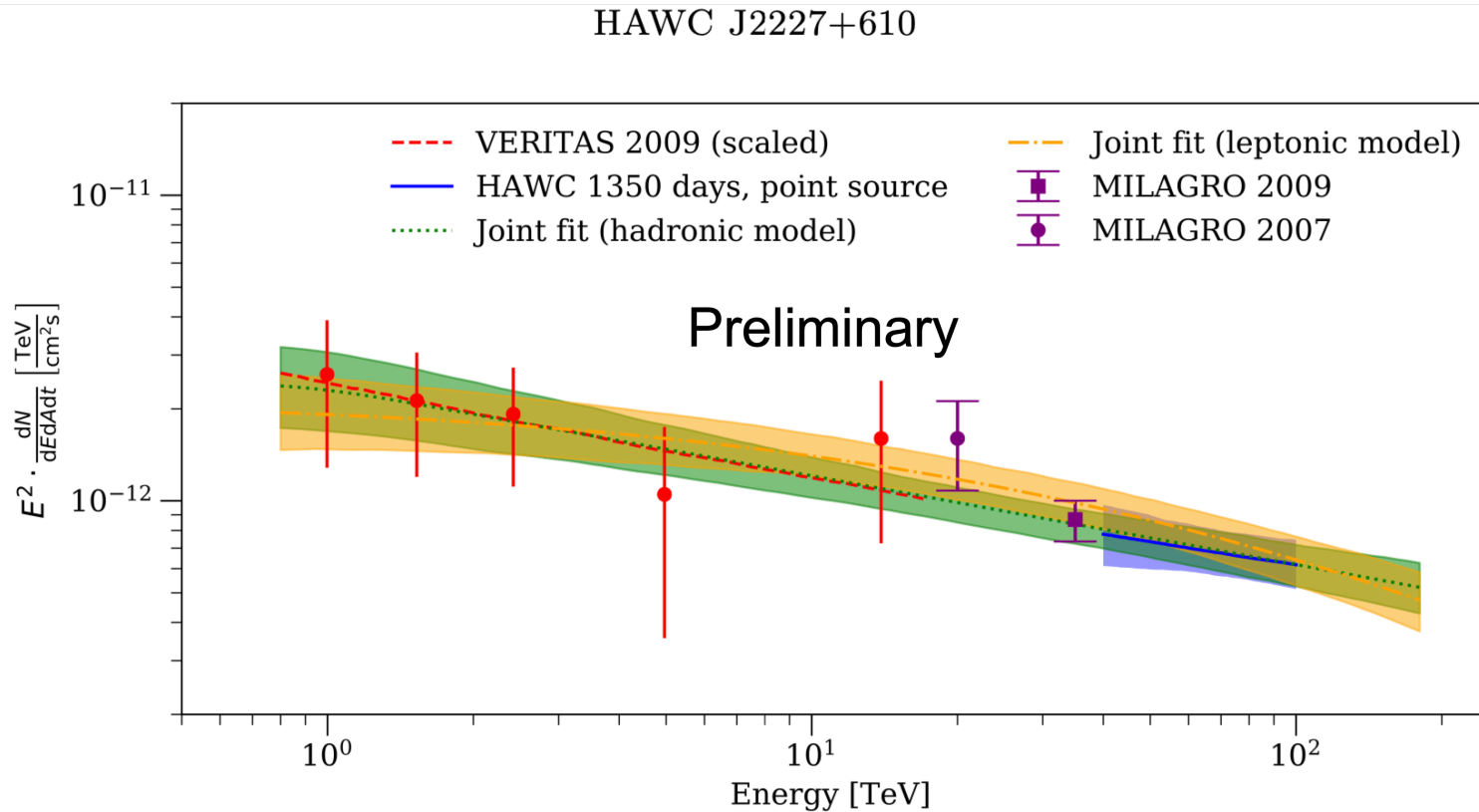
# Boomerang

- SNR G106.3+2.7 is a comet-shaped radio source
- PSR J2229+6114, seen in radio, X-rays, and gamma rays
- Boomerang Nebula is contained in the remnant
- VERITAS source (energy range 900 GeV – 16 TeV)
- The joint VERITAS-HAWC spectrum is well fit by a power law from 800 GeV to 180 TeV
- HAWC emission pointlike, morphology compatible with VERITAS source
- If hadronic, the cutoff energy in the underlying proton spectrum is constrained to be above 800 TeV
- Leptonic mechanism cannot be excluded



# Joint VERITAS-HAWWC Spectrum

## Boomerang - A Galactic Pevatron?



Gamma Spectral Slope : 2.29, Lower limit on Ecut = 120 TeV

Proton Spectral Slope : 2.35, Lower limit on proton Ecut = 800 TeV,  $W_p = 10^{48} (n/50)^{-1}$  erg

Source for LHAASO



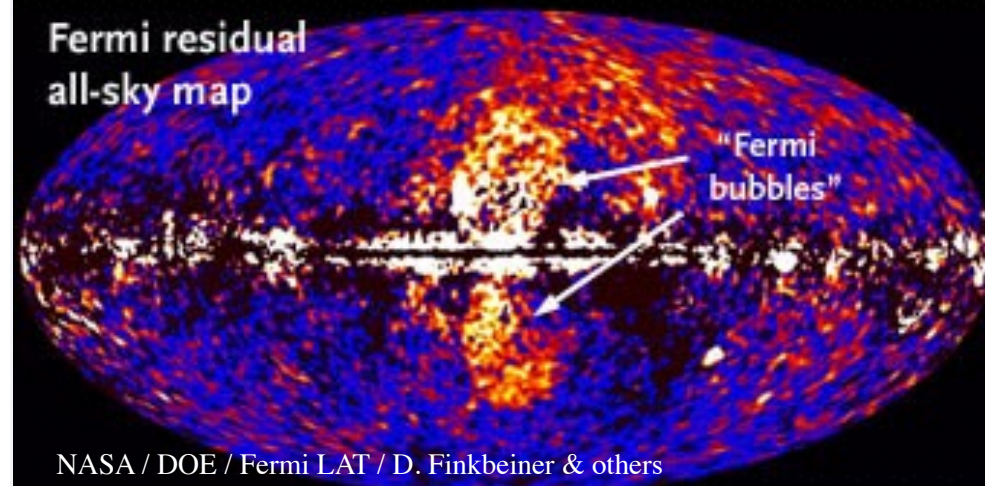
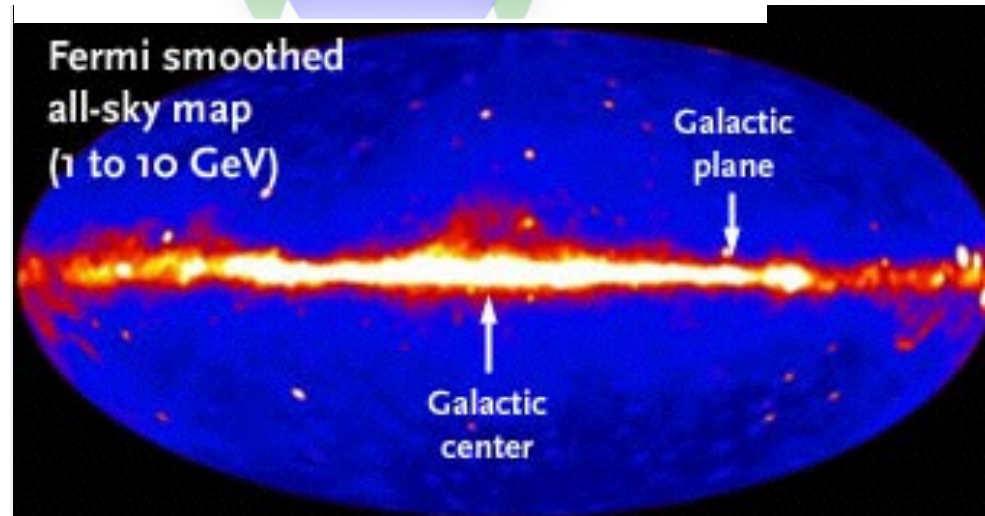
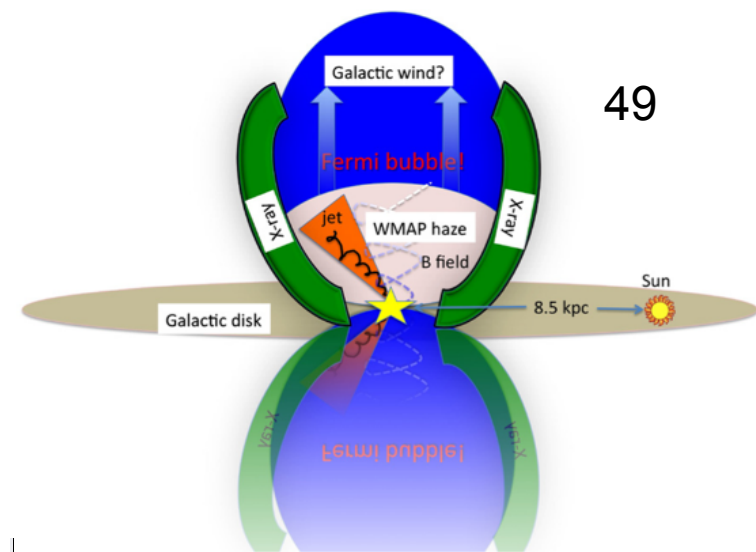
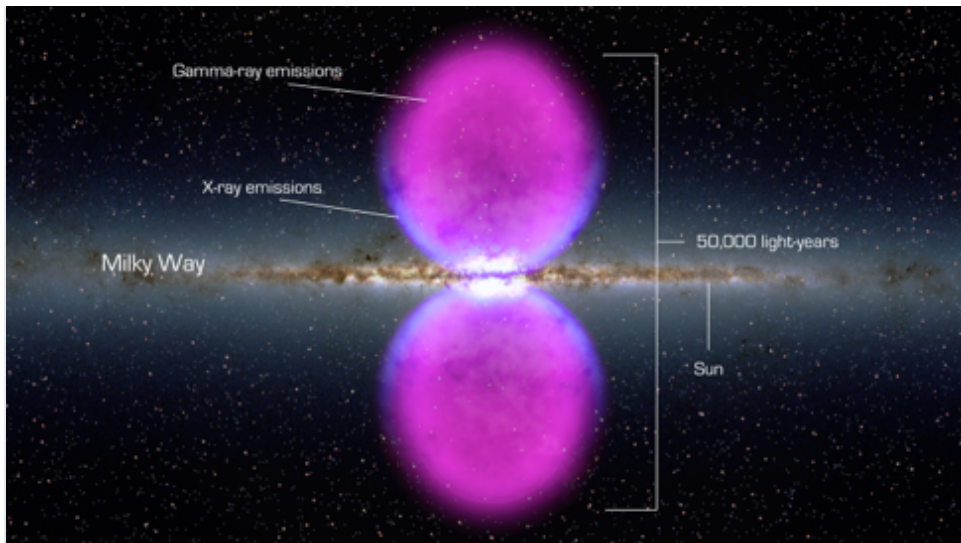
# Fermi bubbles

Large scale, non-uniform structures extending above and below the Galactic center.

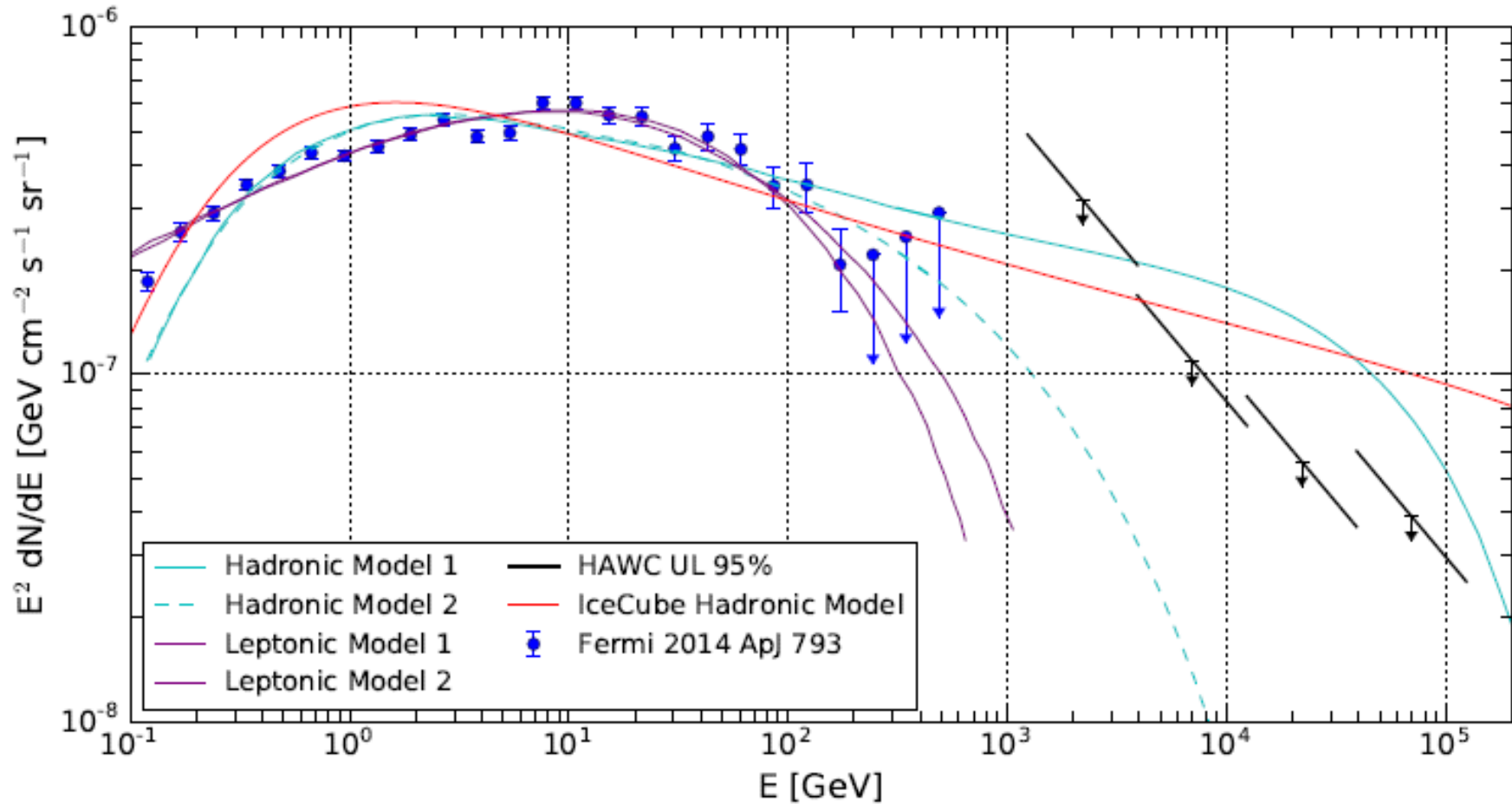
Edges line up with X-ray features.

Correlate with microwave excess (WMAP haze)

Both hadronic and leptonic model fit Fermi LAT data.

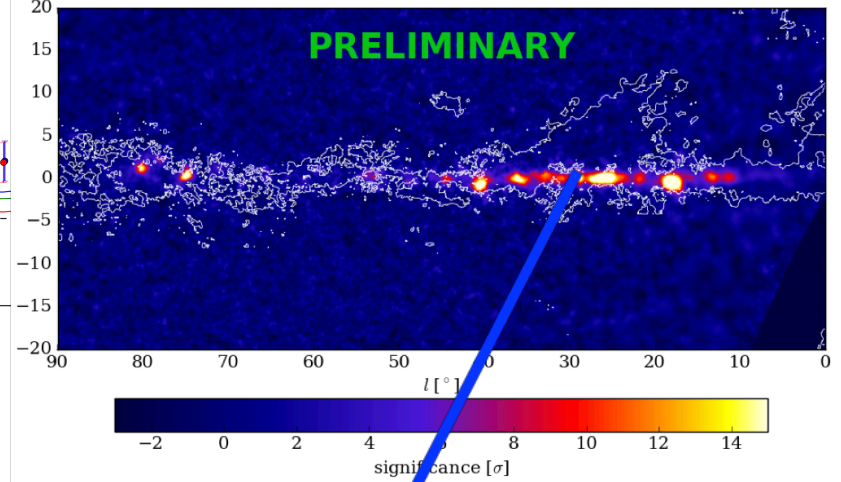
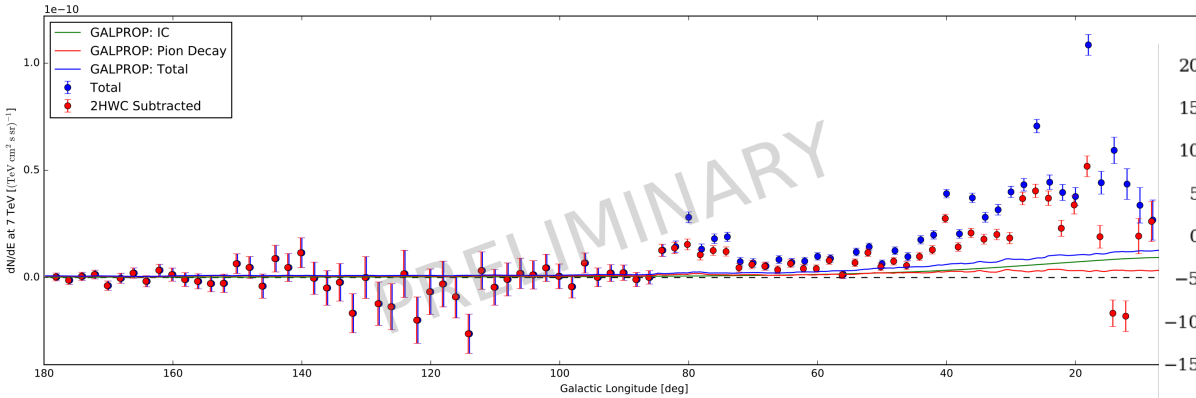


# HAWC 90% CL upper limits



Abeysekara et al, ApJ, 2017

# GDE and Molecular Clouds

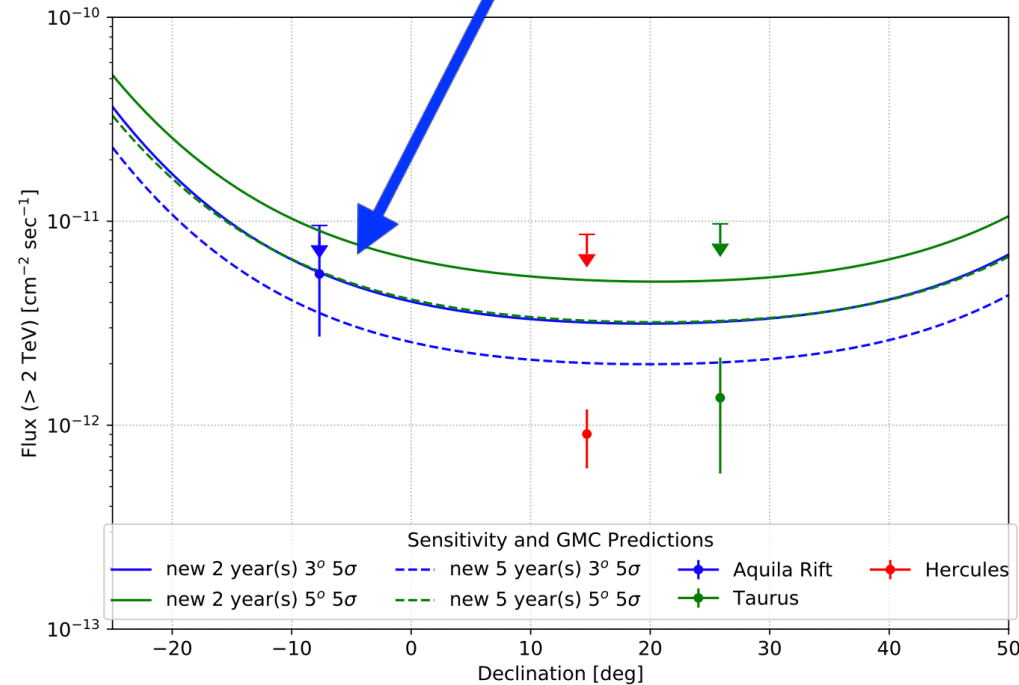


Test of Galactic Diffuse Emission Models at multi-TeV

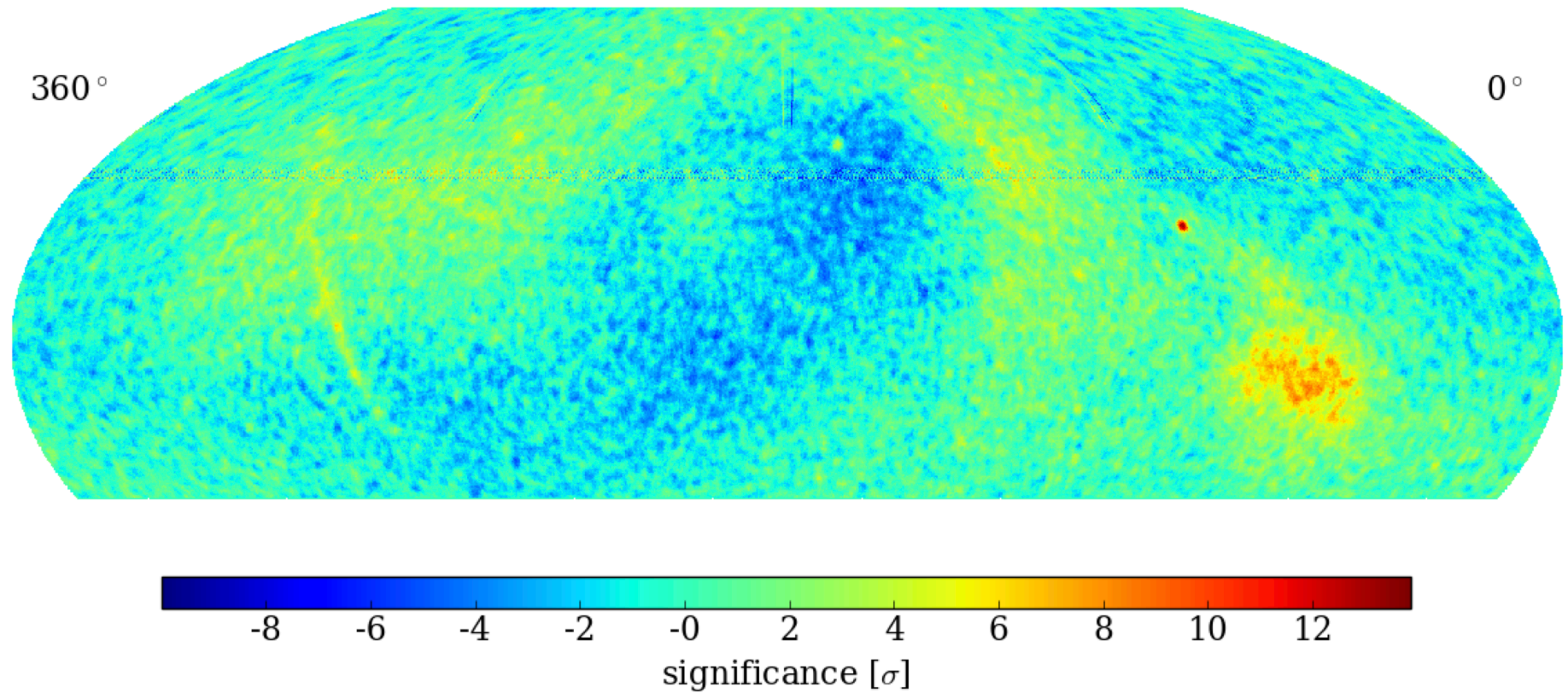
Improve upper limits on Fermi Bubbles by almost an order of magnitude

Unprecedented probe of CR flux a distant galactic regions through their interaction with Large Molecular Clouds using multi-TeV gamma-ray

Direct CR measurement: Update of Large scale anisotropy and localized excesses measurements

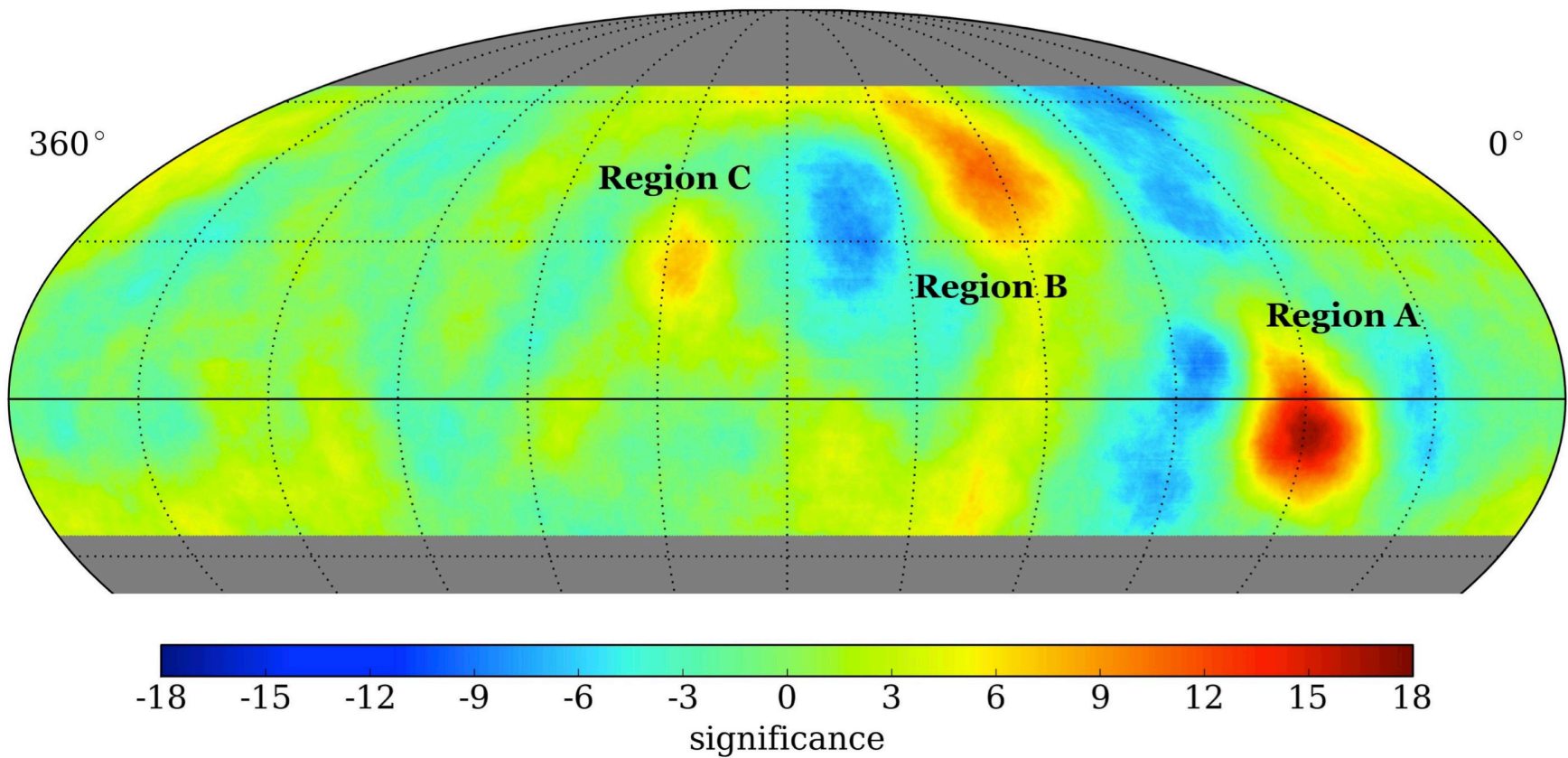


# HAWC - No gamma-ray cut



# Large Scale Anisotropy

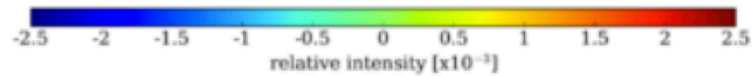
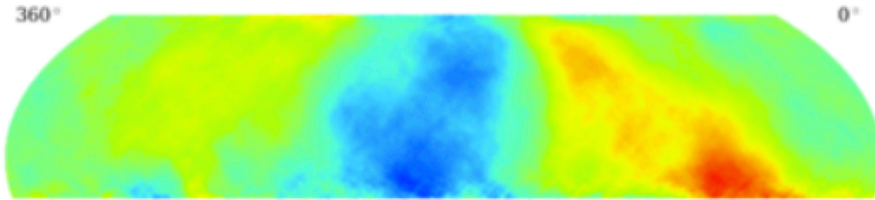
Regions A, B and C are the only statistically significant excesses ( $>5\sigma$  post-trials)



# Energy dependence

~2 TeV

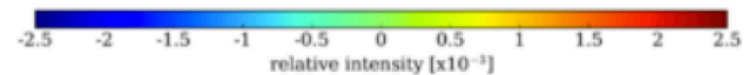
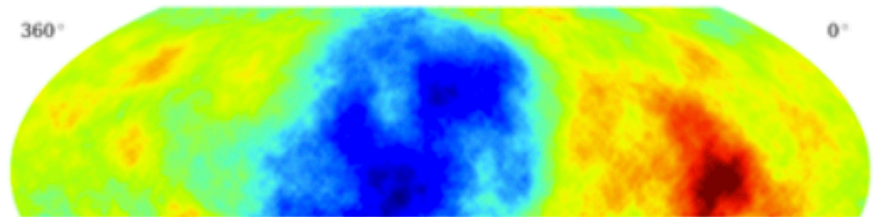
Bin 2



- Large-scale anisotropy for energy bin 2. Median energy is 1.86 (+ 3.03, -1.5)

~13.5 TeV

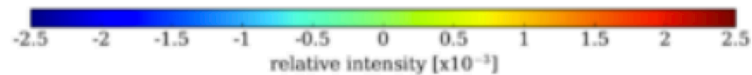
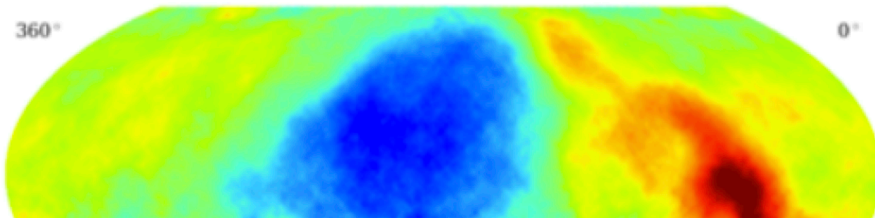
Bin 4



- Large-scale anisotropy for energy bin 4. Median energy is 13.5 (+ 16.0, -9.03)

~5 TeV

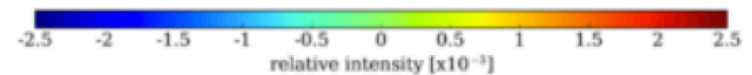
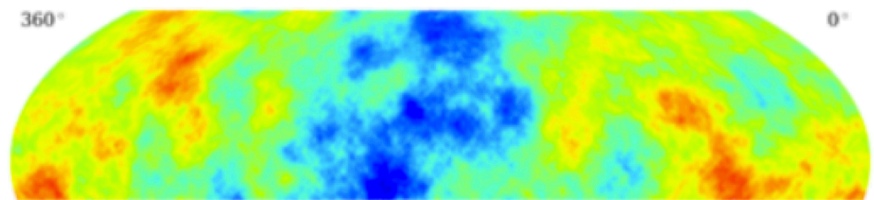
Bin 3



- Large-scale anisotropy for energy bin 3. Median energy is 4.90 (+ 6.85, -3.3)

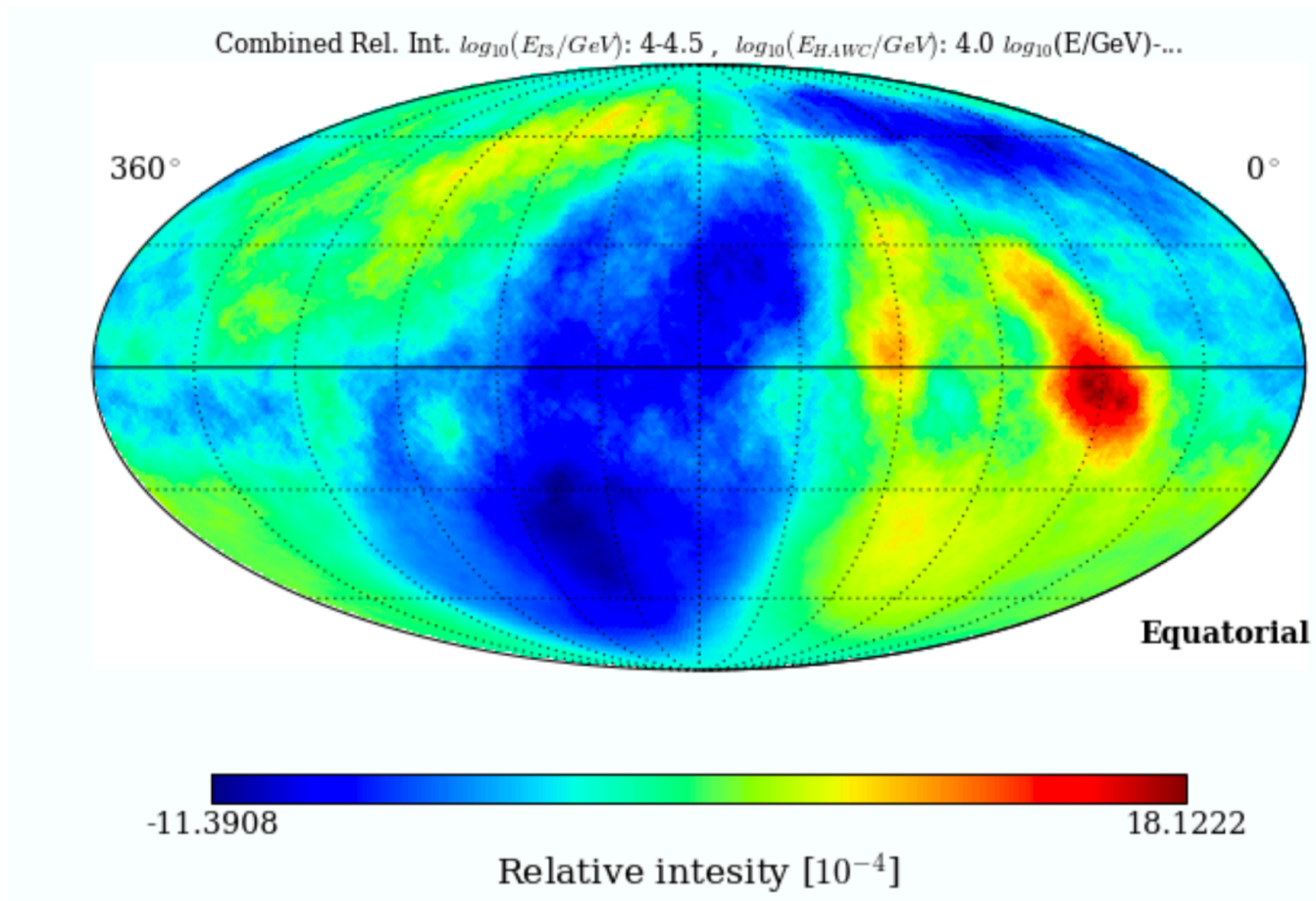
~45 TeV

Bin 5



- Large-scale anisotropy for energy bin 5. Median energy is 44.7 (+ 67.6, -27.7)

# HAWC-IceCube Joint Fit



# Multi-wavelength/Multi-messenger

We have follow-up agreements with:

– Swift

– Fermi-LAT

– IACTs

• FACT

• HESS

• MAGIC

• VERITAS

– AMON

– IceCube

– ANTARES

– LIGO/VIRGO

HAWC-triggered:

- New source candidates lists.
- follow-up observations by IACTs such as VERITAS and MAGIC from Pass I release.
- Flares from known gamma-ray sources.

HAWC ATel #8922  
on Mrk 501 flare

Externally triggered:

- IceCube alert on high confidence neutrino event (highest energy pointed astrophysical track-like).
- Fermi alerts on flaring activities.
- LIGO/VIRGO gravitation wave event follow-up

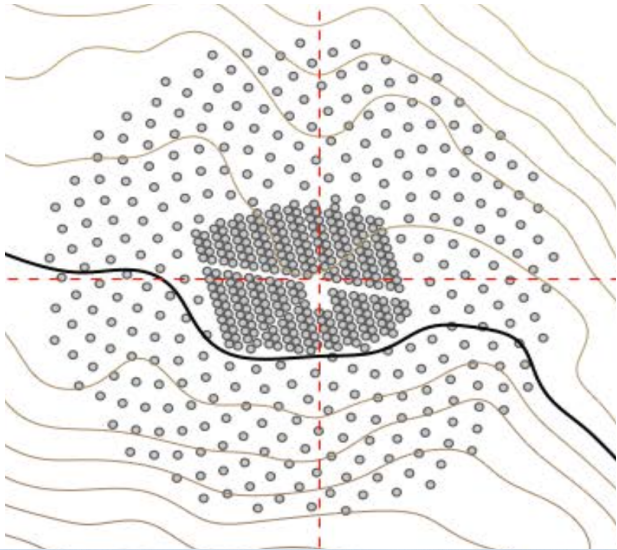
IceCube ATel: #7856  
HAWC Follow-up ATel:  
#7868



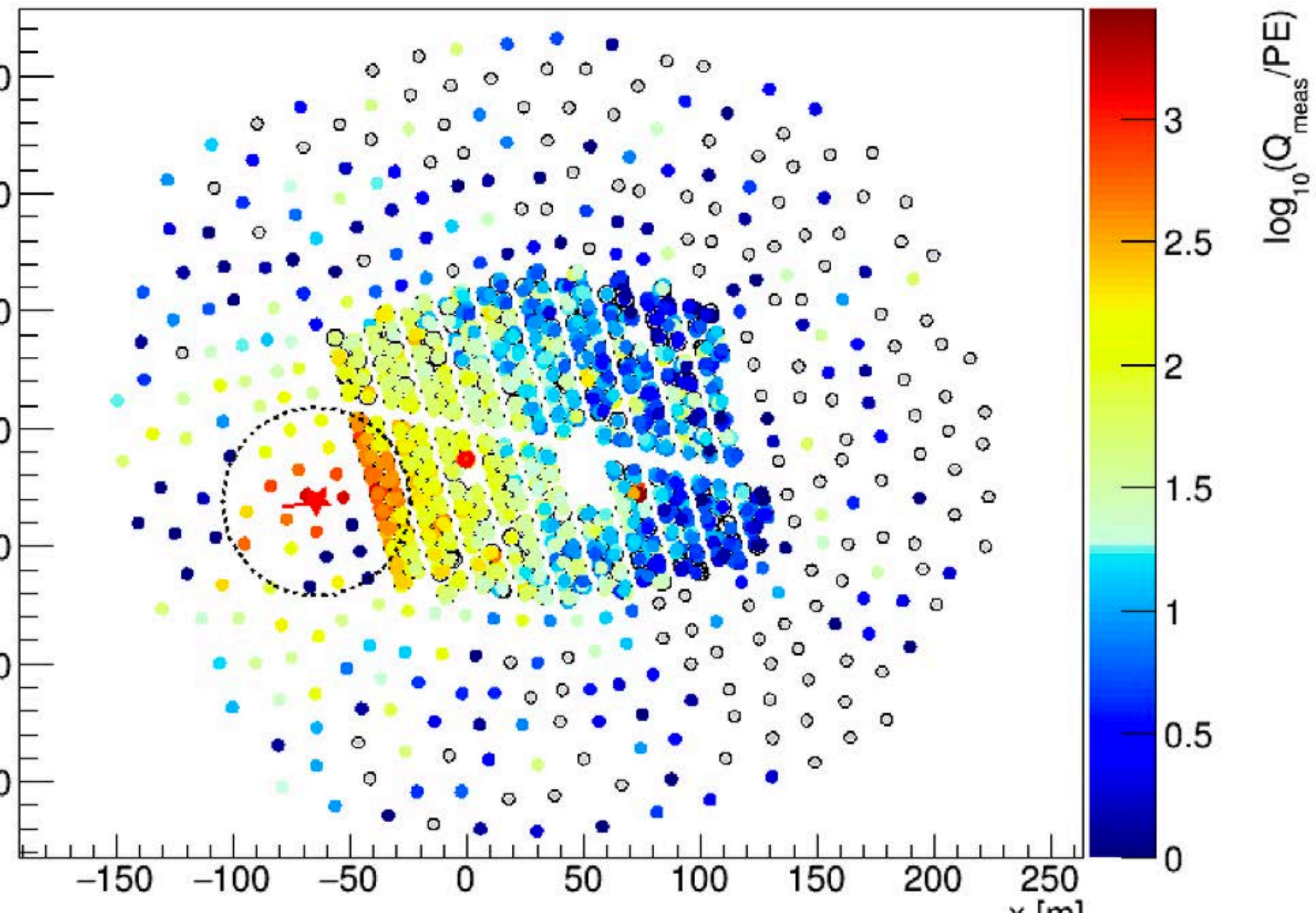
# HAWC with Outrigger



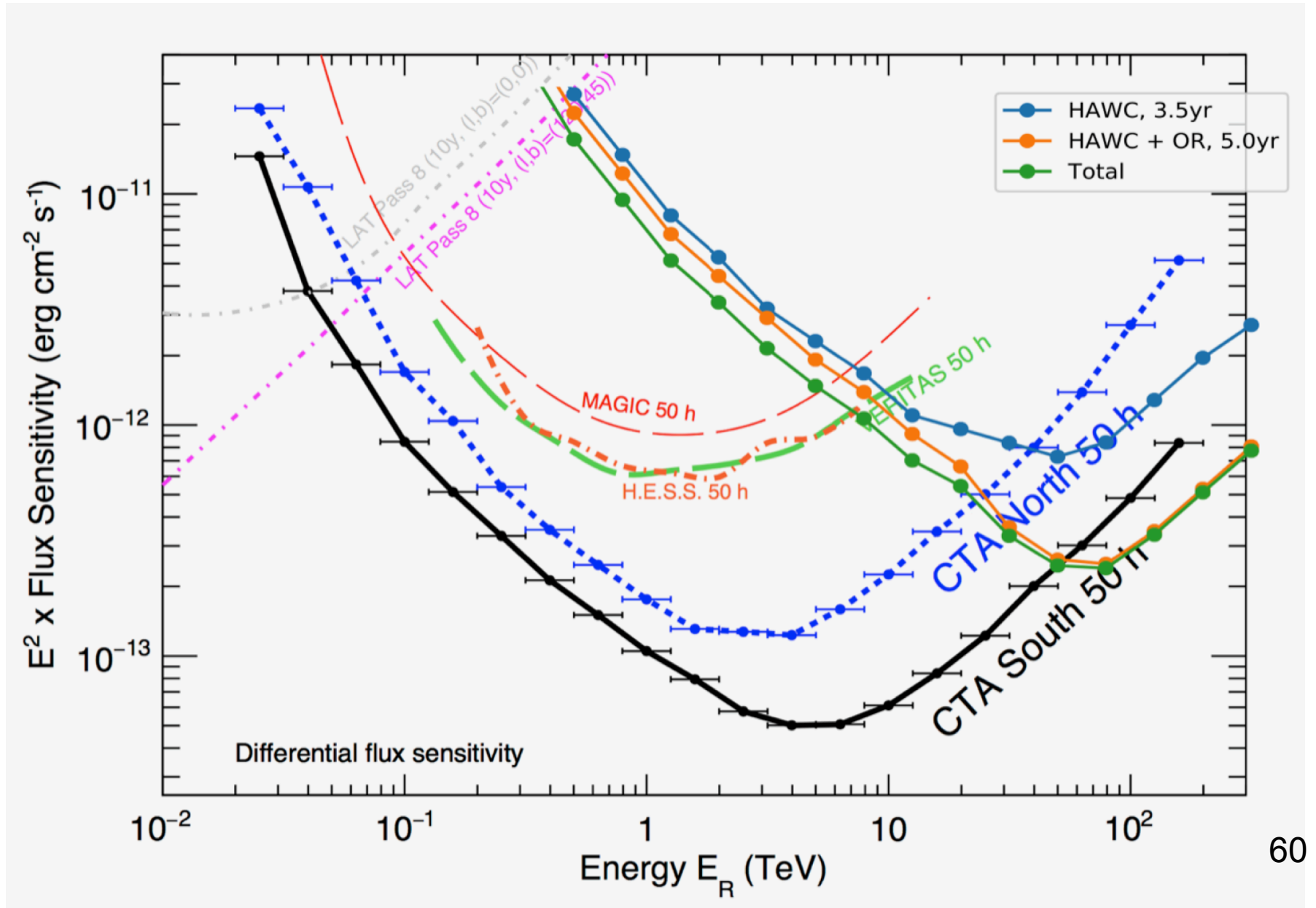
# HAWC with Outrigger



- HAWC has added more detectors to enhance the sensitivity above 10 TeV.
- Outriggers help to accurately determine core position for showers off the main tank array.
- Funded by LANL LDRD, Max Planck Institute in Heidelberg, and CONACyT in Mexico
- Gives angle and energy reconstruction for showers that trigger HAWC but have the core outside the HAWC array
- Expands total effective area by a factor of  $\sim 4$  above  $\sim 10$  TeV with the addition of 350 outrigger tanks
- 100% operational and taking data since August 2018, but we're still refining calibration, reconstruction and analysis algorithms
- HAWC already detects multiple sources greater than 100 TeV. Outriggers will increase this number of sources and characterize their spectra.



# HAWC + Outriggers Sensitivity



# HAWC Strengths

- **High Duty Cycle**  
Transients
- **Sensitivity & Angular Resolution  $> \sim 10$  TeV**  
Highest Energy Accelerators
- **Wide field of view with good angular resolution**  
Extended Emission

# Summary and Outlook

For a relatively small amount of money HAWC is

- surveying the TeV sky with a wide-field of view
- Discovering new classes of sources
- Doing exciting physics
- Unveiling the highest energy sky
- Playing an important role in Multi-messenger astrophysics
- With outriggers and new algorithms progressing outside the  $\sqrt{t}$  regime

# **Backup Slides**

# Cuts used in analysis

$\mathcal{B}$	$f_{\text{hit}}$	$\psi_{68}$	$\mathcal{P}$ Maximum	$\mathcal{C}$ Minimum	Crab Excess Per Transit
1	6.7 - 10.5%	1.03	<2.2	>7.0	$68.4 \pm 5.0$
2	10.5 - 16.2%	0.69	3.0	9.0	$51.7 \pm 1.9$
3	16.2 - 24.7%	0.50	2.3	11.0	$27.9 \pm 0.8$
4	24.7 - 35.6%	0.39	1.9	15.0	$10.58 \pm 0.26$
5	35.6 - 48.5%	0.30	1.9	18.0	$4.62 \pm 0.13$
6	48.5 - 61.8%	0.28	1.7	17.0	$1.783 \pm 0.072$
7	61.8 - 74.0%	0.22	1.8	15.0	$1.024 \pm 0.053$
8	74.0 - 84.0%	0.20	1.8	15.0	$0.433 \pm 0.033$
9	84.0 - 100.0%	0.17	1.6	3.0	$0.407 \pm 0.032$

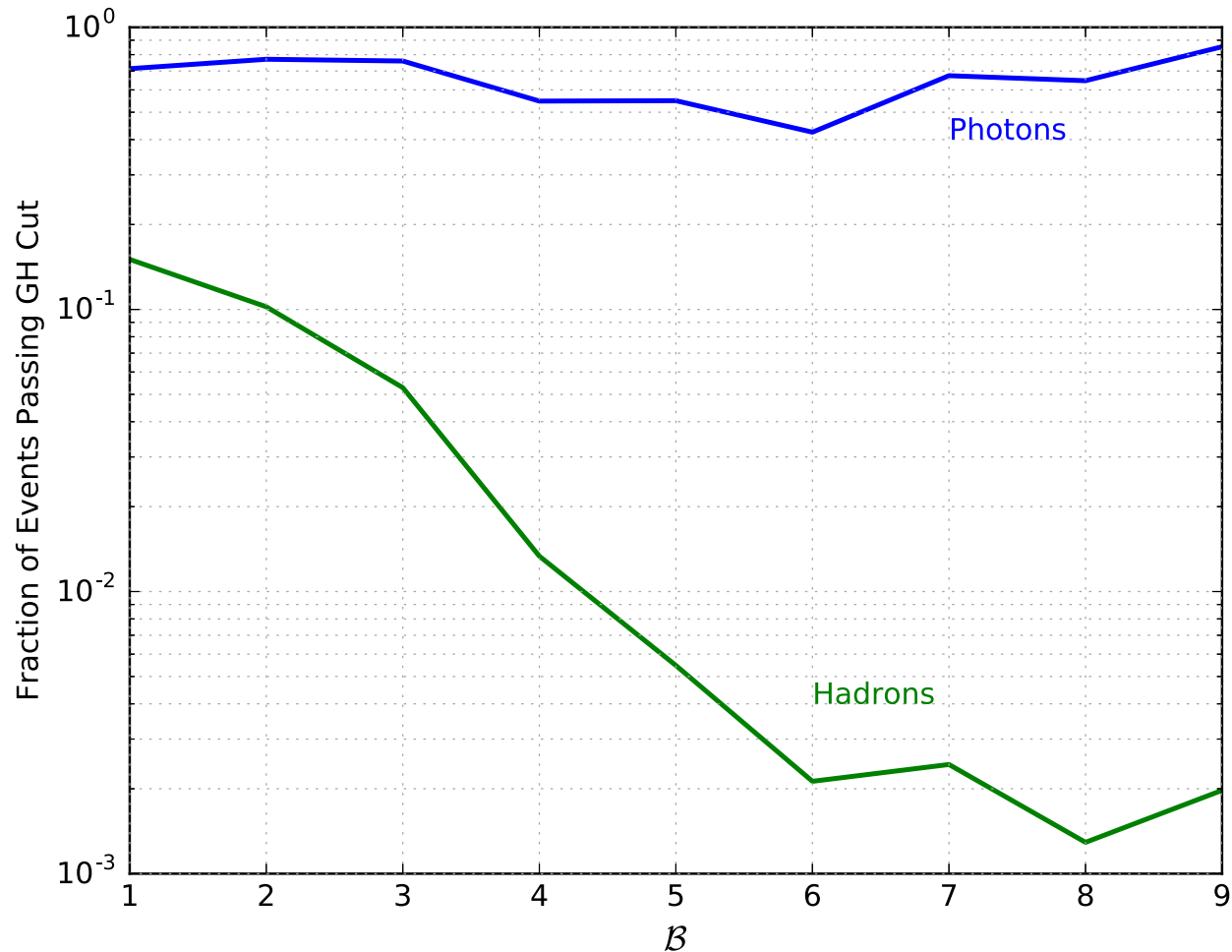
The cuts are chosen to maximize the statistical significance with which the Crab is detected in the first 337 days of the 507-day dataset, leaving the resting days to obtain the Crab spectra without optimisation. The two spectra differ by 10%, assumed as one of the systematics.

Albert et al, 2017



# Cut Efficiency

Albert et al, 2017

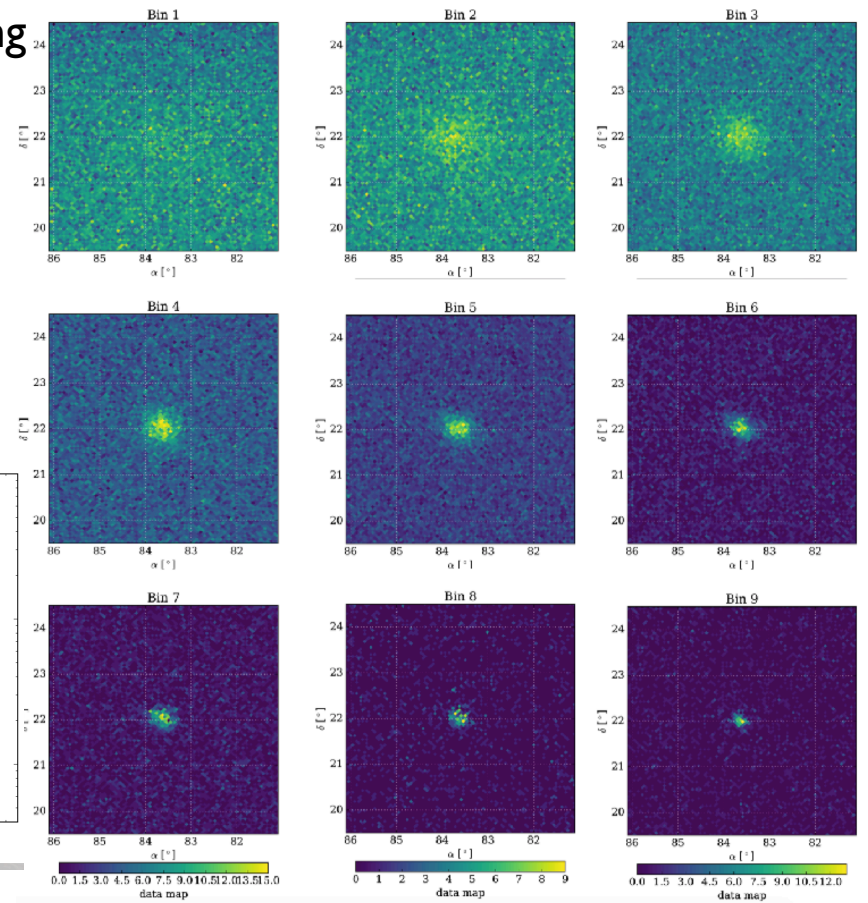
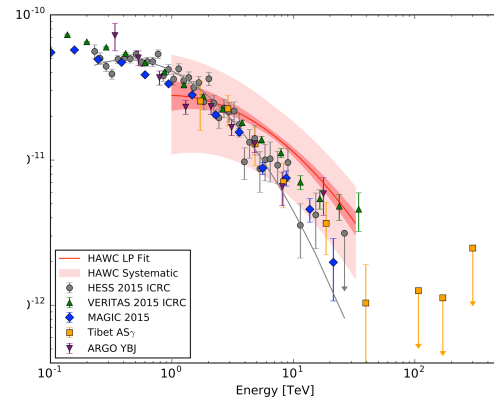
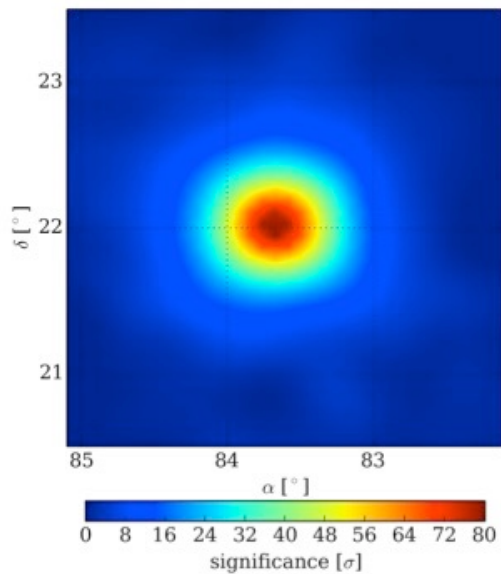


The figure shows the fraction of gamma rays and background hadron events passing photon/hadron discrimination cuts as a function of the event size,  $B$ . Good efficiency for photons is maintained across all event sizes with hadron efficiency approaching  $1 \times 10^{-3}$  for high-energy events.

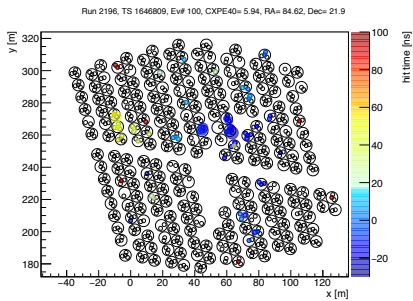
# Searching for sources with HAWC

- Events are sorted by size in  $n$  bins (corresponding to a characteristic energy, S/N ratio and PSF)
- A likelihood framework incorporating detector response and source model tests the presence of sources in the  $n$  maps

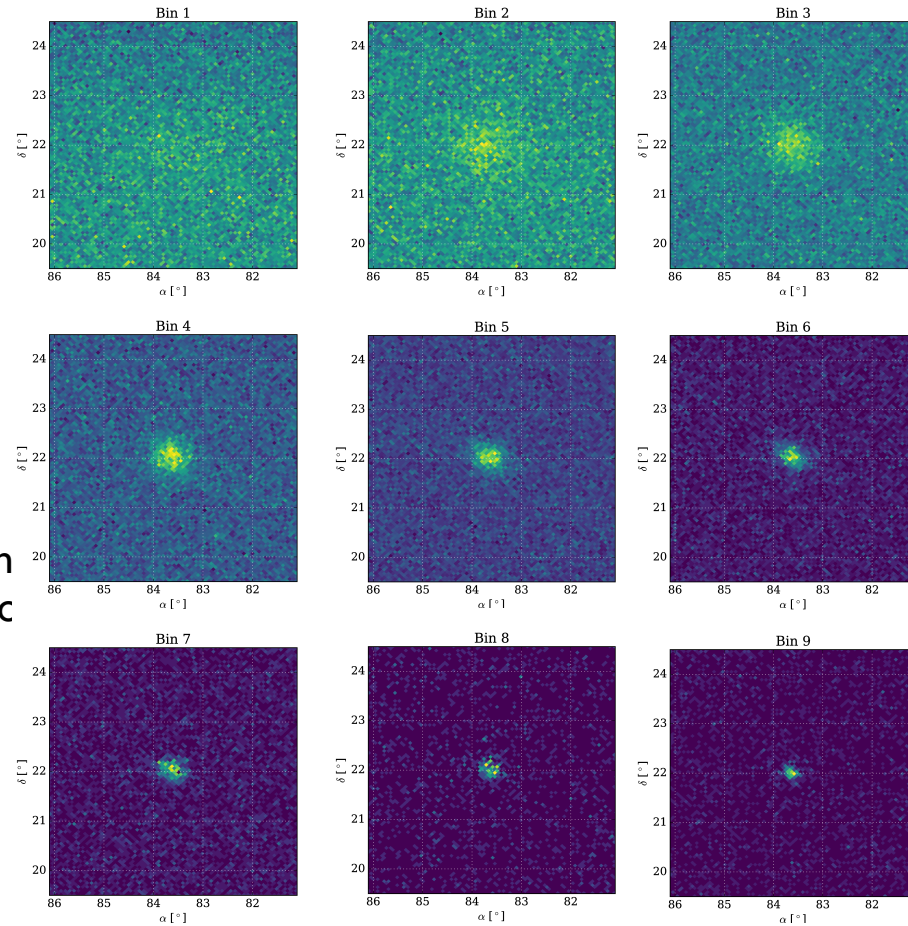
CRAB



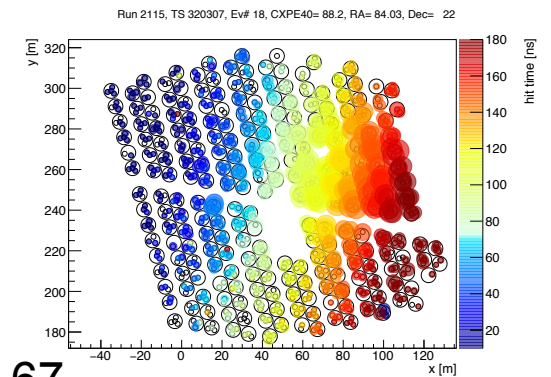
# HAWC Sensitivity



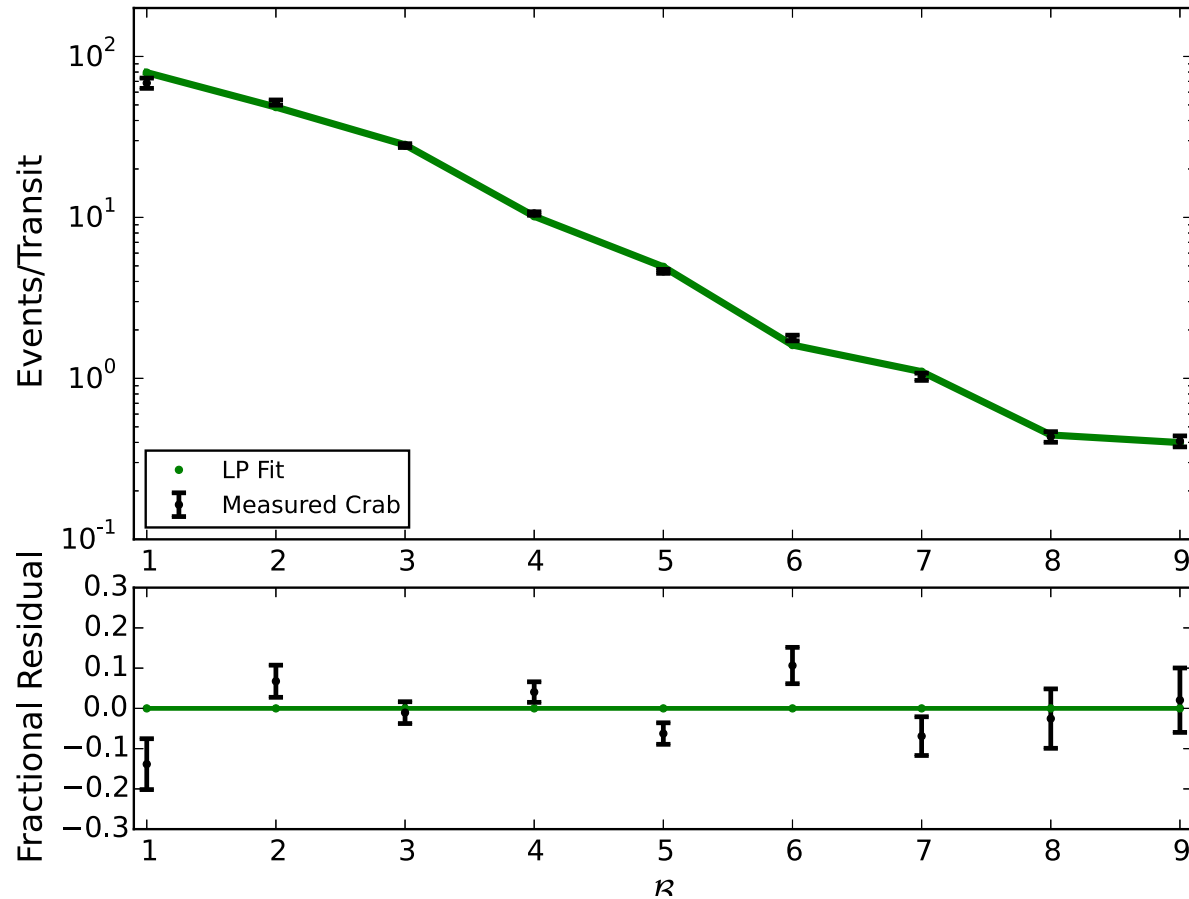
CRAB



The bigger the shower the:  
the better the angular resolution  
the better the background rejectic  
the higher the energy  
the fewer the events

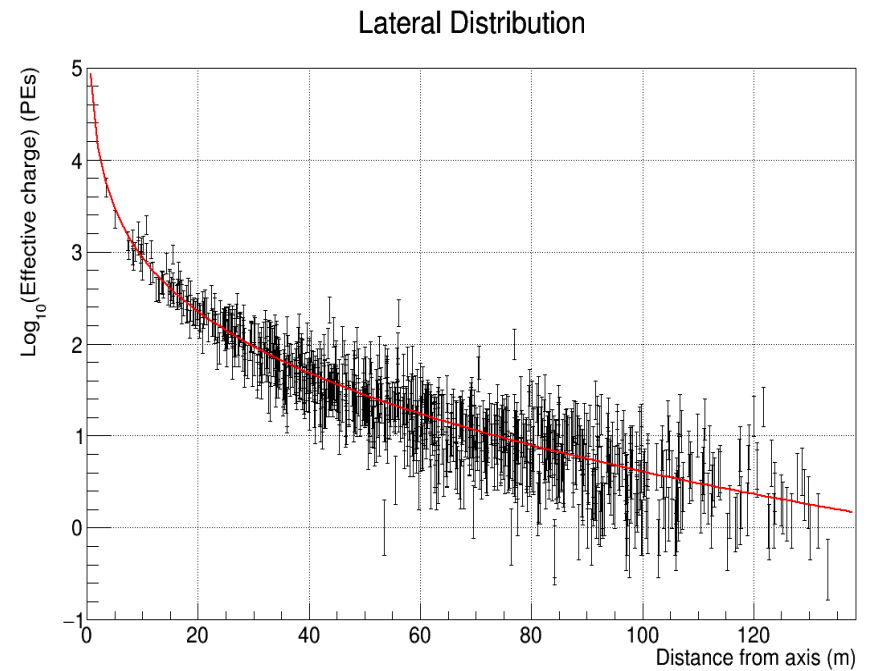
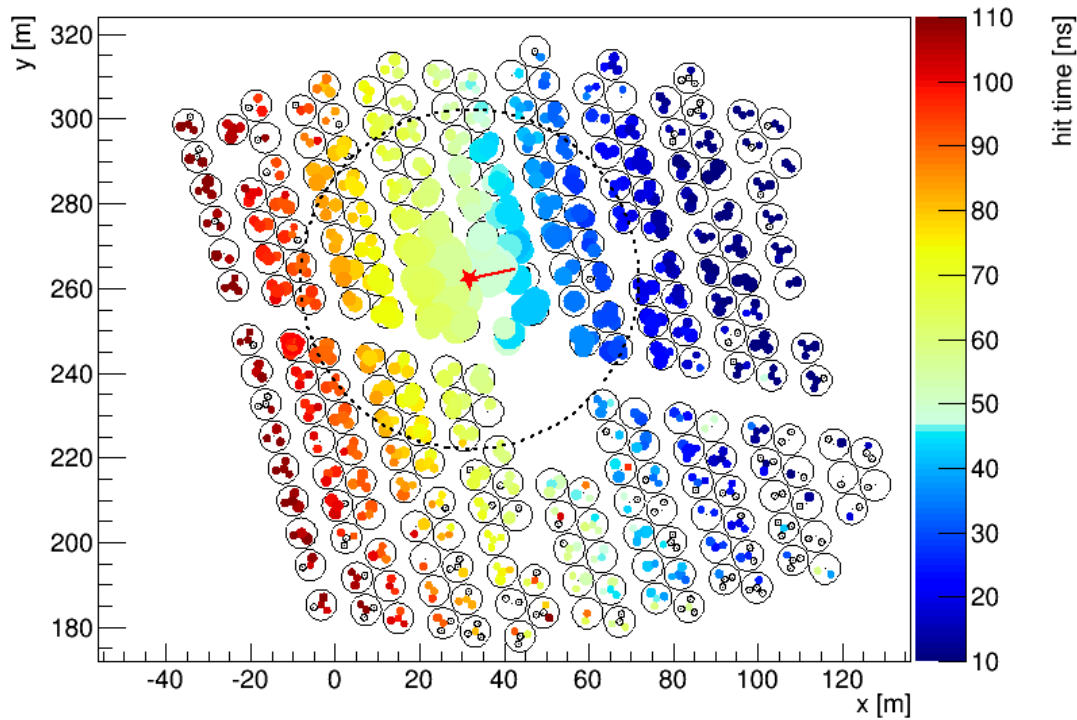


# Number of photons from Crab



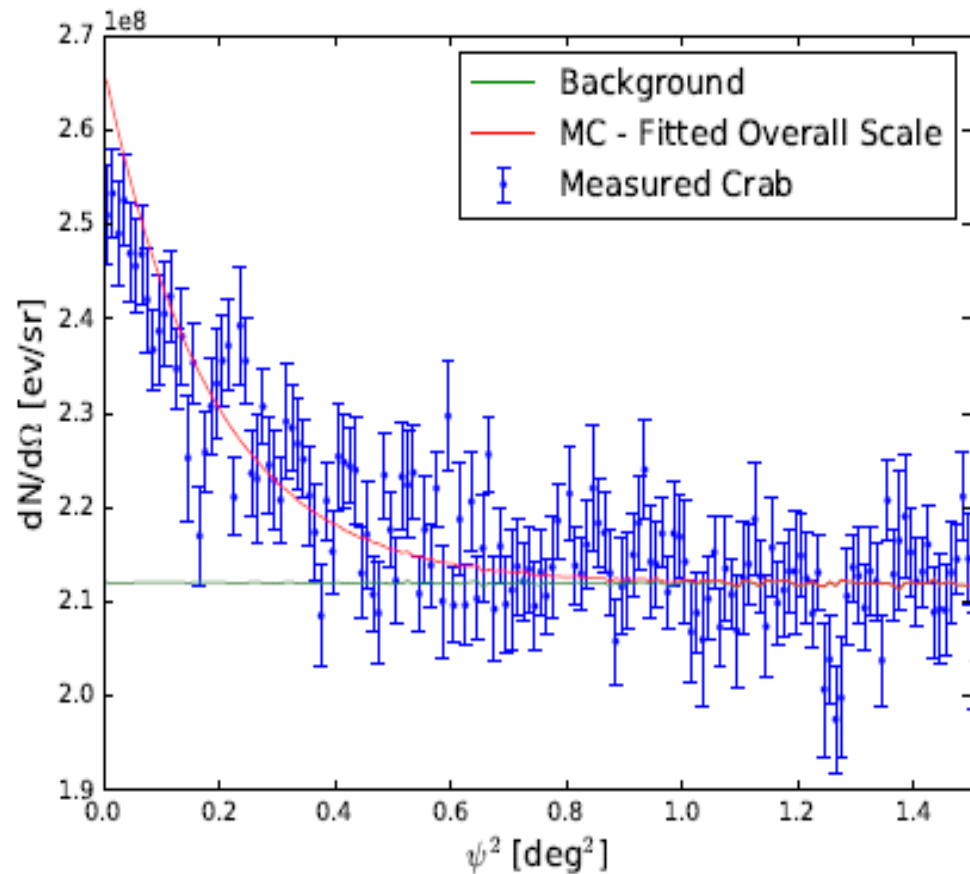
The figure shows the measured, background-subtracted number of photons from the Crab in each B bin. To get the total number of photons, the signal from the Crab is fit for each B separately. The measurements are compared to prediction from simulation assuming the Crab spectrum is at the HAWC measurement. The fitted spectrum is a good description of the data, with no evidence of bias in the residuals.

# Crab gamma-ray candidate

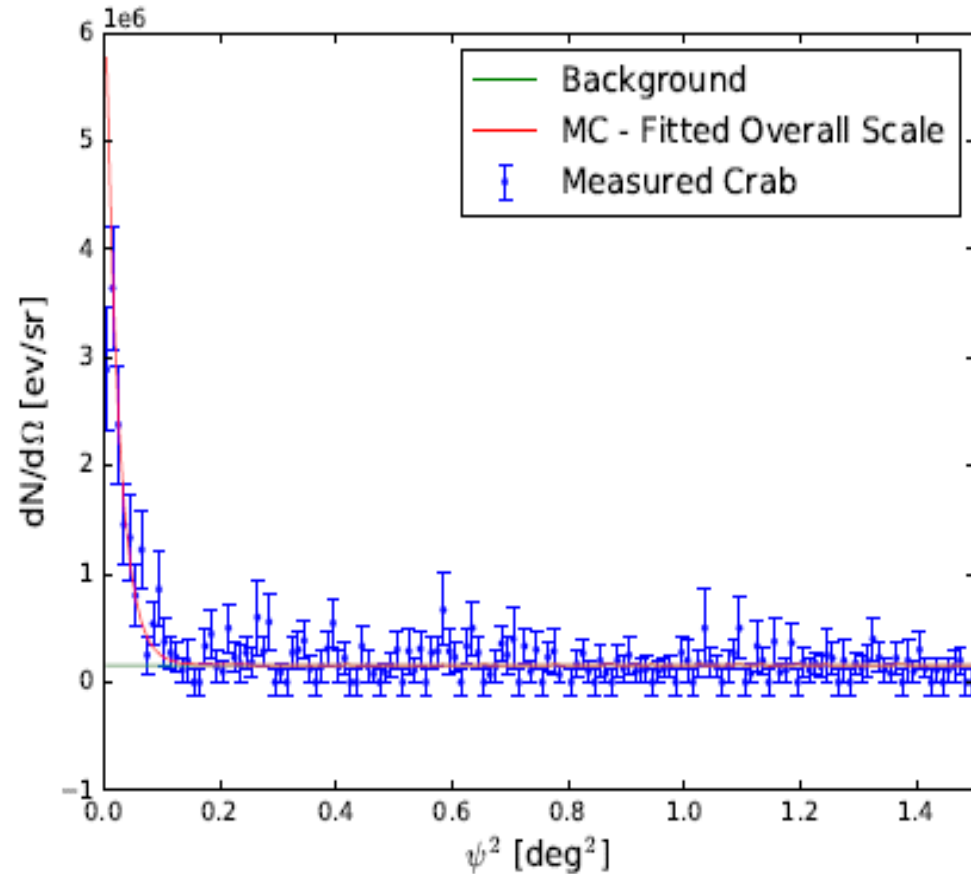


- Event reconstructed within  $0.4^\circ$  of the Crab Nebula.

# Angular Resolution



(c)  $\mathcal{B} = 3$  Angular Profile



(d)  $\mathcal{B} = 8$  Angular Profile

# HAWC Data Volume

**We read in every PMT hit all the time**

Raw data rate - 500MB/s -10 VME Backplanes

**Trigger in Software**

Trigger rate requiring  $\sim 30$  hits in 300ns is  $\sim 25$ kHz

**Process in near real time**

**Rate to disk  $\sim 24$ MB/s  $\rightarrow$   $\sim 2$ TB/day (everyday)**

**Data is moved by portable disk arrays to UNAM**

About once a week it's driven to Mexico City

Moved over Internet II to UMD

**Raw Data plus processed data is stored in Mexico and Maryland**

About a petabyte a year

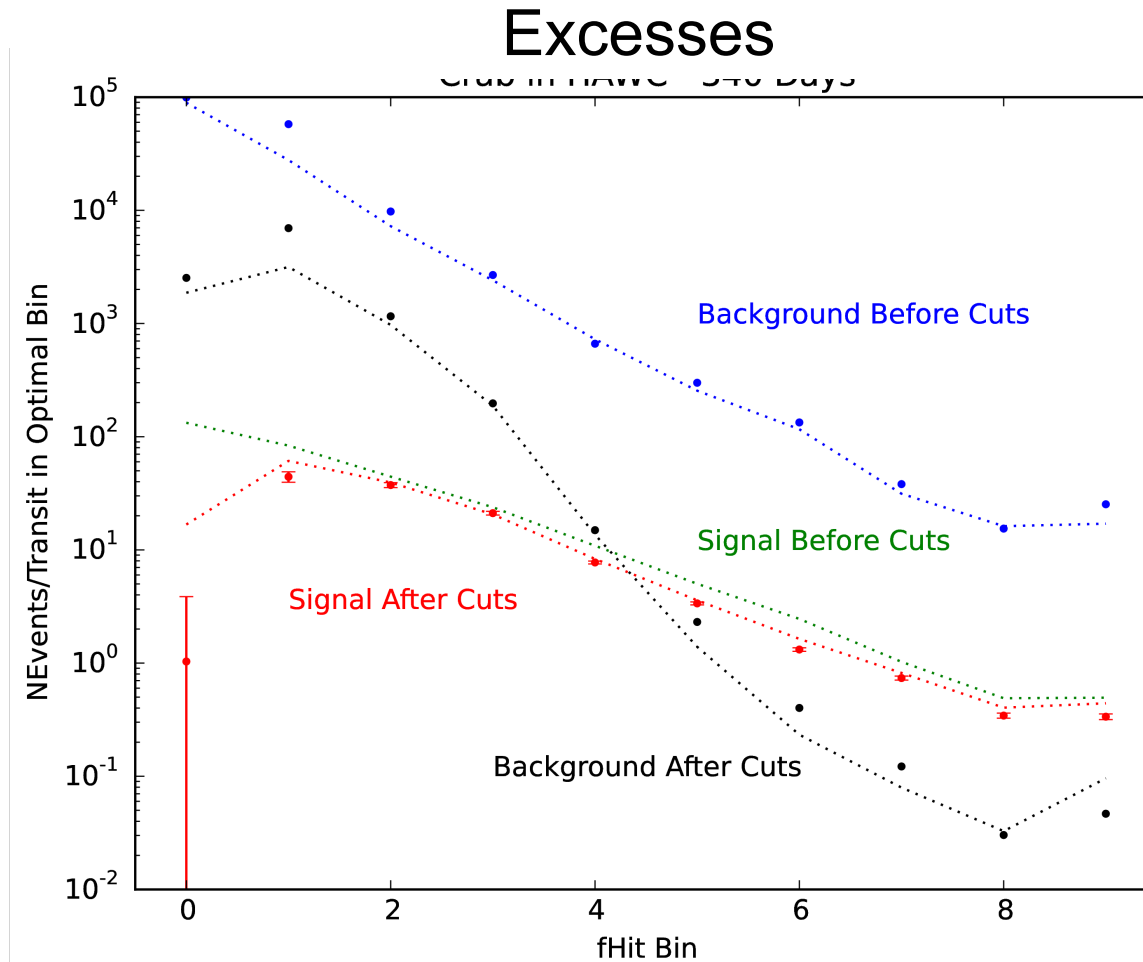
Currently we have about 7.5 PB of storage at UMD



The Data

# Signal and background before and after cuts

72



$\sigma = \text{signal}/\sqrt{\text{background}}$  on Crab per transit: 5-7 integrated over all energy bins.  
In 1128 days we have 162  $\sigma$ , which roughly scales with square root of time and gives 5  $\sigma$ /day